Volume VII

Asadh 2082 (July 2025)

JOURNAL OF LAND MANAGEMENT AND GEOMATICS EDUCATION

An Annual Publication of LMTC

Published by:

Government of Nepal

Ministry of Land Management, Cooperatives and Poverty Alleviation

Land Management Training Center

Dhulikhel, Kavrepalanchok

Nepal

CONTACT US

info@lmtc.gov.np
Land Management Training Centre
Ministry of Land Management, Cooperatives and Poverty Alleviation
Dhulikhel, Kavre, Nepal
G.P.O. Box number. 12695, Kathmandu, Nepal
Phone number. 00977 11 415055/51
Fax. 00977 11 415078

SUBMISSION

Visit http://www.lmtc.gov.np for online manuscript preparation and submission guidelines. Contribution of original unpublished research, review articles, scholarly essays are welcome. The articles will be published only after peer review.

Cover Page

Airborne Laser Scanner (Source: https://aerolaser.es/en/mapping-lidar/)

Terrestrial Laser Scanner (Source: https://luxfootball.lu/terrestrial-lidar-remote-sensing-market-outlook-2025-2030/#google_vignette)

UAV Based Laser Scanner (Source: https://uavcoach.com/lidar-drones/)

Output of LiDAR Survey (https://www.lidarsolutions.com.au/lidar-solutions/lidar-survey-inspection-services/lidar-forest-survey-forestry-inventory-mapping-modelling/)

This issue of "Journal of Land Management and Geomatics Education" is available at www.lmtc.gov.np. All contents can be accessed without registration or subscription.

ADVISORY COMMITTEE

Chairperson
Janak Raj Joshi
Executive Director
Land Management Training Center
M.Sc. in Geoinformation Science and Earth Observation

Members

Prof. Manish Pokharel, PhD
Dean, School of Engineering
Kathmandu University
Doctorate Degree in E-government

Damodar Wagle
Chief Survey Officer
Ministry of Land Management, Cooperatives and Poverty Alleviation
Masters in Geography

Rajendra Raut
Director
Land Management Training Center
Masters in Public Administration

Ram Kumar Sapkota
Director
Land Management Training Center
M.Sc. in Geodesy and Geoinformation

Sudeep Shrestha
Director
Land Management Training Center
M.Sc. in Photogrammetry and Geoinformatics

Lekha Nath Dahal
Director
Land Management Training Center
Masters in Land Administration

EDITORIAL COMMITTEE

EDITOR-IN CHIEF

Ram Kumar Sapkota
Director
Land Management Training Center
M.Sc. in Geodesy and Geoinformation

MEMBERS

Bigyan Banjara
Instructor
Land Management Training Center
M.Sc. in Earth Oriented Space Science and Technology

Bhagirath Bhatt
Instructor
Land Management Training Center
ME in Geoinformatics

Kamal Shahi
Instructor
Land Management Training Center
M.Sc. in Geospatial Technologies

Rheecha Sharma
Instructor
Land Management Training Center
M.Sc. in Geospatial Engineering

EDITORIAL

It's my immense pleasure to present the seventh edition of the Journal of Land Management and Geoinformatics Education, an annual publication of the Land Management Training Centre (LMTC), a certified ISO 9001:2015 institution. In today's era of rapid scientific and technological advancement, the fields of land management and geoinformatics have emerged as critical disciplines, playing a vital role in efficient planning and policymaking, environmental protection, disaster resilience, and evidence-based decision-making. This journal serves as a platform for students, researchers, and practitioners in the geospatial field to share in-depth studies, innovative practices, and evidence-based research in geospatial sciences and land management.

This edition of the journal brings together a wider collection of peer-reviewed research focused on geospatial science and land governance. The articles explore flood risk mapping through AHP and Fuzzy AHP, urban expansion and land-use change, and groundwater potential zoning for sustainable planning. Contributions also examine agricultural land pooling, carbon stock estimation using satellite imagery, and geoid enhancement with UAV data. In addition, this issue features an article that presents some innovative approaches for enhancing service delivery in survey offices. These diverse studies reflect the evolving role of geospatial technologies in addressing importance of geospatial technologies in tackling the critical developmental and environmental challenges faced by today's communities. On behalf of Editorial board, I would like to extend my earnest thankfulness to all contributing authors for their insightful study and research as well as reviewers for their outstanding professional contribution.

Moreover, I am pleased to express my sincere gratitude to Executive Director Mr. Janak Raj Joshi and advisory committee members for their constant support and guidance to bring up this journal. I would also like to articulate my appreciation to Mr. Bhagirath Bhatt and the entire editorial board for their tireless efforts and dedication in bringing this issue to publication.

Furthermore, being the only federal training institution dedicated to capacity building and advancement in the fields of geoinformation and land management in the country, Land Management Training Centre remains strongly committed to becoming a center of excellence in surveying, mapping, and land management. Warmest congratulations on the glorious 57th Anniversary of the Land Management Training Center, a dignified milestone with decades of dedication, and impactful contribution in capacity building in the field of land management and geoinformation

Finally, I invite readers to deeply engage with the articles presented in this edition and to acquire meaningful insights that contribute to the academic and professional pursuits.

Enjoy Reading!

Thank you!!

Message from Dean

It gives me immense pleasure to know that the Land Management Training Centre (LMTC) is preparing to release its seventh edition of the Journal of Land Management and Geomatics Education. Since 2007, Kathmandu University, School of Engineering, has been running the undergraduate program Bachelor in Geomatics Engineering in collaboration with the Land Management Training Center (LMTC), Ministry of Land Management, Co-operatives and Poverty Alleviation. Since then, we have together uplifted and strengthened our collaboration in running graduate (Masters in Land Administration and ME/MS in Geoinformatics) and postgraduate programs (PhD in Land Administration and Geomatics Engineering), thereby producing skilled human resources in the field of land management and geospatial science.

I would like to express my sincere appreciation to the editorial team of the journal and the whole institution for their efforts and the steps they have taken to create such a platform, which is truly inspiring and also essential for the dissemination of knowledge and research within the geospatial and surveyor's community. I would also like to extend my best wishes to the editorial team and LMTC and look forward to collaborating much more in the near future to make more meaningful strides in the surveying and land management sector.

Prof. Manish Pokharel, PhD
Dean, School of Engineering
Kathmandu University

Executive Director's Message!

I am delighted to present the seventh edition of the Journal of Land Management and Geomatics Education. Building on the innovative spirit of our previous editions, this journal continues to be an essential hub for academic rigor, technological advancement, and practical developments in the fields of land management and geomatics. As we navigate an era marked by rapid urbanization, climate vulnerability, and changing spatial challenges, the insights shared in this journal are not merely academic-they are vital catalysts for sustainable development, resilience, and transformative change in Nepal and beyond. Land management and geomatics are crucial fields that connect human development with caring for our planet. These disciplines enable us to make better use of resources, reduce environmental risks, and create fair solutions for communities facing complex social, economic, and ecological changes. Since 1969, the Land Management Training Center (LMTC) has been dedicated to promoting excellence in these areas, continually working to bridge the gap between theory and practice. This journal reflects that commitment by showcasing innovative research that provides professionals, policymakers, educators, and students with the necessary tools to build a sustainable future.

This edition presents a diverse range of research that reflects the interdisciplinary nature in the field of geoinformatics. Contributions cover several critical areas, including advanced methodologies using GIS, remote sensing, and UAV technology to address land-use planning, agricultural optimization, and natural resource management; studies on the impacts of climate change-such as flood susceptibility modeling, aerosol dynamics, and urban heat island effects-offering data-driven strategies for disaster risk reduction; integrated approaches to groundwater zoning, forest biomass estimation, and land administration reforms that emphasize participatory and technology-enabled governance; and breakthroughs in geoid modeling, satellite data fusion, and analytical frameworks like AHP and Fuzzy AHP that enhance spatial decision-making precision. Each article reflects the synergy between academic inquiry and real-world relevance,

highlighting how geospatial intelligence can promote policy coherence, community resilience, and ecological sustainability.

The publication of this edition reaffirms commitment of the center to excellence in education, research, and professional training. Recent milestones, such as our renewed partnership with Kathmandu University, the deployment of LiDAR technology at the center, and the re-certification of our ISO 9001:2015 quality standards, highlight our determination to enhance geomatics education in Nepal. Our training programs, designed for government personnel at both federal and local levels, integrate global best practices with local expertise, nurturing a new generation of leaders prepared to address complex challenges. I extend my heartfelt gratitude to our authors, whose pioneering work forms the foundation of this journal; our reviewers, whose thorough assessments ensure academic rigor; and the editorial team, whose unwavering dedication helped bring this publication. Special recognition goes to our partners in academia, industry, and government, whose collaborative spirit amplifies the impact of our collective efforts.

As we celebrate this edition, I encourage our readers – students, academics, policymakers, and practitioners - to engage thoughtfully with these insights, convert knowledge into action, and contribute to future volumes. The challenges we face, from climate adaptation to equitable land governance, require bold ideas and inclusive dialogue. Let this journal serve as your platform: share your research, provide constructive critiques, and join us in pioneering solutions that align human progress with the planet's limits. I am confident that this edition will inspire innovation, inform policy, and spark the curiosity of future geospatial pioneers. Together, let us continue mapping pathways to sustainability.

Janak Raj Joshi
Executive Director
Land Management Training Center
July, 2025

Table of Contents

List of Peer Reviewers

Mr. Ganesh Prasad Bhatta
Joint Secretary, Ministry of Land Management Cooperatives and Poverty Alleviation

Mr. Susheel Dangol
Deputy Director General, Survey Department

Mr. Punya Prasad Oli
Principal, Himalayan College of Geomatic Engineering and Land Resources Management
Former Director General, Survey Department

Dr. Reshma Shrestha
Associate Professor and Head of Department, Kathmandu University

Dr. Subhash Ghimire
Associate Professor, Kathmandu University

Dr. Him Lal Shrestha
Associate Professor, Kathmandu Forestry College

Dr. Dev Raj Poudyal
Lecturer, University of Southern Queensland, Australia

Mr. Suraj K.C.
Chief Survey Officer, Survey Department

Mr. Sanjeevan Shrestha
Chief Survey Officer, Ministry of Land Management Cooperatives & Poverty Alleviation

Ms. Tina Baidar
Chief Survey Officer, Survey Department

Dr. Uma Shankar Panday
Assisstant Professor, Kathmandu University

Mr. Prakash Ghimire
Instructor, Land Management Training Center

Mr. Shankar K.C.
Survey Officer, Survey Department

Mr. Digbijaya Poudel
Lecturer, Kathmandu University

IDENTIFICATION OF POTENTIAL AGRICULTURAL LAND POOLING SITES IN KASKI DISTRICT USING AHP AND GIS

Dhaka Ram Gaire[1], Shailendra Shahi[1], Oshi Humagain[1], Bir Bahadur Khatri[1], Umesh Bhurtyal[1],Milan KC[2]

[1]Department of Geomatics Engineering, IOE, Pashchimanchal Campus, Pokhara, Nepal

pas077bge016@wrc.edu.np,pas077bge043@wrc.edu.np, pas077bge026@wrc.edu.np, pas077bge014@wrc.edu.np, umbhurtyal@wrc.edu.np

Ministry of Land Management, Agriculture, Cooperatives and Poverty Alleviation, Gandaki Province

kcmilan28@gmail.com

ABSTRACT

This study identifies potential agricultural land pooling sites in Kaski District using an integrated Geographic Information System (GIS) and Analytic Hierarchy Process (AHP) approach. Agricultural land pooling seeks to address land fragmentation and promote efficient collective farming. The study considered four major criteria—slope, land parcel area, proximity to roads, and irrigation access following the Agricultural Land Pooling Program Implementation Guidelines, 2077, from the Ministry of Agriculture and Land Management, Gandaki Province.

Criteria weights were calculated using AHP as follows: Slope (60.57%), Area (23.18%), Irrigation Access (11.04%), and Road Proximity (5.21%). A GIS-based weighted overlay method was applied to create a suitability map, classifying land into four categories: Most Suitable, Suitable, Moderately Suitable, and Low Suitable. The results revealed that about 48% of the land parcels fall under the "Most Suitable" and "Suitable" categories, mostly located in the district's central and southern regions. Field validation was carried out using Kobo Collect, resulting in an overall accuracy of 82.35% and a Kappa coefficient of 0.76, indicating a strong agreement between the model and ground data. This research demonstrates that combining AHP with GIS is an effective method for land pooling site selection and offers valuable insights for expanding future land consolidation initiatives.

KEYWORDS: Land Pooling, Agriculture Land, GIS, AHP, DEM

1. INTRODUCTION

1.1 Background

Nepal is predominantly an agricultural nation, with around 62% of its population involved in farming activities, according to the Agriculture Census 2022/23. Agriculture accounts for approximately 25% of the country's Gross Domestic Product (GDP) and serves as a major source of employment (Nepal Economic Forum, 2023). The overall economic development of Nepal is closely tied to the performance of its agricultural sector.

This research highlights the adoption of modern agricultural practices, focusing particularly on land pooling — a method known locally as *Jagga Ekikaran* or *Chaklabandi*. Land pooling is a practical approach to combined farming, where individual farmers consolidate their fragmented plots into larger, more manageable unitsThe adaptation to modern agricultural tools and technologies—such as harvesters, cutters, and other mechanized equipment—becomes significantly easier with larger and regularly shaped land parcels. These uniform plots not only facilitate efficient use of machinery but also help reduce both the time and cost involved in agricultural practices, ultimately enhancing productivity and promoting sustainable farming. By doing so, farming can be managed more professionally, incorporating entrepreneurial skills and business strategies. The profits generated are distributed among the landowners according to the size of their original landholding. Through land pooling, farmers gain better access to agricultural resources like irrigation systems, road networks, and markets, leading to enhanced productivity and a higher standard of living. This method enables the transition from traditional farming to more modern, efficient techniques. Furthermore, under the Local Self-Governance Act of 1999, municipalities and local authorities can actively promote and implement land pooling initiatives.

Gandaki Province, one of the seven provinces, places high importance on agriculture and is strongly oriented toward agricultural development. It consists of 11 districts with Pokhara as its capital. According to the Ministry of Agriculture and Land Management, Gandaki Province (2077), Agriculture is the primary source of income for

86% of all household. Despite this 24 percent of cultivable land remains uncultivated where irrigation is available only on 36.15 percent of the area. So, this province has initiated Cooperative based farming in agriculture through land pooling program as Province Pride Project in more than 32 places where six of them lies in Kaski district.

Table 1. Land Pooling programs conducted by the Ministry of Agriculture, Land Management and Cooperatives in Kaski District.

S. N.	District	Land Pooling Location	Land Pooling Area (Ropani)	Name of Cooperative/Group	Number of Beneficiary Farmer Families
1	Kaski	Machhapuchhre Gaunpalika - 3	208	Bhume Srijansil krishak Samuha	67
2	Kaski	Pokhara Mahanagarapalika - 23	137	Dharapani (Kayer) Krishi Samuha	35
3	Kaski	Machhapuchhre Gaunpalika - 3	108	Annapurna Mahila Prangarik Sahakari Sanstha Ltd	31
4	Kaski	Rupa Gaunpalika	85	Polyantar Tankakaja Krishak Samuha	118
5	Kaski	Pokhara Mahanagarapalika - 28	55	Birat Krishi Sahakari Sanstha Ltd	20
6	Kaski	Pokhara Mahanagarapalika - 16, Armala	57	Lekali Krishak Samuha	100

This study mainly concerns identifying potential land pooling sites in Kaski district using AHP model and GIS. The criteria are set according to Land Pooling Program Implementation Guidelines, 2077 approved by the Honorable Council of Ministers on 2077/04/31 for land pooling program in Gandaki province.

1.2 Study Area

Kaski district lies at the central of Gandaki province. Spanning an area of 2,017 square kilometres, it is characterized by diverse topography, ranging from flat valleys to steep hills and mountainous terrains. It extends between 27°25' N to 28°30' N latitude and 83°30' E to 84°30' longitude. In terms of terrain, the study area lies in the hilly region of Nepal. The elevation value ranges between 367m -7921m.

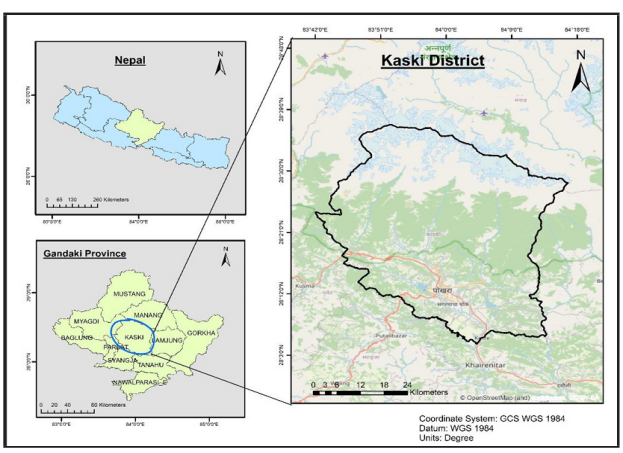

Figure 1. Map of Study Area

2. MATERIALS AND METHODS

2.1 Data Required

Table 2. Data Sources

Data	Resolution	Source	Purpose
DEM	30 m	USGS Earth Explorer	Derived slope from SRTM DEM
Landsat 8	30 m	USGS Earth Explorer	Created LULC map; extracted cropland
Road Network	Vector	OpenStreetMap	Assessed accessibility to land pooling sites
Irrigation	Vector	OpenStreetMap	Access irrigation facility to land pooling sites

2.2 Working Procedures:

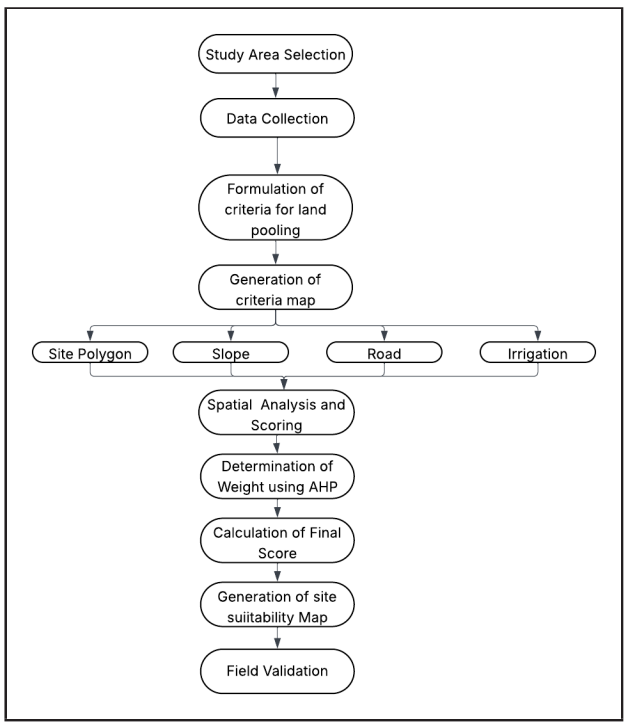

Figure 2: Schematic representation of Methodology

2.2.1 Study Area Selection

Unlike the Terai, where land is flat and well-serviced, the hilly region of Kaski lacks uniform slope, road access, irrigation, and large parcels. This makes it a priority area for identifying suitable agricultural land pooling sites using defined criteria.

2.2.2 Data Collection

DEM, road network, and water sources were collected for spatial analysis along with non-spatial data like the criteria guideline for AHP. Land cover was prepared using Landsat imagery from GEE.

2.2.3 Formulation of Criteria

The criteria and their scoring system were slightly modified from the original guideline to suit the available data and ensure practical applicability in the study area.

2.2.4 Generation of criteria maps using GIS

Slope, road network, and irrigation source maps are not shown, as they were directly derived from reliable sources

like USGS (DEM) and OpenStreetMap, requiring only minimal processing for use in the analysis. The Land Use and Land Cover (LULC) map for the project was created using Landsat imagery. The classification was conducted using the Random Forest (RF) algorithm in Google Earth Engine. To distinguish cropland accurately, other major land cover types such as water, vegetation, settlement, bare land, and snow were also classified. These classes helped exclude non-agricultural areas and improve the accuracy of cropland identification. These land cover classes were chosen to represent the major surface features of Kaski district relevant to land pooling analysis. Although land cover was not used directly as a criterion, it was essential for identifying cropland parcels, which were required for the area-based criterion. Therefore, the land cover map was included to show how cropland parcels were extracted for further analysis.

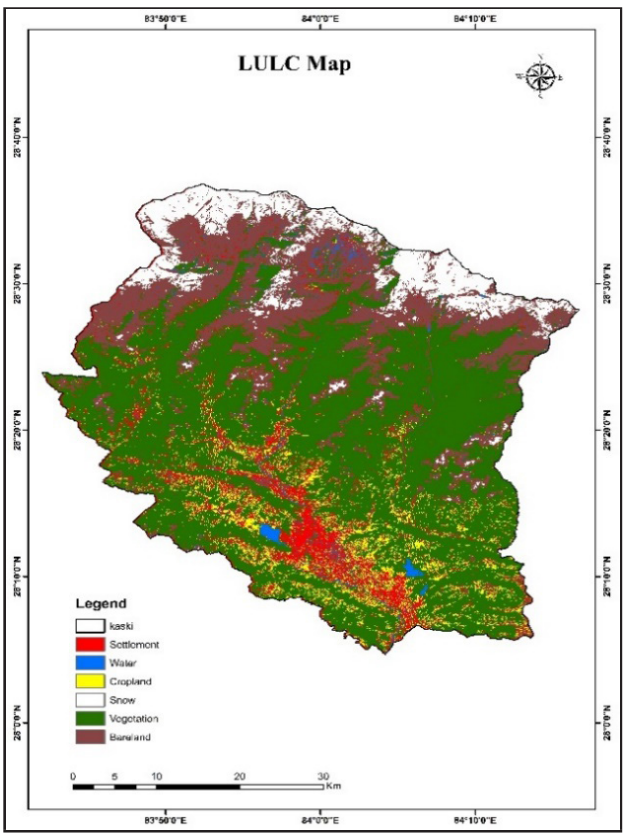

Figure 3: LULC Map of Kaski District

From this imagery, the crop land was extracted and used as a separate layer. This crop land layer was then overlaid on Google Earth Pro, which provided high-resolution satellite imagery for more precise analysis. Using Google Earth Pro's digitizing tools, polygons were manually created to represent the boundaries of the agricultural fields. These digitized polygons were subsequently used to generate a site polygon map, which serves as a key component in the spatial analysis for identifying suitable sites for land pooling.

The confusion matrix below summarizes the performance of the classifier:

Table 3. Confusion Matrix of LULC

Classes	Water	Settlement	Cropland	Snow	Vegetation
Water	22	2	1	0	1
Settlement	2	18	3	0	1
Cropland	0	1	34	0	0
Snow	0	0	0	24	1
Vegetation	0	0	1	0	55
Bare Land	1	2	0	0	3

Table 4. Accuracy Assessment

	Water	Settlement Area	Cropland	Snow
Producer Accuracy	78.57%	60.00%	77.27%	92.31%
Consumer Accuracy	82.14%	62.50%	90.00%	92.31%
Overall Accuracy		81.04%		
Kappa Coefficient		74.20%		

2.2.5 Spatial analysis and scoring

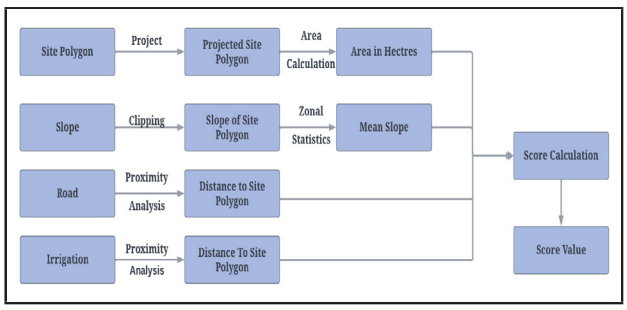

Figure 5. Methodology for Spatial analysis and Scoring

Site polygon analysis

To calculate the area of site polygons for analysis, the data must first be projected into an appropriate **Projected Coordinate System (PCS)** such as UTM, to ensure accurate area measurements. Once reprojected, we use the area calculation tool within the software. The area is typically calculated in hectares.

Slope analysis

The slope map is generated using Digital Elevation Model (DEM) data. To assess the slope for each individual site polygon, zonal statistics are applied, with the mean method used to calculate the average slope within each polygon. This approach allows for a detailed analysis of the topography across the study area, helping to evaluate the suitability of different sites for land pooling based on their slope characteristics.

Road analysis

Proximity analysis is performed using the near tool to calculate the Euclidean distance between each site polygon and the nearest road. This analysis helps in assessing the accessibility of the sites, which is an important factor in determining their suitability for land pooling.

Irrigation analysis

Proximity analysis is performed using the near tool to calculate the Euclidean distance between each site polygon and the nearest waterway. This analysis helps in evaluating the availability of water resources in land pooling sites.

Score Evaluation

Python codes are used in field calculator of attribute table to calculate score for each criterion based on their sub-criteria. Scores are given based on the following sub-criteria set by Ministry of Agriculture and Land Management, Gandaki Province.

Table 5. Sub Criteria for land pooling

Criteria	3=Highest Importance	2=Average Importance	1=Slight Importance
Area	>150 ropani	50-150 ropani	<50 ropani
Slope	0-5Â°	5-10Â°	>10Â°
Road	<100m	100-250 m	>250 m
Irrigation	<50 m	50-100 m	>100 m

2.2.6 Determination of weights using AHP

The Analytical Hierarchy Process (AHP) is a widely used multi-criteria decision-making tool that helps in solving complex problems by structuring them into a hierarchical model consisting of a goal, criteria, and alternatives (Saaty, 1980; Roig-Tierno et al., 2013). It facilitates decision-making in situations where multiple criteria and sub-criteria are involved, especially in cases where interactions between factors are significant (Feizizadeh et al., 2014; Tiwari et al., 1999). AHP is particularly effective in handling both qualitative and quantitative data, allowing the assignment of weights to various decision criteria through pairwise comparisons (Bunruamkaew & Murayama, 2011) AHP allows us to give each factor a **weight** based on its importance and then combine all the results to choose the best option. AHP works very well with **GIS (Geographic Information System)** to create **suitability maps.** These maps help in selecting the best location for things like farming or planning land use (Triantaphyllou & Mann, 1995; Boroushaki & Malczewski, 2008; Bunruamkaew & Murayama, 2011). Because it is both **simple and powerful,** AHP is often used in land suitability analysis for agriculture (Chen et al., 2010a; Akıncı et al., 2013).

The AHP method involves the following key steps and equations:

1. Pairwise Comparison Matrix (PCM):

Construct a matrix A= $[a_{ij}]$, where

a_{ij}= importance of criterion i and j, using Saaty's scale (1-9)

2. Normalize the matrix:

Divide each element by sum of its column:

$$a'_{ij} = \frac{a_{ij}}{\sum_{\{i=1\}}^{\{n\}}\{a_{ij}\}}$$

3. Compute weights:
Average each row of the normalized matrix:

$$W_i = \frac{\sum_{\{j=1\}}^{\{n\}}\{a'_{ij}\}}{n}$$

4. Calculate
Multiply PCM by weight vector - divide result element wise by weights - average:

$$\lambda_{max} = \frac{\sum \frac{(A.W)_i}{W_i}}{n}$$

5. Consistency Index (CI):

$$CI = \frac{\lambda_{max} - n}{n-1}$$

6. Consistency ratio (CR):

$$CR = \frac{CI}{RI}$$

where RI=Random Index. If CR<0.1, consistency is acceptable.

Table 6: AHP Matrix

Criteria	Area	Road	Slope	Irrigation	Criteria Weight
Area	1	5	0.25	3	0.2318
Road	0.2	1	0.125	0.3333	0.0521
Slope	4	8	1	6	0.6057
Irrigation	0.333	3	0.1667	1	0.1104
Sum	5.5333	17	1.5417	10.3333	

This Calculation yield the following results:

λmax = 4.1494

Consistency Index (C.I) = 0.0498

Consistency Ratio (C.R) = 0.0553

Since, the CR (0.0553) is less than 0.1, the pairwise comparison matrix is consistent and Valid for use in AHP.

2.2.7 Calculation of Final score

The final suitability score for each site polygon is calculated using the weighted overlay formula. Instead of using the weighted overlay tool in GIS directly, the formula is applied manually in the attribute table. A new field named "Final Score" is added to the attribute table, and the Field Calculator is used to apply the formula:

Final Score = ∑ (Weight of Criterion× Criterion Value)

This approach integrates multiple criteria, such as slope, proximity to roads, and proximity to waterways, by assigning weights to each factor based on their relative importance determined through the AHP process.

2.2.8 Generation of Site suitability map

The calculated final scores for each site, based on individual criterion values and their respective weights were integrated into a GIS-based weighted overlay analysis, which classified the study area into four suitability classes: Low Suitable, Moderately Suitable, Suitable, and Most Suitable. The final suitability map illustrates the areas prioritized for land pooling based on the selected criteria.

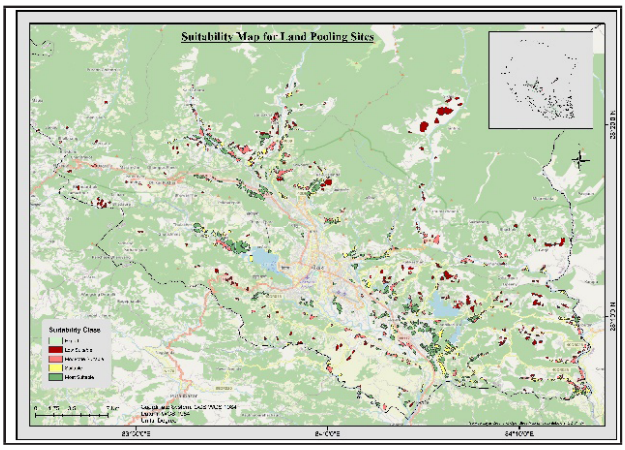

Figure 6. Final Suitability Map for land pooling Sites in Kaski District

2.3 Findings:

The map reveals that most suitable and suitable lands are scattered in the central and southern parts of the Kaski district, particularly around Pokhara Valley. These areas are characterized by relatively flat terrain, good irrigation access, and proximity to existing infrastructure, making them highly viable for land pooling initiatives.

On the other hand, a significant portion of the district (36.75%) falls under low suitability areas. These regions, mostly in the northern and eastern hilly zones, are constrained by rugged topography and lack of accessibility, which pose challenges for large-scale land pooling projects.

The moderately suitable areas, while limited in area (15.38%), might still be potential targets for small-scale or community-led initiatives if complemented with infrastructure development.

Table 7. Area of Suitability Class

Class	Number of Polygon sites	Area in Hectares	Percentage(%)
Most Suitable	168	970.66	22.69
Suitable	154	1077.14	25.18
Moderate Suitable	124	657.89	15.38
Low Suitable	178	1572.24	36.75

2.4 Field Validation and Accuracy Assessment

To validate the suitability classification model, a field verification was conducted. The observed data from the field were compared with the model-predicted classes using a confusion matrix (contingency table). The field data were collected using **Kobo Collect** and the results were analysed using accuracy assessment metrics.

For field validation, a total of 32 ground truth sample sites were selected using stratified random sampling to ensure balanced representation from each suitability class. The sites were distributed among the classes of Most Suitable, Suitable, Moderately Suitable and Low Suitable, with each class containing approximately 8 to 9 sample sites. This approach was adopted to ensure that all categories were adequately represented during the accuracy assessment, enhancing the reliability of the validation results. The location of the sample sites is shown in the map below.

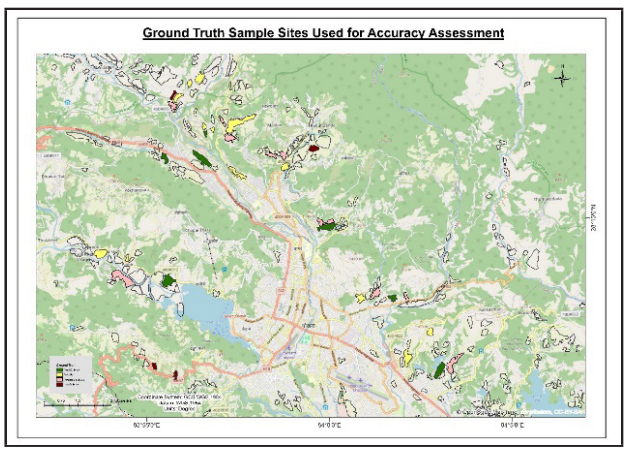

Figure 7. Ground Truth sample site Map

2.4.1 Confusion Matrix (Contingency Table)

The following matrix represents the comparison between the classification results (Model) and the field data (Ground Truth):

Model \ Field	Most Suitable	Suitable	Moderate Suitable	Low Suitable	Row Total
Most Suitable	7	2	0	0	9
Suitable	0	9	1	0	10
Moderate Suitable	0	1	8	0	9
Low Suitable	0	1	1	4	6
Column Total	7	13	10	4	34

This yields the following accuracies:

Accuracy Metric	Most Suitable	Suitable	Moderately Suitable	Low Suitable
Producer's Accuracy	100.00%	69.23%	80.00%	100.00%
User's Accuracy	77.78%	90.00%	88.89%	66.67%
Overall Accuracy	82.35%			
Kappa Coefficient	0.7597			

The field validation of the classification results yielded an overall accuracy of 82.35% and a Kappa coefficient of 0.7597, indicating strong agreement between the classified map and the ground truth data. Most classes achieved high producer's and user's accuracies, with only minor misclassifications. These results confirm that the classification is reliable and suitable for supporting decision-making in the project.

3. CONCLUSION AND RECOMMENDATIONS

3.1 Conclusions

The integration of AHP and GIS in this study has proven to be an effective method for identifying and evaluating potential sites for agricultural Land Pooling within the Kaski district. The final suitability map revealed that nearly half of the analysed area falls under the 'most suitable' and 'suitable' categories, indicating promising zones for future land pooling initiatives. These areas are largely concentrated around relatively flatter terrain with better access to irrigation and infrastructure particularly around Pokhara and its surroundings.

The study highlighted the dominant influence of topographic factors, with slope being the most critical determinant of suitability. The use of a systematic AHP approach provided an objective basis for assigning relative importance to various physical and infrastructural factors, ensuring a balanced and transparent evaluation process.

These results offer significant insights into spatial planning for sustainable land management, especially in a geographically diverse region like Kaski. Moreover, the spatial visualization capabilities of GIS make it easier for planners and decision-makers to interpret complex geospatial relationships, prioritize development zones, and implement policies that align with long-term sustainability goals.

In conclusion, this project provides valuable insight and groundwork that can support policy-level decision-making. The identified suitable areas can serve as reference locations for future land pooling implementation. Therefore, the findings of this research can be highly useful to the Ministry of Agriculture and Land Management of Gandaki Province as a technical basis for promoting and executing land pooling programs at the local and provincial levels.

3.2 Recommendations

Based on the limitations identified during the project in Kaski district, several key recommendations can guide future improvements. First, the model should be enhanced by incorporating additional parameters such as socio-economic factors, land tenure, soil quality, and aspect data, which can provide a more holistic understanding of land suitability. Precision in digitizing parcel boundaries is also crucial and should be achieved using high-resolution satellite imagery or field-verified cadastral datasets. Furthermore, irrigation data should be refined to distinguish between seasonal, permanent, and partial water sources, relying on field verification or official government records rather than generalized OpenStreetMap (OSM) layers. Lastly, to increase the reliability and accuracy of the suitability model, a larger number of field verification sites should be selected across all suitability classes.

The identification of potential land pooling sites through this study should be utilized to improve local-level land use zoning. Land should be categorized into agricultural and residential zones more effectively, with areas deemed suitable for land pooling preserved primarily for agricultural use. Residential development should be discouraged in such zones to protect valuable farmland. This approach should be adopted to support the sustainable management and preservation of agricultural land in the Kaski district, thereby contributing to improved land use planning and long-term food security.

ACKNOWLEDGEMENTS

We sincerely thank the Department of Geomatics Engineering, Pashchimanchal Campus, for the opportunity to undertake this 4th-year project. Our heartfelt gratitude goes to the Ministry of Agriculture and Land Management, Gandaki Province, for their support in providing the necessary data and valuable guidance throughout the project. Their assistance was crucial to the successful completion of our work.

REFERENCES

Faust, A., Castro-Wooldridge, V., Chitrakar, B., & Pradhan, M. (2020). *Land pooling in Nepal: From planned urban "islands" to city transformation* (ADB South Asia Working Paper Series No. 72). Asian Development Bank https://www.adb.org/publications/land-pooling-nepal

Boroushaki, S., & Malczewski, J. (2008). Implementing an extension of the analytical hierarchy process using

ordered weighted averaging operators with fuzzy quantifiers in ArcGIS. *Computers & Geosciences, 34*(4), 399–410. https://www.sciencedirect.com/science/article/pii/S0098300407001471

De Souza, F., Ochi, T., & Hosono, A. (2018). *Land readjustment: Solving urban problems through innovative approach*. JICA Research Institute. https://www.jica.go.jp/jicari/publication/booksandreports/20180228_01.html

Ministry of Agriculture, Land Management and Cooperatives, Gandaki Province. (2020). *जग्गा चक्लाबन्दी कार्यक्रम सञ्चालन मापदण्ड*, २०७७. https://molmac.gandaki.gov.np

Mishra, A., et al. (2015). Identification of suitable sites for organic farming using AHP & GIS. https://www.sciencedirect.com/science/article/pii/S1110982315000289

Saaty, T. L. (1980). *The analytic hierarchy process*. McGraw-Hill.https://www.sciencedirect.com/science/article/pii/0270025587904738

Triantaphyllou, E., & Mann, S. H. (1995). Using the analytic hierarchy process for decision making in engineering applications: Some challenges. *International Journal of Industrial Engineering: Theory, Applications and Practice, 2*(1), 35–44.

https://www.researchgate.net/publication/241416054_Using_the_analytic_hierarchy_process_for_decision_making_in_engineering_applications_Some_challenges

Wittaker, R. (1987). The analytic hierarchy process – what it is and how it is used. *European Journal of Operational Research, 30*(1), 9-26. https://www.sciencedirect.com/science/article/pii/0270025587904738

AUTHOR INFORMATION

Name	:	**Dhaka Ram Gaire**
Academic Qualification	:	BE in Geomatics Engineering
Organization	:	Environment and Geological Service
Current Designation	:	Geomatics Engineer
Work Experience	:	3 months

ASSESSING THE SPATIAL VARIATION OF AEROSOL OPTICAL DEPTH AND ITS RELATIONSHIP WITH LAND USE/LAND COVER IN KATHMANDU VALLEY, NEPAL

Dibikshya Shrestha[1], Aayush Chand[1], Prejika Thapa[1], Bibek Ojha[1]

[1]Department of Geomatics Engineering, Pashchimanchal Campus, IOE, Tribhuvan University, Nepal

jbdibikshyashrestha@gmail.com, aayushchand123321@gmail.com,

thapapreji@gmail.com, bibekojha07@gmail.com

ABSTRACT

Aerosols play a crucial role in influencing atmospheric processes, air quality, and human health. Understanding the relationship between land use/land cover (LULC) and aerosol optical depth (AOD) is essential for developing effective land management and air pollution mitigation strategies. This study investigates the spatial variation of AOD and its association with LULC in Kathmandu Valley, Nepal, during the summer season of 2023. MODIS AOD products and Landsat 8-derived indices, including the Normalized Difference Vegetation Index (NDVI), Normalized Difference Built-up Index (NDBI), and Normalized Difference Water Index (NDWI), were utilized for this purpose. Spatial analysis revealed that lower AOD values were observed over forested areas, while higher concentrations were associated with water bodies, grasslands, and built-up areas. Correlation and regression analyses confirmed a negative relationship between vegetation cover and AOD, and a positive association between built-up areas, water surfaces, and aerosol loading. The study highlights the significant influence of LULC on aerosol distribution and provides essential information for land management and air pollution mitigation strategies.

KEYWORDS: Aerosol Optical Depth, NDVI, NDBI, NDWI, LULC, Kathmandu Valley, Remote Sensing, Air Quality

1. INTRODUCTION

Aerosols, fine solid or liquid particles present within the atmosphere, have a significant influence over environmental conditions, air quality, and public health. They play a vital role in radiative forcing, affecting both local and global climatic conditions by causing variations in the balance of solar radiation (Kaufman et al., 2005; Xie & Sun, 2021). Air pollution constitutes various components, primarily including airborne particulate matter (PM) and gaseous pollutants such as ozone (O3), nitrogen dioxide (NO2), volatile organic compounds (like benzene), carbon monoxide (CO), sulfur dioxide (SO2), among others (Newby et al., 2015), (Article, 2002). Fine particulate matter, specially PM2.5, with diameter less than 2.5 micrometers, has adverse effects on human health, affecting respiratory and cardiovascular diseases. As per the World Health Organization, over seven million people annually suffer diseases related to PM2.5 exposures (WHO, 2018). So, it is important to understand the aerosol behavior and its driving factors, centrally in urbanized and rapidly developing regions where there is an increment in aerosol concentrations due to both natural and anthropogenic sources. Globally, aerosol optical depth (AOD) has been on the rise in industrialized and densely populated regions. Satellite observations and ground-based measurements indicate the increasing trends over Asia, Africa and parts of Latin America, driven by urbanization, vehicular emission. Industrial activities and biomass burning (Van Donkelaar et al., 2013).

Kathmandu Valley, Nepal, is experiencing increasing urbanization, vehicular emissions, and agricultural activities that significantly influence air quality and aerosol distribution in the surrounding atmosphere. The valley's topography, evolving weather conditions, and rapid urban development, lead to intricate aerosol trends that vary both in space and time. Various research has resulted that Aerosol Optical Depth (AOD), which is a measure of the overall concentration of aerosols in the atmosphere, is strongly influenced by land use and land cover (LULC) configurations (Li et al., 2014; He et al., 2016). Land use

changes, especially urban expansion, deforestation, and agricultural intensification have resulted to directly affect aerosol concentrations and its distribution, resulting in increasing air pollution levels (Guo et al., 2012; Xie & Sun, 2021).

Satellite-derived products such as from the Moderate Resolution Imaging Spectroradiometer (MODIS) have proved to be essential in effective monitoring of aerosols at a regional scale. MODIS derived aerosol products have proven to provide consistent, sustainable, and large-scale observations of Aerosol Optical Depth (AOD), making them useful for analyzing aerosol shifts in both time and space (Gupta et al., 2006; Levy et al., 2013). These products offer spatial resolutions of up to 1 km, which allow for more detailed urban areas analysis given their global coverage and availability over two decades, MODIS AOD data have become a standard reference for numerous air quality and urban environmental studies (Remer et al., 2005).

The Kathmandu Valley's aerosol concentrations are influenced by various factors, including urbanization, industrial emissions, and transportation. Previous studies have highlighted the spatial variability of aerosol distribution in urban areas, where dense urban environments with high built-up areas generally tend to have high aerosol concentrations (Li et al., 2014). While areas with vegetation and natural terrains generally show lower aerosol levels due to natural filtration processes (Liu, X., et al. 2018). These variations are also influenced by topography, where lower-lying areas tend to accumulate aerosols due to limited ventilation and increased atmospheric stability (Xie & Sun, 2021).

Kathmandu Valley lacks in detailed studies on AOD variations, as well in relation with LULC, so our research aims to fill this gap by investigating the relationship between aerosol concentration and land cover patterns across the valley. This study will utilize remote sensing data, specifically Landsat 8 imageries and MODIS aerosol products, to analyze the spatial variation of AOD in Kathmandu Valley during the summer of 2024. The study objectives include:

1. Monitoring the spatial variation of AOD during the summer of 2024 and identifying key patterns in aerosol concentration.
2. Quantifying the correlations between AOD values and LULC-related variables, including vegetation indices such as NDVI (Normalized Difference Vegetation Index) and NDBI (Normalized Difference Built-up Index), and NDWI (Normalized Difference Water Index).
3. Assessing the influence of urbanization, agricultural land use, and natural environments on the spatial distribution of AOD.

By understanding the relationship between LULC and AOD in Kathmandu Valley, these findings will help improve land use management, inform air quality control strategies, and ultimately support efforts to reduce aerosol-related pollution in the valley.

2. MATERIALS AND METHODS

2.1 Study Area

This Study focuses on Kathmandu Valley (Figure 1), a bowl-shaped basin in the lesser Himalayas of central Nepal, spans 933.73 km² between 27.403° N and 27.818° N latitude and 85.189° E and 85.5657° E longitude. Its valley floor averages 1,425 m above mean sea level and is enclosed by the Shivapuri (2,732 m), Phulchowki (2,695 m), Nagarjun (2,095 m), and Chandragiri (2,551 m) ranges. The Bagmati River flows through the basin, which includes the administrative districts of Kathmandu, Bhaktapur, and Lalitpur.

A subtropical continental semi-humid climate (mean annual temperature ~18.3 °C; rainfall ~1,440 mm) and the bowl-shaped topography promote pollutant accumulation from biomass burning, vehicular emissions, and construction dust. Its diverse land cover and complex terrain provide an ideal setting to examine how vegetation, urban, agricultural, and water bodies influence Aerosol Optical Depth.

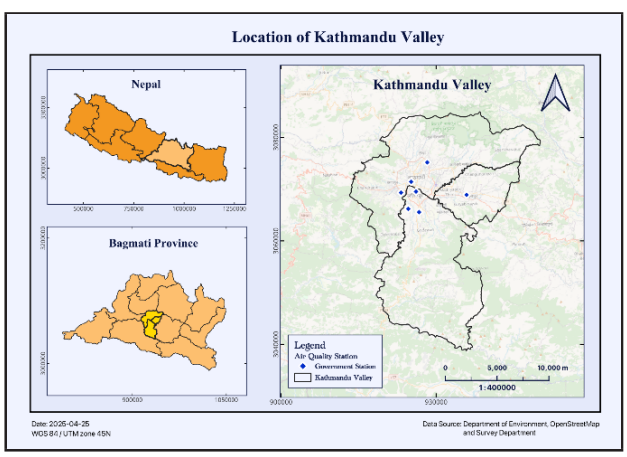

Figure 1. Location of Kathmandu Valley

2.2 Data Sources and Preprocessing

2.2.1 MODIS AOD: Processed in Google Earth Engine (GEE) by filtering the MCD19A2 granules for the Kathmandu Valley boundary and the period February 1 to July 1, 2023. We selected the Optical_Depth_055 band, applied a scale factor of 0.001, computed a seasonal mean composite, and clipped it to the study area.

2.2.2 Landsat 8 Surface Reflectance: Using GEE, Collection 2 Level-2 images with <10% cloud cover were filtered by date and region. Bands SR_B3 (Green), SR_B4 (Red), SR_B5 (NIR), and SR_B6 (SWIR1) were exported as seasonal mean rasters at 1 km resolution after compositing and reprojection to EPSG:32645.

2.2.3 Local Processing Environment: In Google Colab, we installed and imported Python packages—rasterio, numpy, pandas, geopandas, shapely, scikit-learn, matplotlib—for raster resampling, extraction, and statistical analysis after data export from GEE.

2.3 Derivation of Spectral Indices

Landsat 8 Collection 2 Level-2 images were processed in Google Earth Engine (GEE) to derive spectral indices representing vegetation, built-up structures, and surface water. These images provide surface reflectance values, which were converted using a radiometric scaling formula: applying a multiplier of 0.0000275 and an offset of –0.2 to convert raw DN values to reflectance.

Three indices were computed for each image:

- **NDVI (Normalized Difference Vegetation Index):**

  NDVI (Normalized Difference Vegetation Index) is used to assess vegetation cover based on the difference between near- infrared (NIR) and red reflectance.

  $$NDVI = (NIR - Red) / (NIR + Red) \quad (1)$$

- **NDBI (Normalized Difference Built-up Index):** NDBI (Normalized Difference Built-up Index) is used to assess built-up areas based on shortwave infrared (SWIR1) and NIR reflectance.

  $$NDBI = (SWIR1 - NIR) / (SWIR1 + NIR) \quad (2)$$

- **NDWI (Normalized Difference Water Index):**

  NDWI (Normalized Difference Water Index) is used to detect water bodies based on green and NIR reflectance.

  $$NDWI = (Green - NIR) / (Green + NIR) \quad (3)$$

In Landsat 8 Collection 2 Level-2 images, Red = SR_B4, Green = SR_B3, NIR = SR_B5, and SWIR1 = SR_B6. These indices were calculated per scene after cloud filtering and composited to create seasonal mean images that were then reprojected to 1 km resolution (EPSG:32645) and exported as GeoTIFFs for further analysis.

2.4 Data Integration and Preprocessing

All data layers were projected to EPSG:32645 and resampled to match the 30 m resolution of the LULC raster. MODIS AOD and Landsat indices were resampled using bilinear interpolation in Python. This alignment ensured pixel-level consistency for statistical correlation analysis.

2.5 Statistical Analysis

Pixel-level values of AOD, NDVI, NDBI, NDWI, and LULC were extracted and analyzed in Python. Summary statistics (mean, min, max, std. dev.) of AOD were calculated for each LULC class. Area proportions were derived using pixel counts and the known pixel area (0.0009 km² for 30m resolution). Correlation coefficients were computed between AOD and LULC-related indicators. Regression analysis was conducted to visualize and quantify the relationships between AOD and the selected indices.

3. RESULTS

3.1 Land Use/Land Cover Composition

Land use/ Land Cover were classified using the Maximum Likelihood method in ArcMap. Five classes were defined: water body, built-up areas, forest, farmland and grassland. Training samples were digitized manually. Accuracy was accessed using over 50 validation points per class via Google Earth imagery. The classification of land use/land cover revealed that grassland (27.90%), forest (25.58%), and farmland (25.00%) dominate the Kathmandu Valley, while built-up areas and water bodies occupy 20.86% and 0.66% of the total area respectively (Table 2). The spatial distribution (Figure 3) of these categories illustrates that grassland and forest areas are mainly located on the periphery, while built-up areas are concentrated in the valley core.

Table 2. Area statistics of LULC types

LULC Type	Area (km²)	Proportion (%)
Water body	6.17	0.66
Built-up areas	194.62	20.86
Forest	238.72	25.58
Farmland	233.29	25.00
Grassland	260.37	27.90

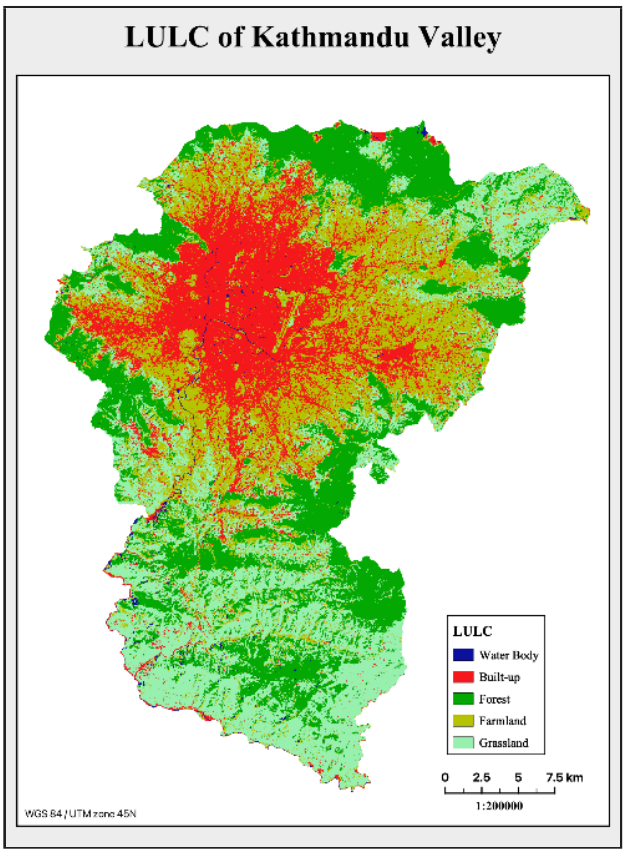

Figure 3. LULC of Kathmandu Valley

3.2 AOD Distribution by LULC Class

Analysis of mean AOD values (Table 4) highlights pronounced differences among LULC types. Water bodies record a mean AOD of 0.451 (SD = 0.051), as these low-lying surfaces trap aerosols under stable atmospheric conditions. Grasslands follow with a mean of 0.447 (SD = 0.062), reflecting dust entrainment in exposed terrains during the dry season. Built-up areas have a mean AOD of 0.441 (SD = 0.025), consistent with urban emissions from vehicles and construction activities. Farmland shows a mean of 0.433 (SD = 0.031), influenced by tillage, harvesting, and biomass burning. Forests exhibit the lowest mean AOD at 0.401 (SD = 0.048), underscoring canopy uptake and deposition processes.

Table 4. AOD statistics in different LULC type

LULC Type	Min	Max	Mean AOD	SD
Built-up areas	0.320	0.622	0.441	0.025
Farmland	0.305	0.621	0.433	0.031
Forest	0.304	0.618	0.401	0.048
Grassland	0.304	0.622	0.447	0.062
Water body	0.324	0.621	0.451	0.051

The spatial pattern (Fig. 5) demonstrates that transitional zones—particularly grassland adjacent to urban fringes and water margins—experience elevated and highly variable aerosol loading, combining natural dust sources and anthropogenic contributions. In contrast, built-up areas maintain relatively uniform AOD levels, indicative of steady emission rates. Forested corridors consistently show lower aerosol burdens, supporting their critical role as natural sinks in the valley's aerosol dynamics.

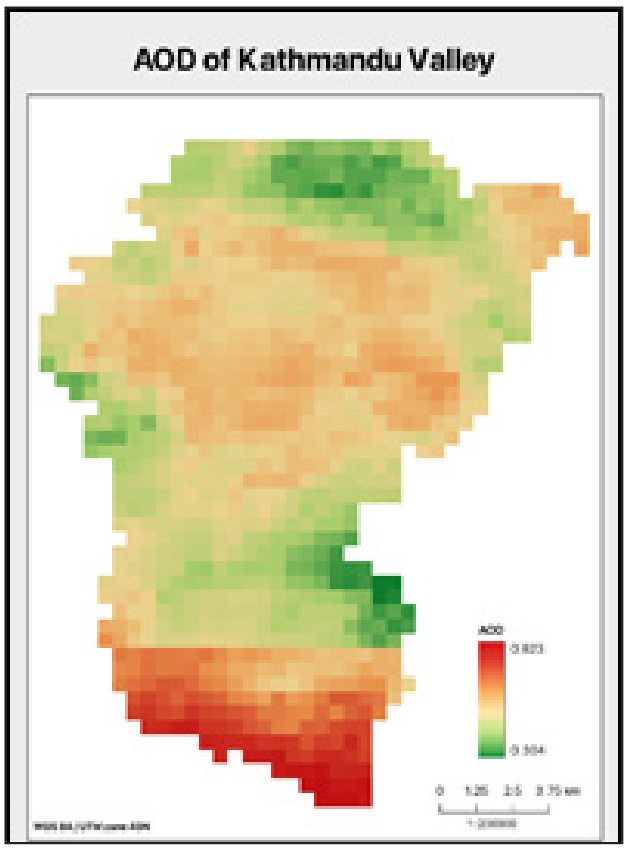

Figure 4. Spatial distribution maps of AOD

3.3 AOD and Vegetation/Built-up/Water Indices

The interaction between AOD and surface characteristics is further elucidated by comparing aerosol levels with three spectral indices (Figs. 7–9; Table 6). NDVI values above 0.5 in peripheral forests coincide with the lowest AOD readings (<0.42), illustrating the effectiveness of dense vegetation in sequestering particles. Conversely, NDBI peaks (up to 0.45) in central Kathmandu correspond to zones of elevated AOD (>0.44), highlighting urban emissions as a primary aerosol source. NDWI, though generally low (<0.2), shows localized increases near water bodies where AOD also rises, suggesting that moisture-rich areas may experience aerosol retention under stable atmospheric layers.

Quantitatively, Pearson correlations (Table 6) reveal a significant inverse relationship between AOD and NDVI (r = –0.168), affirming the noise-reduction capacity of green cover. A strong positive correlation between AOD and NDBI (r = 0.360) highlights built environments as hotspots for particulate matter. The positive although weaker correlation with NDWI (r = 0.169) points to the role of surface moisture and topographic depressions in modulating aerosol concentrations.

When examining binary LULC metrics, the proportion of forest cover (PerForest) shows the highest negative correlation with AOD (r = –0.361), while the proportion of built-up land (PerCon.) exhibits a positive correlation (r = 0.115). These results collectively demonstrate that spectral indices can serve as effective proxies for predicting spatial patterns of aerosol loading across heterogeneous landscapes.

Table 6. Correlation coefficients between AOD and LULC-related variables

Variable	AOD
NDVI	-0.168
NDBI	0.360
NDWI	0.169
PerWater	0.034
PerCon.	0.115
PerForest	-0.361
PerFarm	0.030
PerGreen	0.211

3.4 Regression Analysis

The linear regression plots illustrate the degree of relationship between AOD and NDVI, NDBI, and NDWI. AOD shows a slight negative trend with NDVI, and modest positive trends with both NDBI and NDWI. These trends visually support the statistical outcomes of the Pearson correlation analysis, providing intuitive evidence that dense vegetation helps lower AOD, while built-up and lowland water-prone regions may accumulate aerosols.

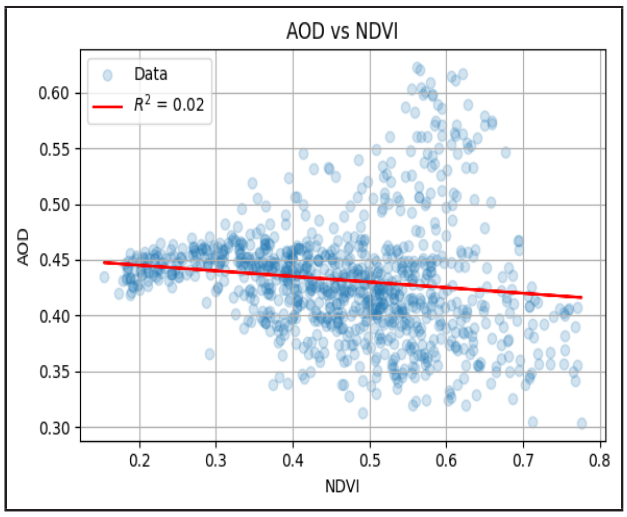

Figure 10. Regression plot of AOD vs NDVI

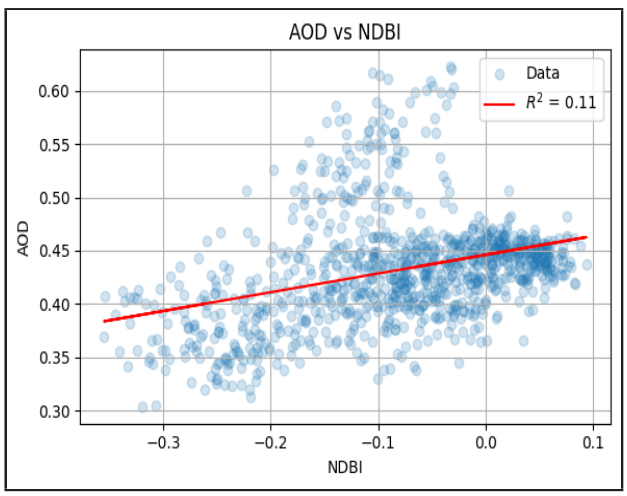

Figure 11. Regression plot of AOD vs NDBI

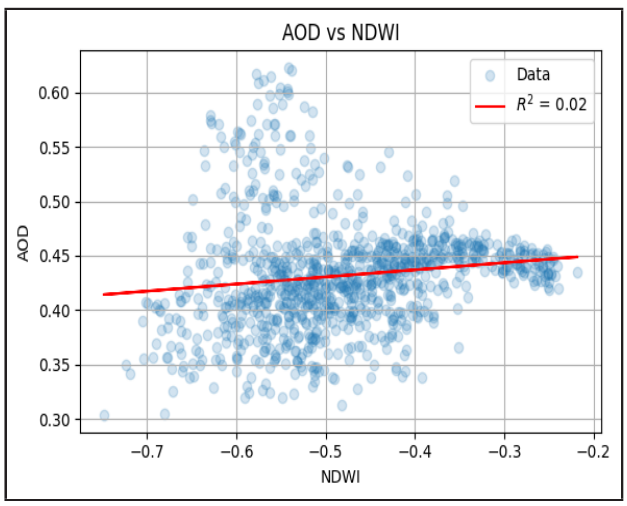

Figure 12 Regression plot of AOD vs NDWI

4. DISCUSSION

The spatial variation of Aerosol Optical Depth (AOD) in Kathmandu Valley from February to July 2023 reflects the influence of land use and land cover (LULC) on aerosol concentrations. Mean AOD values ranged from 0.401 in forested areas to 0.451 over water bodies, indicating moderate aerosol loading. A low overall standard deviation (0.0536) suggests relatively consistent spatial distribution despite varying terrain and land cover.

Vegetated areas such as forests recorded the lowest AOD levels, supported by negative correlations with NDVI (−0.127) and PerForest (−0.217), indicating that dense vegetation helps reduce aerosol concentrations through natural filtration and dry deposition (Liu et al., 2018). In contrast, built-up areas exhibited higher AOD values, with Built-up areas and NDBI showing positive correlations (0.115 and 0.337, respectively), highlighting the impact of urbanization and human activities like traffic and construction on air pollution.

Interestingly, water bodies showed relatively high mean AOD and the largest variability (standard deviation 0.078), likely due to their low-lying locations that favor aerosol entrapment. The weak positive correlation with NDWI (0.133) may also reflect influences of topography and atmospheric stability.

Agricultural lands showed a notable aerosol presence, with a mean AOD of 0.433 and the highest correlation (0.218) among all LULC types. This is likely linked to seasonal agricultural practices such as tilling, harvesting, and biomass burning during the pre-monsoon period.

While these findings underscore the role of LULC in aerosol distribution—with vegetation acting as a mitigating factor and urban/agricultural areas contributing to higher concentrations—there are notable limitations. The use of seasonal averages may mask short-term variations in AOD, and the MODIS AOD product's coarse resolution could reduce accuracy when matched with finer-scale Landsat-based indices. Furthermore, the absence of meteorological data such as wind speed, temperature, or humidity limits understanding of aerosol dispersion dynamics.

Future research should incorporate higher temporal resolution data, integrate meteorological parameters, and validate findings with ground-based air quality monitoring to enhance reliability and policy relevance.

5. CONCLUSION

By integrating MODIS AOD products with Landsat-derived NDVI, NDBI, and NDWI indices, this study has clearly demonstrated that land cover types exert significant control over aerosol loading in Kathmandu Valley. Forested areas recorded the lowest mean AOD (0.401), underscoring the efficacy of dense vegetation in removing particles, while grasslands and water bodies exhibited the highest levels (0.447 and 0.451, respectively) due to surface dust entrainment and topographic trapping. Built-up zones showed consistently elevated AOD (0.441), highlighting urban emissions as key contributors to poor air quality. Correlation and regression analyses of AOD (r = –0.168 for NDVI; r = 0.360 for NDBI; r = 0.169 for NDWI) reinforce these spatial patterns.

Although the use of seasonal composites and resampled rasters may obscure short-term dynamics, and the exclusion of meteorological variables limits dispersion insights, the robust relationships observed advocate for nature-based solutions and targeted land use policies. Specifically, expanding urban green corridors, controlling construction dust, and protecting remaining forest patches can help mitigate aerosol pollution. Future work should integrate in-situ air quality measurements, high-frequency satellite observations, and local meteorological data to refine temporal analyses and extend the methodology beyond Kathmandu Valley for national-scale air quality management.

REFERENCES

Guo, J., Zhang, X., Che, H., Gong, S., An, X., Cao, C., ... & Zhang, W. (2012). Spatial and temporal variations of aerosol optical depth and their correlation with influencing factors over central China. *Atmospheric Research*, *104–105*, 96–106. https://doi.org/10.1016/j.atmosres.2012.01.011

He, Y., Xu, H., Sun, Z., Zhang, Y., Wang, Y., & Gu, J. (2016). Spatiotemporal variations of aerosol optical depth in relation to land use and socio-economic factors. *Science of The Total Environment*,*568*,689–699. https://doi.org/10.1016/j.scitotenv.2016.06.152

Kaufman, Y. J., Tanré, D., Remer, L. A., Vermote, E. F., Chu, A., & Holben, B. N. (2005). The effect of aerosol particles on the radiation budget of the Earth and the implications for climate change. *Atmospheric Environment*, *39*(1), 1–8. https://doi.org/10.1016/j.atmosenv.2004.09.027

Li, Y., Wang, Y., Wang, J., & Wang, X. (2014). Aerosol optical depth and its relation to land use/land cover in urban areas. *Atmospheric Environment*, *94*, 547–555. https://doi.org/10.1016/j.atmosenv.2014.06.009

Newby, D. E., Mannucci, P. M., Tell, G. S., Baccarelli, A. A., Brook, R. D., Donaldson, K., ... & Mills, N. L. (2015). Expert position paper on air pollution and cardiovascular disease. *European Heart Journal*, *36*(2), 83–93. https://doi.org/10.1093/eurheartj/ehu458

van Donkelaar, A., Martin, R. V., Spurr, R. J. D., Drury, E., Remer, L. A., Levy, R. C., & Wang, J. (2013). Optimal estimation for global ground-level fine particulate matter concentrations. *Journal of Geophysical Research: Atmospheres*, *118*(11), 5621–5636. https://doi.org/10.1002/jgrd.50479

World Health Organization. (2018). *Ambient (outdoor) air quality and health*. https://www.who.int/news-room/fact-sheets/detail/ambient-(outdoor)-air-quality-and-health

Xie, Q., & Sun, Q. (2021). Monitoring the spatial variation of aerosol optical depth and its correlation with land use/land cover in Wuhan, China: A perspective of urban planning. *International Journal of Environmental Research and Public Health*, *18*(3), 1132. https://doi.org/10.3390/ijerph18031132

Article, O. (2002). Personal exposure monitoring of particulate matter, nitrogen dioxide, and carbon monoxide, including susceptible groups. *[Journal Name]*, *[Volume(Issue)]*, 671–679.

AUTHOR INFORMATION

Name : **Dibikshya Shrestha**

Academic Qualification : BE in Geomatics Engineering

Organization : IT Maps

Current Designation : Intern

ASSESSMENT OF LANDSAT-8 AND SENTINEL-2 IMAGERY FOR ESTIMATION OF ABOVEGROUND BIOMASS AND CARBON STOCKS IN CHURE FORESTS OF NEPAL

Er. Bhagirath Bhatt [1], Upama Ashish Koju [2], Reshma Shrestha[3]

[1]Land Management Training Centre, Nepal – *bhagirath.bhatt@nepal.gov.np*

[2] Forest Action Nepal – *upamakoju@gmail.com*

[3] Kathmandu University – *reshma@ku.edu.np*

ABSTRACT

Forests play a crucial role in global carbon cycles and biodiversity conservation. Quantifying forest aboveground biomass (FAGB) helps in assessing carbon emission and sequestration and can reduce uncertainty in monitoring global carbon cycles and climate change. Remote sensing techniques have proved to be a cost-effective way to estimate FAGB with timely and repeated observations and recommended by United Nations Framework on Climate Change (UNFCC) to assess FAGB and carbon stock for Reduction of Emissions from Degradation and Deforestation Program (REDD+). This research presents an assessment of freely available Landsat-8 and Sentinel-2 imagery for estimating FAGB in the Chure forests of Nepal using Multiple Regression Analysis. Sentinel-2 and Landsat 8 missions are similar, but Sentinel-2 has higher spatial resolution and collects data from the red-edge region of the electromagnetic spectrum while Landsat has one of the largest temporal ranges of imagery range from 1970s. Twelve variables derived from Landsat-8 and fifteen variables derived from Sentinel-2 imageries were used in the study. Forest inventory data of 225 plots collected by the Forest Research and Training Centre (FRTC) in 2017 and 2018 through field measurements, were used to train and validate the model. The correlation of FAGB measured in each plot and variables extracted from the Landsat-8 and Sentinel-2 optical imageries were assessed by the Pearson correlation coefficients. Multiple Linear Regression was applied based on chosen variables to develop the models for estimating FAGB for the whole study area. The R-squared values of 0.78 and 0.68 and standard error of estimate 45.98 and 40.29 were obtained respectively for the Sentinel-2 and Landsat-8 based estimation models. The estimated results were validated by considering R^2 and RMSE values between observed and estimated FAGB. The values of R^2 and RMSE between observed and estimated FAGB were 0.70 and 45.02 tons/ha and 0.77 and 34.33 tons/ha for Landsat-8 and Sentinel-2 images respectively. The results of the study showed that both Sentinel-2 and Landsat-8 imageries are viable for FAGB and carbon stocks estimation. However, with high R2 and low RMSE value Sentinel-2 based model outperforms the Landsat-8 based model and it seems to be better suited for FAGB estimation in Chure area for the studied year. Overall, the research highlights the potential of Sentinel-2 and Landsat-8 imagery for FAGB estimation and emphasizes the importance of utilizing multi-source data and advanced modelling techniques for accurate and reliable FAGB mapping. The study also revealed that Chure forests are of considerable significance as they store substantial amounts of carbon despite disturbance from different anthropogenic activities.

KEYWORDS: Forest Above Ground Biomass, Landsat-8 Imagery, Sentinel-2 imagery, Carbon stock, Chure Forests, Vegetation Indices, Multiple Regression Analysis

1. INTRODUCTION

Climate change is a critical issue that the world is currently facing(Shrestha et al., 2025). The main cause of this problem is changes in land use due to increased human activities such as deforestation, burning fossil fuels, and expanding industries(Ning et al., 2023). These activities result in high levels of carbon dioxide (CO_2) in the atmosphere, along with other greenhouse gases (GHG), which trap thermal energy(Nunes, 2023). This global warming phenomenon causes climate change and, as a result, can lead to natural disasters such as earthquakes, floods, droughts, wildfires, high temperatures, and other related events(Hassan, 2024). Forests play a crucial role in mitigating atmospheric CO_2 levels(Alkama & Cescatti, 2016; Psistaki et al., 2024)

Approximately 40% of the Earth's terrestrial carbon is stored in tropical rainforests, making them a significant contributor to the global carbon cycle (Mauya et al., 2015). However, rapid deforestation threatens this vital function, resulting in 12-20% of total anthropogenic CO_2 emissions despite their ecological importance (Collins, 2015). The United Nations Framework Convention on Climate Change (UNFCCC) had introduced an initiative named the Reduction of Emissions from Degradation and Deforestation Program (REDD+) which provides financial incentives to developing countries to conserve and manage forests in their countries that effectively reduce emissions resulting from anthropogenic activities (Mermoz et al., 2015). Such initiatives require transparent, comprehensive, steady, comparable, and precise national and subnational measurement, reporting, and verification (MRV) systems to monitor and evaluate the forest biomass /carbon stock and the resulting carbon emissions (Lallo et al., 2017).

Forest above-ground biomass (FAGB) represents the largest carbon pool in forest ecosystems (Güneralp et al., 2014). However, human activities such as deforestation can lead to a reduction in forest area, which can cause the deterioration of the FAGB, carbon stock (CS), which not only diminishes CO_2 sequestration but also results in the release of stored carbon back into the atmosphere thereby, aiding to the global warming (Chinembiri et al., 2013). Precise measurement of FAGB is essential for effective forest management, climate change mitigation through REDD+, sustainable forest management, and efforts to conserve and enhance forest carbon stocks. Therefore, it is essential to rapidly and accurately estimate and monitor FAGB across diverse spatial and temporal scales. This is crucial for significantly reducing uncertainties in carbon stock assessments and providing valuable insights for strategic forest management plans (Pan et al., 2013).

Nepal possesses abundant forest resources, covering around 44.74 % of its total land area, equivalent to 6.2 million hectares (DFRS, 2018). According to a report by the Food and Agriculture Organization (FAO) in 2015, the estimated amount of living biomass in Nepalese forests was 484 million tons. This comprises 359 million tons of FAGB and 126 million tons of below-ground biomass (BGB). However, these figures are presented at a national scale and lack the necessary granularity for effective planning (FAO, 2015).

In general, FAGB can be estimated through three available methods: model-based simulations, measurements from traditional ground inventories, and retrievals from remote-sensing datasets(Su et al., 2016). Model-based simulation methods usually provide FAGB estimations from local to global scales based on model inputs (e.g., radiation, climate surfaces, and elevations) instead of the actual FAGB distribution (Li et al., 2022). Traditional forest inventory methods (e.g., direct harvest methods and indirect allometric modelling methods) can provide reliable information on biomass at local or regional scales (Torre-Tojal et al., 2022). However, taking ground measurements is labor- intensive and expensive when used for large areas, and is time-consuming for a nationwide forest survey. Compared with the forest inventory approach, remote-sensing techniques significantly improve the efficiency of FAGB mapping in large areas and areas that are difficult to access (Ehlers et al., 2022). By linking with ground inventory data, FAGB can be estimated from remote sensing datasets using statistical models. Typically, passive optical remote sensing [e.g., Moderate Resolution Imaging Spectroradiometer (MODIS) of 250m resolution, Landsat Thematic Mapper (TM) of 30m resolution and radar techniques [e.g., phased array L-band synthetic aperture radar (PALSAR) of 10m resolution and Shuttle Radar Topography Mission (SRTM) of 30m resolution] have become primary data sources for estimating FAGB, because of their availability(Su et al., 2016).

In the past three decades, Landsat images have been mostly used for forest AGB estimation mainly because of the freely accessible long archive images with medium spatial resolution (Nguyen et al., 2020). Landsat 8 is a multispectral imagery with medium spatial resolution which is one of the most suitable open-source sensors for extracting land cover and forestry applications. Landsat 8 has a fine spectral resolution, high resolution (15 meters) in the panchromatic band, 30 meters in multispectral imagery, and a radiometric resolution of 12 bits (Ke et al., 2015). Karlson (2015) evaluated the utility of Landsat images in Sudano-Sahelian Woodlands for Tree Canopy Cover and biomass assessment. Gizachew et. al. (2016) reported that applications of Landsat satellite products are boundless and are used most extensively for biomass and vegetation analysis due to their free data availability, spatial coverage, and high temporal resolution. Many previous studies have used Landsat products for biomass estimation by developing relationships between field

data and different vegetation indices (Ou et al., 2019; Priatama et al., 2022; Turgut & Günlü, 2022; Zhang et al., 2023). Many researchers worked on Landsat data and explored the behavior of various spectral indices such as the Normalized Difference Vegetation Index (NDVI), Enhanced Vegetation Index (EVI), Soil Adjusted Vegetation Index (SAVI), and Modified Soil Adjusted Vegetation Index (MSAVI) (Imran & Ahmed, 2018a; Qiu et al., 2020; Tang et al., 2022).

Sentinel-2 is a polar-orbiting satellite equipped with a multi-spectral instrument, MSI sensor, launched on 23 June 2015 by the European Space Agency (ESA), provides a significant improvement in spectral coverage, spatial resolution, and temporal frequency over the current generation of Landsat sensors(Castro Gómez, 2017). The spectral configuration of Sentinel-2 is comparable to some commercial satellite data, such as Worldview-2 and RapidEye, because of the presence of the red-edge band, but is further improved by incorporating shortwave infrared bands (SWIR). The unique characteristics of Sentinel-2 as compared to commercial satellites is the only inclusion of the red edge band, which is important for vegetation assessment and monitoring (Ramoelo et al., 2015).

While various studies have highlighted the utility of both Sentinel-2 and Landsat-8 data for forest assessments across diverse ecosystems, there exists a critical knowledge gap regarding their comparative effectiveness in estimating forest aboveground biomass and carbon stocks in the distinctive context of Nepal's Chure Forests. The Chure region is characterized by its ecological complexity, ranging from subtropical to temperate forests, and is located at the foothills of the Himalayas. These forests are essential components of Nepal's landscape, influencing climate regulation, water resources, and biodiversity conservation. However, they are also vulnerable to anthropogenic pressures such as deforestation, land use changes, and degradation.

This research aims to bridge the aforementioned research gap by conducting a comprehensive assessment of Landsat-8 and Sentinel-2 imageries for estimating forest aboveground biomass and carbon stocks within the Chure Forests of Nepal. This study uses multiple regression analysis techniques to derive the relationships between variables derived from Landsat-8 and Sentinel-2 imageries and FAGB calculated from field plots and hence calculates FAGB and carbon stocks in the entire region. By exploring the capabilities of these satellite imageries, this study provides insights into their applicability, accuracy, and limitations in this unique forest ecosystem. The findings of this study will contribute valuable information to guide forest management strategies, inform policy decisions, and support Nepal's commitment to sustainable development and climate change mitigation.

2. MATERIALS AND METHODS

2.1 Study Area

The study was conducted in the Chure region of Nepal. The geographical location of the study area is 80° 09' 25"E to 88° 11' 16"E longitude and 26° 37' 47"N to 29° 10' 27"N latitude (Subedi et al., 2022) as illustrated in Figure 1. The area of the Chure region is about 1,898,263 hectares and occupies 12.80% of the area of the entire country (DFRS, 2014; Thapa et al., 2023). It extends in an east-west direction, covering 37 of the 77 districts in the country. Forests cover the highest proportion of the total area of the Chure region (72.37%; 1,373,743 ha) (DFRS, 2014). The study area has a typical tropical forest with undulating topography. Major species of this region are Sal, Pine, Khair, and Sissoo (DFRS, 2014a). The Chure region has a sub-tropical to warm temperate climate that is characterized by hot and sub-humid summers, intense monsoon rain, and cold dry winters (DFRS, 2014). The average annual minimum temperature in this region ranges from 12°C to 19°C, while the average annual maximum temperature ranges from 22°C to 30°C (DFRS, 2014). The precipitation pattern in the Chure region is variable, with the highest annual rainfall occurring in the Koshi and Bagmati provinces. The total annual rainfall varies from a minimum of 1,138 mm to a maximum of 2,671 mm (DFRS, 2014b).

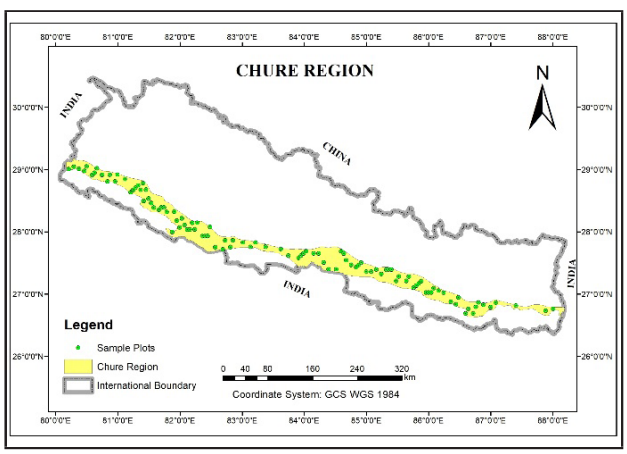

Figure 1. Study Area Map

2.2 Data and Software

The study utilized two types of secondary data - satellite imagery and forest inventory data. The multitemporal time series of Landsat-8 and Sentinel-2 images from 2017 to 2019 were obtained from Google Earth Engine (GEE). The multitemporal time series data were used as the data over whole Chure region was collected during this time period. Further, the multitemporal time series image helps to minimize the errors due to the effect of cloud and shadows in individual images (Chen et al., 2021; Qi et al., 2022). Forest cover map of ESA was used for masking the forest area. In addition, the Forest Research and Training Centre (FRTC) provided forest inventory data for field sample plots. This data included information on tree height and Diameter Breast Height (DBH), which allowed for the calculation of FAGB for the sample plots. More details on the satellite images used are given in Table 1.

Table 1. Specifications for Satellite Imagery

SN	Satellite Image	Number of Bands Used	Spatial Resolution (m)	Cloud Cover (%)	Time
1.	Landsat-8	2,3,4,5,6,7	30m	Less than 3 %	Multitemporal (2017 to 2019)
2.	Sentinel-2	2,3,4,5,6,7,8	10m and 20m	Less than 3 %	Multitemporal (2017 to 2019)

Table 2 shows the software and tools used for image download, processing, analysis and mapping.

Table 2. Software and Tools Used in the Study

Software/Platform	Purpose
Google Earth Engine	For image download, image processing and extracting vegetation indices
QGIS	Mapping and Analysis
SPSS	For Statistical Analysis

2.3 Methods

The amount of FAGB and carbon stocks in the study area were estimated and mapped using field data and information from remote sensing data, particularly Landsat-8 and Sentinel-2 imagery. The imagery was obtained from GEE, and its pre-processing and processing were also performed in GEE.

Vegetation indices such as NDVI, EVI, GDVI, GNDVI, NDWI, RGR, SAVI, and SLAVI and Tasselled Cap Brightness, Greenness and Wetness indices were derived from Landsat 8 image. The vegetation indices derived from the Sentinel-2 image were NDVI, EVI, GDVI, GNDVI, IRECI, RGR, SAVI, NDI45, SR, Red Edge 1 NDVI, Red Edge 2 NDVI and Red Edge 3 NDVI and Tasselled Cap Brightness, Greenness and Wetness indices.

First, the statistical correlation tests were performed between FAGB and variables derived from Landsat-8 and Sentinel-2 imagery. The variables combination that had a high coefficient of determination and low standard error of estimate were selected as the final estimation variables. Further, variables with high multicollinearity were excluded to ensure the most accurate and reliable results. Models were developed for each of the imageries, i.e., Landsat-8 and Sentinel-2, by considering the coefficient of selected variables and constant values from multiple linear regression analysis. The developed model was used to estimate the productivity of FAGB and carbon stocks in the study area. Figure 2 presents summary of the methodology adopted for the estimation of FAGB in the study area.

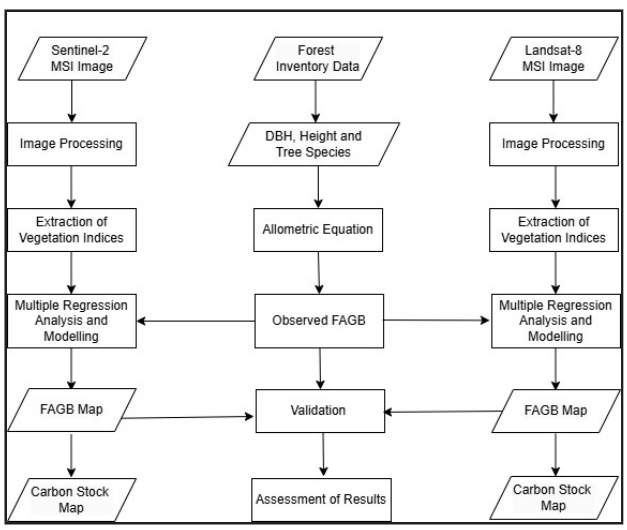

Figure 2. Methodological flowchart of Study

2.3.1 Image Pre-processing: Landsat-8 and Sentinel-2 atmospherically corrected surface reflectance imageries were pre-processed and processed in GEE. The pre-processing of image included masking out cloud and cloud shadows, masking saturated pixels and scaling the bands. The resolution of all Landsat-8 bands was 30m while bands of 10m and 20m were used in case of Sentinel-2 image. The 10m resolution bands were resampled to 20m before analysis to maintain consistency in data. The image was clipped to the shape of the study area.

2.3.2 Vegetation Indices: The vegetation indices layers were derived using pre-processed Landsat-8 and Sentinel-2 bands in GEE. Twelve indices were selected based on their performance in previous studies (Koju et al., 2019; Nguyen et al., 2020; Tian et al., 2023). Table 8 shows all the vegetation indices derived from Landsat-8 bands.

Table 3. Landsat 8 Bands, Vegetation Indices and Tasselled Cap Indices

Estimation Variables	Formula/Description	Reference
Vegetation Indices		
NDVI	(B5-B4)/(B5+B4)	(Pettorelli et al., 2005)
RGR	B4/B3	(Sims & Gamon, 2002)
GDVI	$(B5^2- B4^2)/(B5^2+ B4^2)$	(Karlson et al., 2015)
GNDVI	(B5- B3) / (B5+ B3)	(Wang et al., 2007)
EVI	{2.5*(B5-B4)}/{B5+(6*B4-7.5* B2) +1}	(Hasanah et al., 2020)
SAVI	1.5*(B5 - B4)/(B5 + B4+0.5)	(Huete, 1988)
SR	B5/ B4	(Bannari et al., 1995)
NDWI	(B5- B7)/(B5+ B7)	(Jackson et al., 2004)
SLAVI	B5/(B4+ B7)	(Karlson et al., 2015)
Tasseled Cap Indices		(Samarawickrama et al., 2017)
Brightness		
(0.3029 * B2) + (0.2786 * B3) + (0.4733 * B4) + (0.5599 * B5) + (0.5080 * B6) + (0.1872 * B7)		
Wetness		
(0.151 * B3) + (0.197 * B4) – (0.328 * B5) + (0.340 * B6) – (0.711 * B7)		
Greenness		
(0.6685 * B4) – (0.2848 * B3) – (0.0002 * B5) – (0.0721 * B6) – (0.5020 * B7)		

Table 4. Sentinel-2 Bands, Vegetation Indices and Tasselled Cap Indices

Estimation Variables	Formula/Description	Reference
Vegetation Indices		
NDVI	(B8-B4)/(B8+B4)	(Gitelson & Merzlyak, 1997)
RGR	B4/B3	(Sims & Gamon, 2002)
NDI45	(B5-B4)/B5+B4)	(Frampton et al., 2013)
GDVI	$(B8^2-B4^2)/(B8^2+B4^2)$	(Karlson et al., 2015)
GNDVI	(B8-B3)/(B8+B3)	(Wang et al., 2007)
IRECI	(B7-B4)/(B5/B6)	(Frampton et al., 2013)
EVI	{2.5*(B8-B4)}/{B8+(6*B4-7.5*B2) +1}	(Hasanah et al., 2020)
SAVI	1.5*(B8-B4)/(B8+B4+0.5)	(Karlson et al., 2015)
SR	B8/B4	(Karlson et al., 2015)
RE1 NDVI	(B8-B5)/(B8+B5)	(Fernández-Manso et al., 2016)
RE2 NDVI	(B8-B6)/(B8+B6)	
RE3 NDVI	(B8-B7)/(B8+B7)	
Tasseled Cap Indices		(Samarawickrama et al., 2017)
Brightness		
(0.3029 * B2) + (0.2786 * B3) + (0.4733 * B4) + (0.5599 * B8) + (0.5080 * B11) + (0.1872 * B12)		
Wetness		
(0.151 * B3) + (0.197 * B4) –(0.328 * B8) + (0.340 * B11) – (0.711 * B12)		
Greenness		
(0.6685 * B4) – (0.2848 * B3) – (0.0002 * B8) – (0.0721 * B11) – (0.5020 * B12)		

2.3.3 Extract Pixel Values of Explanatory Variables

The pixel values for each variable derived from Landsat-8 and Sentinel-2 were extracted in GEE and exported in CSV format. The field plot locations (latitude, longitude) were used as a reference while extracting the values of indices. The value of the indices within the radii of 20m was taken into consideration to maintain consistency with FAGB values of ground sample plots. Buffer of 20m radius was created for each point representing the plot locations. The minimum, maximum and mean values of indices within the plot were extracted. But the mean values of indices were used as it produced results with highest accuracy.

2.3.4 Statistical Analysis

Statistical analysis was carried out using SPSS software. Correlation analyses were made before model development to know the relation between estimation variables and observed FAGB. The relation between independent variables(indices) and dependent variable (observed FAGB) was assessed based on the value of correlation coefficient. Further, scatter plot was made between each of the independent variables (indices) and dependent variable (observed FAGB). Multicollinearity between variables was tested based on the tolerance value, Eigen value and Variation Inflation Factor (VIF). The variables with tolerance value greater than 0.2 and VIF less than 5 were chosen for the multiple linear regression and variables not satisfying the condition were excluded from the analysis (Shrestha, 2020; Tranmer et al., 2020).

2.3.5 Model Development using Regression Analysis

The objective of regression analysis is to quantify the relationship between a dependent variable and one or more independent variables (Shrestha, 2020). Regression implies a cause-and-effect relationship in which a change in the value of an independent variable will result in an expected average change in the dependent variable. The quantitative relationship is expressed by an equation and its graphic representation. The square value of the correlation coefficient (R^2) is called the coefficient of determination. It can be interpreted as indicating the percentage of variation in one variable that is associated with other variables.

Multiple Linear regression models were developed on SPSS software to assess the relationship between each VIs and observed FAGB. The model was evaluated based on the values of coefficient of determination (R2) and standard error of estimate. The best model was developed by integrating those variables with high R2 and a lower standard error value. The equation obtained from the multiple linear regression model was then used to estimate FAGB. The R2 was preferred since it has a standard measure with values ranging from 0 to 1. The R2 also shows the percentage of the variability explained by the model. Thus, making it easy to understand the relationship between the independent and dependent variables (Ji & Peters, 2007). The equation obtained from the multiple regression model was then used to estimate FAGB.

2.3.6 Validation of Estimated FAGB

The FAGB estimated from the developed model was validated by using validation data comprising of FAGB of ground sample plots. Observed FAGB of 33 plots was used for validation of the results. RMSE between observed and estimated FAGB was computed to determine the effectiveness of the models by using the formula given in Equation 1. A model with low RMSE error is considered suitable for FAGB prediction.

$$RMSE = \sqrt{\sum_{i=1}^{n}(FAGB_o - FAGB_e)^2/n} \quad 1$$

where, $FAGB_o$ is Observed FAGB Value (Dependent Variable), $FAGB_e$ is estimated FAGB Value (Independent Variable), n is number of samples.

3. RESULTS AND DISCUSSION

3.1 Observed FAGB

Based on field data different tree species were found in the forest. Altogether data of 225 plots were used for the study. There were 44 trees on average on a plot of 1256.63 m2. The maximum number of trees recorded was 136 and the minimum was 8. Similarly, the average tree height was 12m with a maximum of 43 m and a minimum was 4 m. From the observed field data, an average FAGB of 209.73 tons/ha, a minimum FAGB of 27.77 tons/ha and, the maximum FAGB OF 402.15 tons/ha was found. The descriptive statistics of the field plot data is given in Table 5.

Table 5: Descriptive Statistics of Observed FAGB

No. of Plots	Mean	Minimum	Maximum	Standard Deviation
225	209.73	27.77	402.15	80.04

3.2 Model Development for FAGB Prediction

3.2.1 Model Development for FAGB Estimation using Landsat-8 Variables: The model was developed using SPSS software based on variables that have a good correlation with the observed FAGB using multiple regression analysis. The estimation model has an R^2 value of 0.68 and the standard error of the estimate was 45.98. Only two variables were selected to develop the model and others were excluded due to multicollinearity. A multicollinearity test was done and variables having multicollinearity effect were discarded by the model based on the values of Variation Inflation Factor (VIF), tolerance values, and eigen values (Shrestha, 2020; Tranmer et al., 2020). The estimation variables selected for model development are NDVI and Greenness. Many studies have found that NDVI and Greenness have good correlation with FAGB and are the most important estimation variables for FAGB estimation (Dube & Mutanga, 2015; Imran & Ahmed, 2018; Koju et al., 2019; Turgut & Günlü, 2022). The results of the multiple regression analysis are shown in Table 11 and Table 12. The evaluation metrics of the estimated model are consistent with the study by Koju et. al. 2019 in which the R^2 value of the models for FAGB estimation ranged from 0.65 to 0.72 (Koju & Zhang, 2019).

3.2.2 Model Development for FAGB Estimation using Sentinel-2 Variables:

The model was developed using SPSS software based on variables that have a good correlation with the observed FAGB using multiple regression analysis. The estimation model has an R^2, adjusted R^2, and standard error of estimate values of 0.78, 0.77, and 40.29 respectively. Only five variables were selected to develop the model and others were excluded because of their lower coefficient of determination values and multicollinearity. The process of the multicollinearity test was similar to the one mentioned in section 4.3.1 (Shrestha, 2020; Tranmer et al., 2020). The variables selected for model development are Red to Green Ratio, NDVI, RE3NDVI, Greenness, and Brightness. The results of multiple regression analysis are shown in Table 13 and Table 14. The measures of assessment for the estimation model comply with the research done by Singh et. al. 2023 in Sal Forest of Western Terai, Nepal where the R^2 value of the estimation models ranged from 0.72 to 0.77 for different estimation variables (Singh et al., 2023).

3.3 Mapping FAGB and Carbon Stock

3.3.1 Mapping FAGB and Carbon Stock Using Landsat-8 Model

The estimated FAGB map was produced by using equation 2 obtained from multiple regression analysis.

$$FAGB_{L8} = 603.292*NDVI + 1346.431*Greenness - 146.167 \quad 2$$

The forest area extracted from the land cover map was considered (ESA, 2019). The estimated FAGB map for the study area is shown in Figure 3. From the FAGB distribution in the map, it can be seen that over the area the FAGB was mostly from 100 to 300 tons/ha. However, in some areas that are close to built-up and agricultural areas, the FAGB of less than 100 tons/ha was found due to anthropogenic activity. In a few areas with dense forest which are far from anthropogenic activities and difficult to access, an FAGB of greater than 300 tons/ha was found. An average FAGB of 219.55 tons/ha was found in the study area.

Finally, a carbon stock map was produced by multiplying FAGB with carbon conversion factor of 0.47 (IPCC, 2003). Figure 4 presents the map of carbon stocks calculated from the FAGB map. Because this map was produced based on FAGB, it has a similar trend in the carbon stocks distribution. The area that has difficulties in accessibility has the largest carbon stocks with the amount higher than 150 tons/ha. The carbon stocks with the amount of less than 50 tons/ha were found in the easily accessible area that was near the road and other land cover types.

3.3.2 Mapping FAGB and Carbon Stock using Sentinel-2 Model

The estimated FAGB map was produced by using equation 3 obtained from multiple regression analysis.

$$FAGB_{S2}=634.846*NDVI-348.090*RE3NDVI-69.298*RGR+150.578*BRIGHTNESS+902.941*GREENNESS-74.685 \quad 3$$

The forest area extracted from the land cover map was considered (ESA, 2019). The estimated FAGB map for the study area is shown in Figure 5. From the FAGB distribution in the map, it can be seen that over the area the FAGB was mostly from 100 to 300 tons/ha. However, in some areas that are close to built-up and agricultural areas the FAGB of less than 100 tons/ha was found due to anthropogenic activity. In a few areas with dense forests which are far from anthropogenic activities and difficult to access, an FAGB of greater than 300 tons/ha was found. An average FAGB of 212.96 tons/ha was found in the study area.

Finally, a carbon stock map was produced by multiplying FAGB with the carbon conversion factor of 0.47 (IPCC, 2003). Figure 6 presents the map of carbon stocks in the forest calculated from the FAGB map. Because this map was produced based on FAGB, it has a similar trend in the carbon stocks distribution.

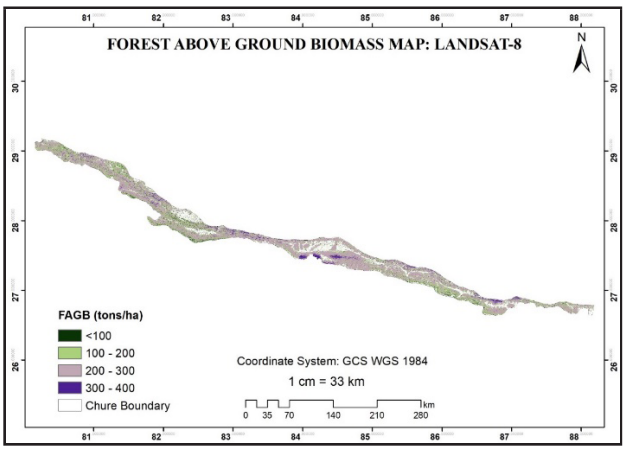

Figure 3. FAGB Map of Chure Forests using Landsat-8 Model

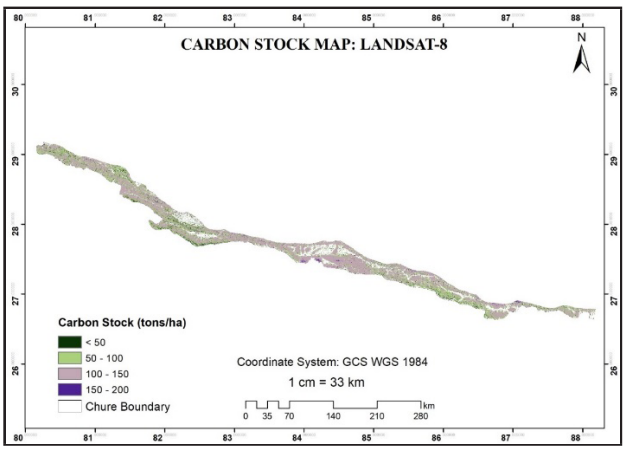

Figure 4. Carbon Stock Map of Chure Forests Based on Landsat-8 Model

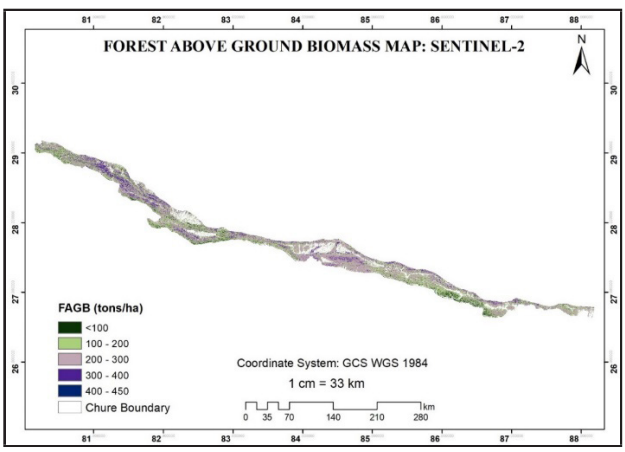

Figure 5. FAGB Map of Chure Forests using Sentinel-2 Model

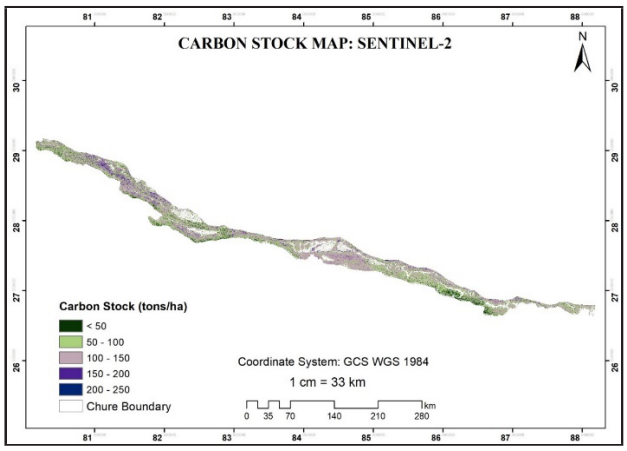

Figure 6. Carbon Stock Map of Chure Forests Based on Sentinel-2 Model

3.4 Validation of Estimated FAGB

3.4.1 Validation of FAGB Estimated from Landsat-8 Explanatory Variables: 15% of total sample plots i.e., 33 plots were used for validation of the estimated FAGB from the model. Estimated FAGB for these thirty-three plots were extracted and correlated with observed FAGB. The dependent (observed FAGB) and independent (estimated FAGB) variables have a good correlation with coefficient of determination 0.70 indicating approximately 70% of the observed FAGB is explained by the estimated FAGB. Since they have a good correlation, it was selected to map the final FAGB and carbon stock. The scatter plot diagram of estimated FAGB versus observed FAGB is shown in Figure 7. The RMSE error between observed and estimated FAGB was found 45.02 tons/ha. The validation results of the model are close to that of the study by Koju et. al. 2019 where the values of R^2 and RMSE error were 0.79 and 63 tons/ha respectively (Koju & Zhang, 2019). The results of our study show that the FAGB can be estimated within acceptable accuracy limits using Landsat-8 imagery.

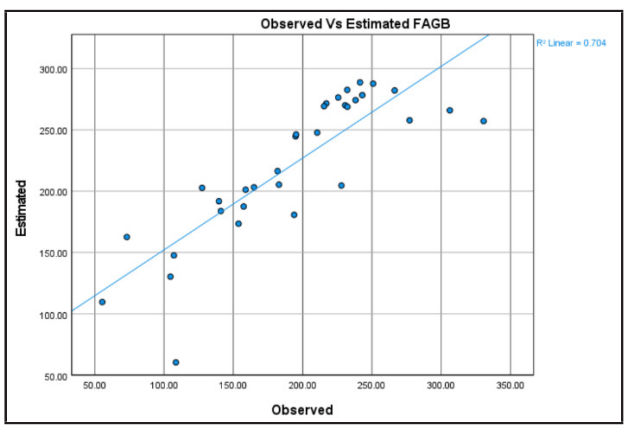

Figure 7. Scatter Plot of Observed Vs Landsat-8 Estimated FAGB

3.4.2 Validation of FAGB Estimated from Sentinel-2 Explanatory Variables: Estimated FAGB for these thirty-three plots were extracted and correlated with observed FAGB. The dependent (observed FAGB) and independent (estimated FAGB) variables have a good correlation with a coefficient of determination of 0.77. It indicates that approximately 77% of the observed FAGB was explained by the estimated model. Since they have a good correlation, it was selected to map the final FAGB and carbon stock. The RMSE error between observed and estimated FAGB was found 34.33 tons/ha. The scatter plot between observed and estimated FAGB is shown in Figure 8. The R^2 and RMSE values are in agreement with that of the research by Askar et. al. 2018 where the R^2 and RMSE values were 0.74 and 27 tons/ha respectively (Askar et al., 2018).

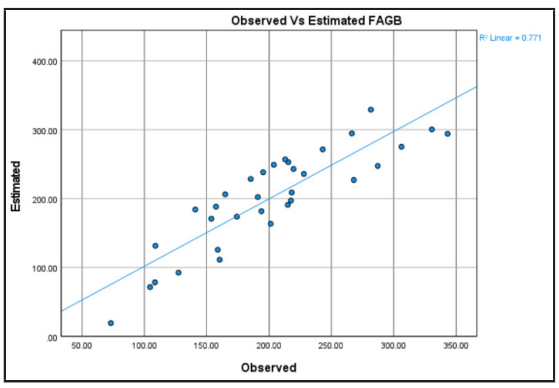

Figure 8. Scatter Plot of Observed Vs Sentinel-2 Estimated FAGB

4. CONCLUSION

This study has been conducted to develop and evaluate remote sensing-based models for estimating FAGB and carbon stocks in Chure forests of Nepal using variables derived from Sentinel-2 and Landsat-8 satellite imagery. Vegetation indices and Tasseled Cap indices from both imageries were combined with field data of 225 plots to assess the effectiveness of each dataset in estimating FAGB. The R-squared values of 0.78 and 0.68 and standard error of estimate 45.98 and 40.29 were obtained respectively for the Sentinel-2 and Landsat-8 estimation models.

The average FAGB productivity in the Chure forests from this study is 219.55 tons/ha and 212.96 tons/ha for Landsat-8 and Sentinel-2 based models respectively. The models were validated by using observed FAGB data of 33 ground sample plots. The value of R^2 obtained from the scatter plot between observed and estimated FAGB were 0.70 and 0.77 for Landsat-8 and Sentinel-2 based data respectively. Further, the RMSE error between observed and estimated FAGB were 45.02 tons/ha and 34.33 tons/ha respectively indicating estimation models developed from both imageries are viable for FAGB estimation. However, with high R^2 and low RMSE value Sentinel-2 based model outperforms the Landsat-8 based model and it seems to be better suited for FAGB estimation in Chure area for studied year. The finer spatial and spectral resolution of Sentinel-2 allows for a more detailed characterization of forest structure and biomass distribution, leading to more accurate estimations. However, in some scenarios where temporal trend of FAGB over decades is needed, Landsat image could be more useful.

Overall, this study highlights the potential of Sentinel-2 and Landsat-8 imagery for FAGB estimation and emphasizes the importance of utilizing multi-source data and advanced modelling techniques for accurate and reliable FAGB estimation and mapping. The study also revealed that Chure forests are of considerable significance as they store suitable amounts of carbon despite disturbance from different anthropogenic activities. These insights can contribute to REDD+ initiatives by supporting efforts to quantify carbon stocks, reduce emissions from deforestation, and promote sustainable forest management practices in the Chure forests of Nepal, aligning with global climate change mitigation goals. Further research and validation efforts are necessary to improve the robustness and applicability of remote sensing-based approaches in FAGB estimation.

REFERENCES

Alkama, R., & Cescatti, A. (2016). Climate change: Biophysical climate impacts of recent changes in global forest cover. *Science*, *351*(6273), 600–604. https://doi.org/10.1126/science.aac8083

Bannari, A., Morin, D., Bonn, F., & Huete, A. R. (1995). A review of vegetation indices. *Remote Sensing Reviews*, *13*(1–2), 95–120. https://doi.org/10.1080/02757259509532298

DFRS. (2014). Churia Forests of Nepal. In *Forest Resource Assessment Nepal*.

Fernández-Manso, A., Fernández-Manso, O., & Quintano, C. (2016). SENTINEL-2A red-edge spectral indices suitability for discriminating burn severity. *International Journal of Applied Earth Observation and Geoinformation*, *50*, 170–175. https://doi.org/10.1016/j.jag.2016.03.005

Frampton, W. J., Dash, J., Watmough, G., & Milton, E. J. (2013). Evaluating the capabilities of Sentinel-2 for quantitative estimation of biophysical variables in vegetation. *ISPRS Journal of Photogrammetry and Remote Sensing*, *82*, 83–92. https://doi.org/10.1016/j.isprsjprs.2013.04.007

Gitelson, A. A., & Merzlyak, M. N. (1997). Remote estimation of chlorophyll content in higher plant leaves. *International Journal of Remote Sensing*, *18*(12), 2691–2697. https://doi.org/10.1080/014311697217558

Hasanah, A., Supriatna, & Indrawan, M. (2020). Assessment of tropical forest degradation on a small island using the enhanced vegetation index. *IOP Conference Series: Earth and Environmental Science*, *481*(1). https://doi.org/10.1088/1755-1315/481/1/012061

Hassan, N. E. (2024). *Global warming : Causes , impacts and urgent strategies for a sustainable future : A review Global warming : Causes , impacts and urgent strategies for a sustainable future : A review*. *September*. https://doi.org/10.30574/gscarr.2024.20.3.0338

Huete, A. R. (1988). A soil-adjusted vegetation index (SAVI). *Remote Sensing of Environment*, *25*(3), 295–309. https://doi.org/10.1016/0034-4257(88)90106-X

Jackson, T. J., Chen, D., Cosh, M., Li, F., Anderson, M., Walthall, C., Doriaswamy, P., & Hunt, E. R. (2004). Vegetation water content mapping using Landsat data derived normalized difference water index for corn and soybeans. *Remote Sensing of Environment*, *92*(4), 475–482. https://doi.org/10.1016/j.rse.2003.10.021

Karlson, M., Ostwald, M., Reese, H., Sanou, J., Tankoano, B., & Mattsson, E. (2015). Mapping tree canopy cover and aboveground biomass in Sudano-Sahelian woodlands using Landsat 8 and random forest. *Remote Sensing*, *7*(8), 10017–10041. https://doi.org/10.3390/rs70810017

Ning, C., Subedi, R., & Hao, L. (2023). Land Use/Cover Change, Fragmentation, and Driving Factors in Nepal in the Last 25 Years. *Sustainability (Switzerland)*, *15*(8). https://doi.org/10.3390/su15086957

Nunes, L. J. R. (2023). The Rising Threat of Atmospheric CO2: A Review on the Causes, Impacts, and Mitigation Strategies. *Environments - MDPI*, *10*(4). https://doi.org/10.3390/environments10040066

Pettorelli, N., Vik, J. O., Mysterud, A., Gaillard, J. M., Tucker, C. J., & Stenseth, N. C. (2005). Using the satellite-derived NDVI to assess ecological responses to environmental change. *Trends in Ecology and Evolution*, *20*(9), 503–510. https://doi.org/10.1016/j.tree.2005.05.011

Psistaki, K., Tsantopoulos, G., & Paschalidou, A. K. (2024). An Overview of the Role of Forests in Climate Change Mitigation. *Sustainability (Switzerland)*, *16*(14). https://doi.org/10.3390/su16146089

Samarawickrama, U., Piyaratne, D., & Ranagalage, M. (2017). Relationship between NDVI with Tasseled cap Indices : A Remote Sensing based Analysis. *International Journal of Innovative Research in Technology*, *3*(12), 13–19.

Shrestha, R., Kadel, R., Shakya, S., Nyachhyon, N., & Mishra, B. K. (2025). Awareness and Understanding of Climate Change for Environmental Sustainability Using a Mix-Method Approach: A Study in the Kathmandu Valley. *Sustainability (Switzerland)*, *17*(7), 1–25. https://doi.org/10.3390/su17072819

Sims, D. A., & Gamon, J. A. (2002). Relationships between leaf pigment content and spectral reflectance across a wide range of species, leaf structures and developmental stages. *Remote Sensing of Environment*, *81*(2–3), 337–354. https://doi.org/10.1016/S0034-4257(02)00010-X

Subedi, B., Lamichhane, P., Magar, L. K., & Subedi, T. (2022). Aboveground carbon stocks and sequestration rates of forests under different management regimes in Churia region of Nepal. *Banko Janakari*, *32*(1), 15–24. https://doi.org/10.3126/banko.v32i1.45442

Thapa, P. B., Lamichhane, S., Joshi, K. P., Regmi, A. R., Bhattarai, D., & Adhikari, H. (2023). Landslide Susceptibility Assessment in Nepal's Chure Region: A Geospatial Analysis. *Land*, *12*(12). https://doi.org/10.3390/land12122186

Wang, F., HUANG, J., TANG, Y., & WANG, X. (2007). New Vegetation Index and Its Application in Estimating Leaf Area Index of Rice. *Rice Science*, *14*(3), 195–203. https://doi.org/10.1016/s1672-6308(07)60027-4

AUTHOR INFORMATION

Name	: Er. Bhagirath Bhatt
Academic Qualification	: ME in Geoinformatics
Organization	: Land Management Training Center
Current Designation	: Instructor
Work Experience	: 10 years
Published Article	: 2

WINGS OVER THE GEOID: EMPLOYING AIRBORNE GRAVITY DATA IN GEOID DETERMINATION

Er. Sushmita Timilsina
Survey Department- *qust04sharma@gmail.com*

ABSTRACT

This study focuses on the application of airborne gravity data to develop a regional geoid model of Nepal in the Remove-Compute-Restore (RCR) framework. In the scenario of difficulties presented by the rugged landscape of Nepal and the limited availability of terrestrial gravity data, airborne gravity measurements serve as an effective input dataset for geoid modeling. The research utilizes the XGM2019e for the reduction of long-wavelength signal reduction and employed LSC to compute geoid residuals, with model covariance functions established from spherical harmonic degree variances. Although greater discrepancies are observed in mountainous areas and near national borders due to the scarcity of data, the findings indicate reasonable geoid residuals, especially inside the boundary. The study suggested that higher-resolution airborne gravity surveys can be a feasible and economical approach for geoid determination in areas such as in Nepal that are either inaccessible or lack sufficient data.

KEYWORDS: GGM, Geoid, RCR, airborne gravity

1. INTRODUCTION TO GEOID

Geoid is defined as the equipotential surface that coincides with Mean Sea Level (MSL). It is defined as "one of the equipotential surfaces of the Earth's gravity potential, of which the (mean) surface of the oceans forms a part" (Hofmann-Wellenhof & Moritz, 2005, p1). Geoid is a complex surface and the most relevant physical figure of the Earth. Therefore, the significance of geoid modeling is well comprehended from former times. Precise determination of geoid has been done for several decades in engineering and science.

1.1 Gravity data for geoid determination

Today, many precise measurements on earth are possible with the application of modern satellite geodetic techniques such as GNSS, but GNSS alone cannot provide orthometric height. The ellipsoid heights provided by the GNSS are not quite useful for practical applications such as large construction or water flow [Hwang.et.al, 2007]. Among many available observables, gravity data is desired as the prime observables for geoid determination. This is because the geoid is defined by the Earth's gravity field and is the surface where the gravity potential remains constant. Therefore, geoid determination methods such as Stoke's integral or spherical harmonics use gravity anomalies. The calculations integrate gravity anomalies to compute geoid undulations.

1.2 Difference between ground and airborne gravity measurement

Gravity data can be obtained from different platforms, such as from the surface itself, airborne and spaceborne. Ground and airborne gravity measurements differ notably not only in their observation surfaces but by many other factors. Ground-based gravity data are collected as discrete samples from a continuous gravity field and airborne gravity measurements are taken along smoother, well-defined flight paths. The most critical difference between these two types of observations is in their frequency characteristics. Unlike ground data, airborne gravity measurements must be processed before they can be used for geoid modeling. Because airborne data is affected by high-frequency noise—mainly from aircraft movement and GNSS signal variations—low-pass filtering is applied, which removes these high frequencies. Unfortunately, this also eliminates useful high-frequency gravity information, presenting a major limitation of airborne gravimetry [(Meyer, 2014)].

2. DATA USED FOR GEOID DETERMINATION

For this study, airborne gravity data covering the whole of Nepal was used as the main input. The overall accuracy of the collected airborne gravity data was estimated to be 3.3 mGal (Forsberg, 2013). Figure 1 shows the observed gravity anomaly in mGal along the flight line. The reason behind

using airborne gravity data is that Geoid determination using airborne gravity data is a powerful approach, especially in regions where terrestrial measurements are sparse or inaccessible (e.g., mountainous, forested, or polar areas). Just like Nepal. Furthermore, two Global Geopotential Models were analyzed; EGM2008 and XGM2019e. This Earth's gravitational potential model (EGM) was developed using the least square combination of the ITG-GRACE03S gravitational model up to degree and order 180 and its associated error covariance matrix, with the gravitational information obtained from a global set of area-mean of free-air gravity anomalies defined on a 5 arc minute equiangular grid (Pavlis et.al, 2012). XGM2019e is a combined global gravity field model that includes the latest satellite model, GOCO06s, in the longer wavelength area with terrestrial measurements over land and ocean of gravity anomalies having a resolution of 15' for the shorter wavelengths (Zingerle et.al, 2019).

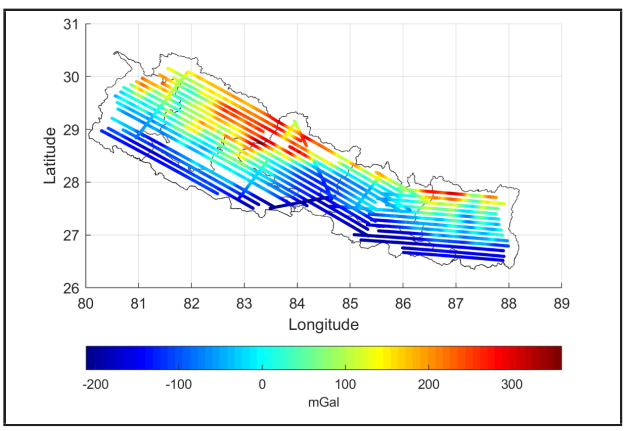

Figure 1. Observed gravity anomaly (mGal) along the flight line

3. BASIC WORKFLOW OF GEOID DETERMINATION

After filtering the high frequency from airborne gravity data, the general Remove-Compute-Restore method can be used for regional/local geoid modelling. Remove-Compute-Restore method is based on the assumptions that the gravity signal observed at certain location is the sum of its long, medium and short wavelength (Gaetani, 2016). The long wavelength component can be characterized by the application of GGM. Removing the effects of long wavelength component removes the gravity signal from Earth's crust, upper mantle and long wavelength topographic signals. This reduction acts as high pass filter to the observed data. Usually, the medium to short wavelength component are due to high frequency topographic effect. This effect can be removed by the use of Residual Terrain Correction. The remaining short wavelength component has mean and standard deviation near to zero. Gravimetric geoid model computation basically comprises of following components:

$$\Delta g = \Delta g_{GGM} + \Delta g_{topo} + g_{res} \quad (1)$$

where Δg_{GGM} is the long wavelength component (trend field), Δg_{topo} is the topography related short/medium wavelength component, and g_{res} is the residual short/medium wavelength component. g_{res} is residual terrestrial gravity quantities that can address the local effects such as density anomalies. The determination of geoid of Nepal was done using air borne gravity data and Least-Squares Collocation approach in Remove-Compute-Restore framework.

3.1 REDUCTION: Gravity Model Simulation

The GGM that results in the best statistical fit to gravity observations is considered the most suitable for modeling of the long-wavelength signal of the gravity field (Zhang 1997). Therefore, the removal or reduction of the long wavelength component from the observed gravity anomaly was done by using the best possible global model. The gravity simulation between global models (EGM2008 and XGM2019e) suggests that XGM2019e fits better to the input data than EGM2008 (Timilsina et.al., 2021). The terrestrial data in XGM2019e is augmented with topographically derived gravity over land (Earth2014), and it is complete up to spherical harmonic degree and order 5539 (Zingerle et al., 2019). So, the medium and long wavelength components of the gravity anomaly are reduced in a single step. Therefore, XGM2019e was chosen for further computations in this study.

The reduction step of gravity anomalies using XGM2019e undergoes following

$$\Delta g_{red} = \Delta g_{obs} - \Delta g_{GEM} \quad (2)$$

where Δg_{obs} is the input observed gravity anomaly, Δg_{GEM} is the gravity anomaly computed using XGM2019e at same position as input data, and Δg_{red} is the reduced gravity anomaly obtained by subtracting long to medium wavelength component of gravity anomaly computed using XGM2019e from the input observation.

3.2 COMPUTE: Least-Squares Collocation

The least squares collocation (LSC) method was used to compute geoid residuals from gravity anomalies. LSC has been widely applied in geodesy for estimating the gravity

field of the Earth both locally and globally (Gaetani, 2016). The main aspect of this method is the statistical interpretation of proper covariance functions of the gravity data as a kernel function which describes the spatial correlation of the observations. Determination of Covariance Function is one of the main parts of the Least-Square Collocation. Figure 4 shows that with the increase in the distance there is a decrease in the covariance value, and with a further increase in distance the empirical covariance function (ECF) oscillates around zero. This is a good indicator that no significant trend is left in the reduced input data. From this data, the variance of gravity anomaly and the correlation length of the covariance function were computed to derive a model covariance function that can properly model the empirical data.

The Model Covariance function is derived to fit our empirical covariance function and later to be used as the basis covariance function for LSC. The Model Covariance function is derived from the degree variances of the GGM. Degree variances are the sum of square of spherical harmonic coefficients, which describe the decay of gravity signal or reflects the signal power contained in all coefficients of same degree. The degree range for the model covariance is chosen such that it matches best with ECF. Here, the degree ranges 455 to 2000 show the best results for the empirical data. There is not much change in the covariance function for the degrees above 2000. Figure 4 shows quite good agreement of MCF and ECF for distances of less than 20km. Also, the model covariance function oscillates around zero with increasing distance. Thus, determined MCF was used as the covariance function to proceed to Least-Squares Collocation.

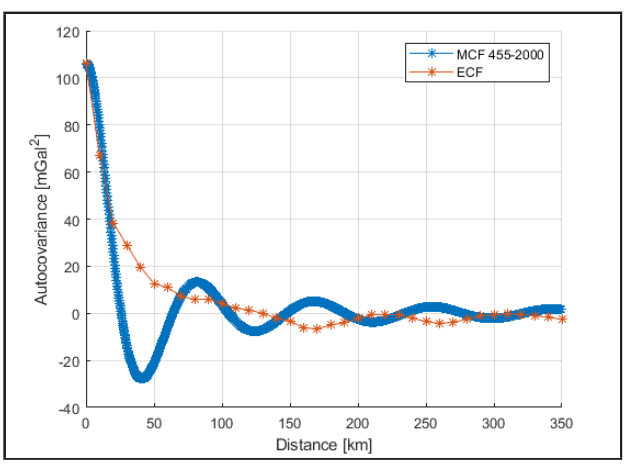

Figure 2. Comparison ECF (Computed from input gravity anomaly) and MCF (Computed from XGM2019e) for degree range 455-2000

The output gravity anomalies were estimated/predicted using the input gravity anomalies at the same stations. The input and output gravity quantities were made the same in order to test if the model that we used fits the input. The geoid residuals in Figure 6 show that the geoid residuals obtained from LSC are quite reasonable. The residual range is between 2.5 meters. Inside the country's boundaries, the residual is even smaller. Higher values are seen in the major mountainous regions of the country. The lack of terrestrial data at the border and outside the country's border has resulted in higher residuals.

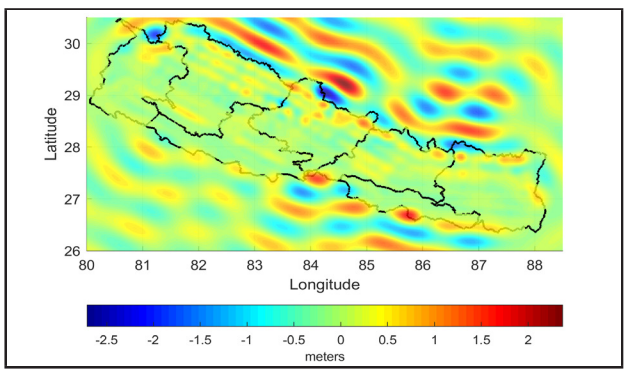

Figure 3. Geoid Residuals computed from LSC

3.3 RESTORE

Restoring is the part where we restore back the long and medium wavelength component that was reduced in the reduction process. The restoring of geoid height is done as following:

$$N = N_{res} + N_{GGM} \quad (3)$$

where N is the final geoid value obtained after adding the N_{GGM} computed from the XGM2019e to the geoid residuals N_{res} computed using LSC. The final geoid is presented in Figure 4. The geoid value ranges between -60 to -10 meters which means the ellipsoid height and orthometric height differs from around -60 to -10 meters.

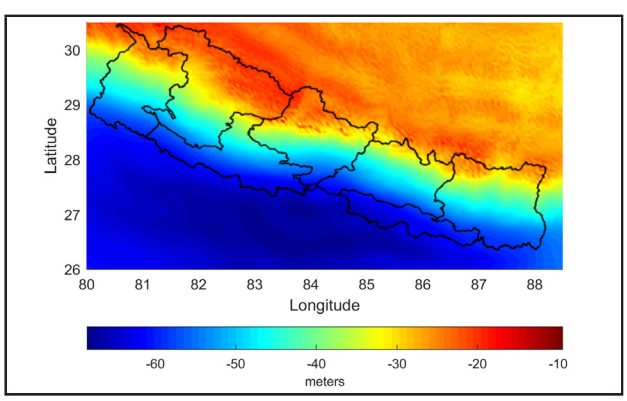

Figure 4. Final Geoid

4. CONCLUSION AND OUTLOOK

This study successfully demonstrated the use of airborne gravity data for geoid determination over Nepal, which is characterized by complex topography and limited terrestrial gravity coverage. By employing the Remove-Compute-Restore method within a Least-Squares Collocation framework, and using the XGM2019e global gravity model for long- and medium-wavelength signal reduction, a regional geoid model was developed with reasonable accuracy. The comparison between empirical and model covariance functions showed good agreement, validating the statistical approach adopted in the LSC process. Although residuals were generally small within Nepals boundaries, higher discrepancies in mountainous and border areas highlight the limitations imposed by sparse or absent ground data. The determination of geoid using airborne gravity can be done. The high frequency signal for the determination of a complete geoid signal would be possible with the availability of high-quality terrestrial observations or denser airborne data with rather low flight altitudes above ground, which in this case is not available. It is helpful in covering areas where ground gravity data is missing with rapid data collection over large areas, typically with larger spatial resolution, in a cost-effective manner.

REFERENCES

Barthelmes, F. (2014). Global Models. Potsdam: GFZ German Research Centre for Geosciences.

Bucha, B., & Janák, J. (2014). A MATLAB-based graphical user interface program for computing functionals of the geopotential up to ultra-high degrees and orders: Efficient computation at irregular surfaces. Computers and Geosciences, Volume 66, 219-227.

Cheinway Hwang, Y.-S. H. (2007). Geodetic and geophysical results from Taiwan airborne gravity survey: Data reduction and accuracy assessment. Advancing Earth and Space sciences.

Forsberg, R., Olesen, A. V., Einarsson, I., Manandhar, N., & Shreshtha, K. G. (2013). Geoid of Nepal from Airborne Gravity Survey. International Association of Geodesy Symposia.

Gaetani, C. I. (2016). COVARIANCE FUNCTION MODELLING IN LOCAL GEODETIC APPLICATIONS USING THE SIMPLEX METHOD. Boletim de Ciências Geodésicas, 22(2), 342-357.

Hofmann-Wellenhof Bernhard, M. H. (2005). Physical Geodesy. SpringerWienNewYork.

Manandhar, N., & K.C, S. (2018). Geoid Determination and Gravity Works in Nepal. Nepalese Journal on Geoinformatcs, Vol. 17, 7-15.

Meyer, U. (2014). Gravity method, Airborne. Springer Nature.

Moritz, H. (1980). Advance Physical Geodesy. Karlsruhe.

Nikolaos K. Pavlis, S. A. (2012). The development and evaluation of the Earth Gravitational Model 2008 (EGM2008). Journal of Geophysical Research, Vol. 117.

Pail, R. (2014). CHAMP-, GRACE-, GOCE-Satellite Projects. In Encyclopedia of Geodesy. Springer, Cham.

Ramouz Sabah, Y. A. (2019). IRG2018: A regional geoid model in Iran using Least Squares Collocation. Stud Geophys Geod 63, 191–214.

Rene Forsberg, A. V. (2013). Geoid of Nepal from Airborne Gravity Survey. International Association of Geodesy Symposia.

Ruffhead, A. (1987). AN INTRODUCTION TO LEAST-SQUARES COLLOCATION. Survey Review, Volume 29, Number 224, 85-94.

Timilsina S., Pail. R., Willberg M., (2021), Regional Geoid for Nepal using Least Square Collocation. Terrestrial, Atmospheric and Oceanic Sciences

U.S. National Geospatial-Intelligence Agency (NGA), E. D. (21. May 2020). EGM2008 - WGS 84 Version. Von https://earth-info.nga.mil/GandG/wgs84/gravitymod/egm2008/egm08_wgs84.html abgerufen

Zingerle, P., Pail, R., Gruber, T., & Oikonomidou, X. (2019). The experimental gravity field model XGM2019e. GFZ Data Services.

AUTHOR INFORMATION

Name	:	**Sushmita Timilsina**
Academic Qualification	:	M.Sc. in Geodesy and Geoinformation
Organization	:	Survey Department
Current Designation	:	Survey Officer
Work Experience	:	10 years
Published Article	:	7

GROUND WATER POTENTIAL ZONING USING GIS AND AHP: CASE STUDY OF BAGMATI RIVER BASIN, NEPAL

Er. Kamal Shahi

Land Management Training Center - *kamal.shahi502@gmail.com*

ABSTRACT

Groundwater supplies around the world are under tremendous pressure due to overuse and noticeable climatic changes over time. The requirement to assess groundwater potential and aquifer productivity rise along with the global need for potable water for human consumption, agriculture, industrial applications and to maintain the ecological balance. GIS based techniques are being widely used to determine the potential zones for ground water as it provides quick and first-hand information for further decision making. In this study, factors affecting the potential of groundwater availability such as material factors like geology, near surface and sub-surface soil features, structure, and drainage patterns and replenishment factors like rainfall, land use type, slope and lineament density were used in the GIS platform to perform the Multi Criteria Decision Analysis (MCDA) and weight allocation for each thematic layer was determined by AHP method . Bagmati river basin of Nepal having the area of 4337 sq.km was delineated in five categories namely Very Low, Low, Moderate, High and Very High as the potential of ground water availability. The result showed that 1 % of study area falls in the Very Low zone, 25 % in the Low zone, 45 % in the Moderate zone, 17 % in the High and 12% in the Very High zone of ground water potential. Also ground water potential zones were cross validated with reference to the available groundwater sources in the study region. Most of the available ground water sources lie in the high and very high zone of ground water potential within the basin.

KEYWORDS: Groundwater Potential, Bagmati River Basin, GIS, AHP, MCDA

1. INTRODUTION

Water present beneath Earth's surface in rock and soil pore spaces and in the fractures of rock formations. About 30 percent of all readily available freshwater in the world is groundwater. So, it's the most important and vital natural resource of water for domestic, industrial, agricultural and many other development works. Groundwater is a significant source of water for agricultural and drinking purposes in Nepal also. Approximately twenty percent of irrigated agriculture, mostly in the Terai, uses groundwater and over fifty percent of people in the Kathmandu Valley use groundwater, frequently through shallow wells, as do eighty percent of people in Siwalik (USAID, 2021). according to the country report of UNICEF,2020, more than one third of the total population of Nepal don't have the access to the improved sanitation and furthermore more than ten percent of the total population don't even have the access to the basic water facilities. However, only ten percent of the total potential renewable ground water is being extracted annually (USAID, 2021). So, these facts infer that although Nepal couldn't have used all the potential of ground water resource to manage the basic water and improved sanitation facilities, there is unbalanced extraction of groundwater which is affecting the natural recharge cycle and the ecology.

Exploration and effective management of groundwater, a valuable natural resource, are crucial to choosing the best places for groundwater recharge, monitoring wells, water supply, and groundwater quality (Jha et al., 2010). The presence of groundwater is influenced by several physio-climatic and hydrogeological factors, including lithological structures, primary and secondary porosity, slope angle, geomorphological landforms, land use/land cover, drainage pattern, distribution and intensity of rainfall, and other physio-climatic conditions, which aid in identifying groundwater potential zones (Melese et al., 2021).

The groundwater potential varies spatially because of the large regional variation in the processes governing groundwater occurrence. However, the development of geospatial and remote sensing technologies to collect and analyse spatial data has made them effective tools in hydrogeology, notably for the assessment of ground water potential zones (Arnous, 2016; Dadgar et al., 2017). Traditionally, expensive and time-consuming ground surveys using geological, geophysical and hydrogeological tools and techniques have been used to identify, delineate and map the groundwater potential zones (Israil et al.,

2006). Literatures reveal that several researchers have been using GIS to delineate groundwater potential zones with the integration of statistical approach such as simple additive weight (SAW) and analytic hierarchy process (AHP) (Israil, et al., 2006; Jaafarzadeh et al., 2011; Jha et al., 2010; Karki et al., 2021) and, machine learning (Kumar P. et al., 2016, Kumar R. et al., 2021; Machiwal et al., 2011). AHP is the most popular and widely used of Multi-Criteria Decision Analysis (MCDA) techniques to delineate groundwater prospecting zones. Hence, this research work will focus on the identification and classification of ground water potential zone in Bagmati river basin (BRB) using the integrated approach of AHP and GIS. The output of this research will provide valuable information to develop sustainable groundwater resource in BRB area. Also, this research will also create a suitable model to be implemented in other river basins of Nepal to delineate the ground water potential and ultimately sustainable groundwater management of the whole country.

2. METHODOLOGY

2.1 Study Area

The BRB encompasses 4337 sq. km and has an elevation range of 55 to 2903 m. It is physically bound between 85° 1′ E to 85° 57′ E longitude and 26° 45′ N to 27° 49′ N latitude (Figure 1(b)). The Bagmati River has six tributaries: Bishnumati, Dhobikhola, Manahara, Nakkhu, Balkhu, and Tukucha. The Bagmati River finds its source in the northern mountain highlands of Kathmandu, Baghdwar (at an altitude of 2690 m) and flows through Nepal's 196 km long section before merging with the Ganges in India.

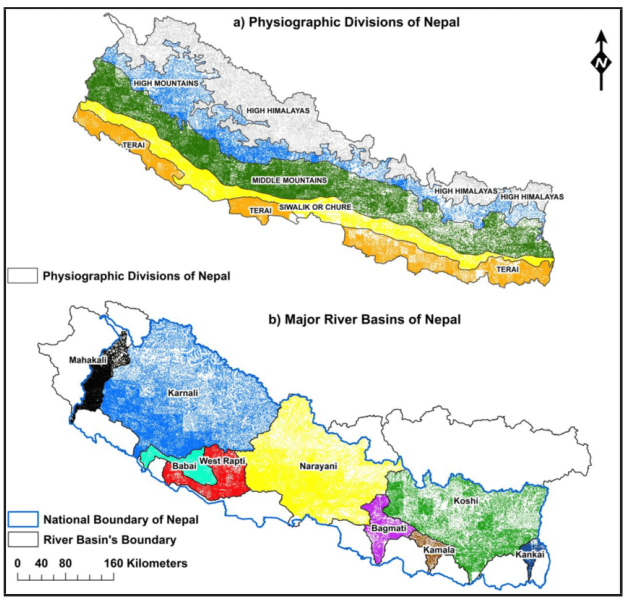

Figure 1(a) Physiographic (above) and Major River watershed basins (below) of Nepal (Karki et al., 2021)

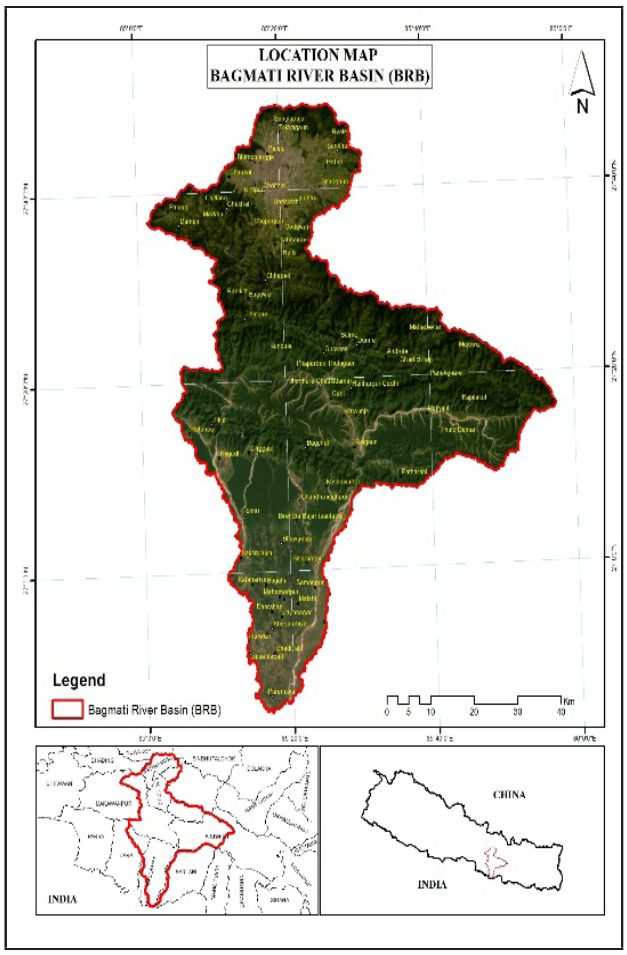

Among nine watershed of Nepal, Bagmati river basin is the small river basin lies on the southern part of the country, and it consists of Middle Mountain, Siwalik region and Terai region as shown in Figure 1(a).

Although aquifers are frequently transboundary and can be damaged by groundwater pumping in India, lowland parts in the Terai have extremely productive alluvial aquifers (250 m deep) and robust recharging. Hard rock aquifers in the Siwalik have erratic groundwater availability, and productivity and recharge are average. Only few studies of groundwater potential in the Bagmati River Basin which is responsible for the water supply of countries' big cities, capital Kathmandu, Bhaktapur, Lalitpur, Chitwan etc...

2.2 Methodological flowchart

Geospatial multi-criteria decision analysis was carried out in the GIS environment to delineate the ground water potential of the BRB using the seven criteria's namely geology, soil, annual rainfall, slope, drainage density, lineage density, land use/land cover. Overall methodological flow diagram is shown in Figure 2.

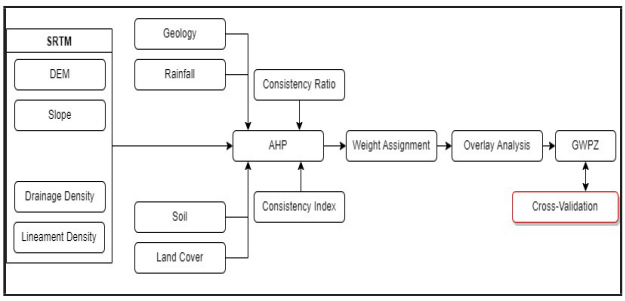

Figure 2. Flow chart of overall methodology

2.3 Data

Data required to prepare such layers was collected from various sources and formats as shown in Table 1.

Table 1. Data properties (Source, resolution, and format)

Data layer	Agency	Portal	Resolution
Global digital elevation model	NASA and JSS	https://www.earthdata.nasa.gov/	30m
Land use land cover	ICIMOD	http://rds.icimod.org/	30m
Geology	U.S. Geological Survey, Central Energy Resources Team	http://energy.cr.usgs.gov	
Soil	FAO-UNESCO World soil map	https://data.apps.fao.org/	
Annual rainfall	ICIMOD	http://rds.icimod.org/	100m

2.4 Data preparation

Pre-processing of each layer was performed to prepare the above mentioned seven layers using ArcGIS v10.8. First, BRB extent and boundary were delineated using DEM and hydrology tool and used as the study area. All data layers were clipped to the extent of study area and resampled to the raster of 30m resolution. WGS 1984 spheroid with UTM 45 N projection was used as the coordinate reference system.

Seven thematic influencing parameters such as slope, soil, geology, LULC, drainage density, lineage density and rainfall were prepared using the data collected as mentioned above.

2.4.1 Drainage Density: Drainage density indicates the closeness of the streams channel and can be calculated as the total length of streams and waters in the watershed divided by the total area of the drainage watershed. DEM was used to extract the drainage lines in the watershed and kernel density function available in ArcGIS was used to calculate the drainage density as shown in Figure 2. The drainage density has the inverse relationship with groundwater potential. Higher the drainage density, there is less probability of ground water potential (Choudhari et al., 2014). So, drainage density map of the watershed was categorized into five class as per the natural break classification method and rank was assigned from 1-9 such that lower density gets the higher rank and vice versa (Table 5) and drainage density map is shown in Figure 3.

2.4.2 Slope: Slope is one of the important factors for the ground water potential as slope determines the amount of water available for recharge and the ruggedness in the terrain of any watershed. Terrain having lower slope prevents the runoff and allows higher infiltration of water to recharge the ground water (Singh et al., 2018). The slope for this study was generated from the SRTM DEM and classified into five class. Rank for each class was assigned from 1-9 inversely with the slope value as shown in Table 5 and slope map is shown in Figure 4.

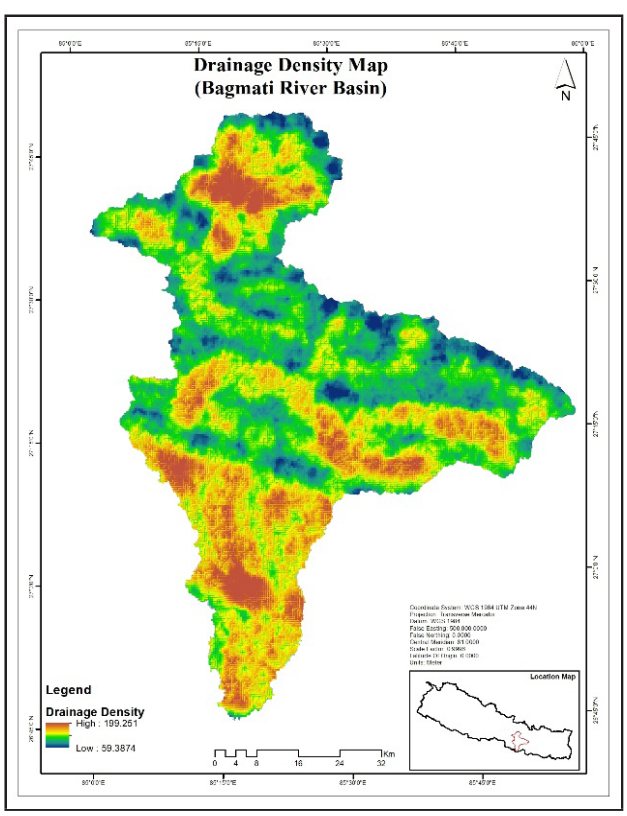

Figure 3. Drainage density map

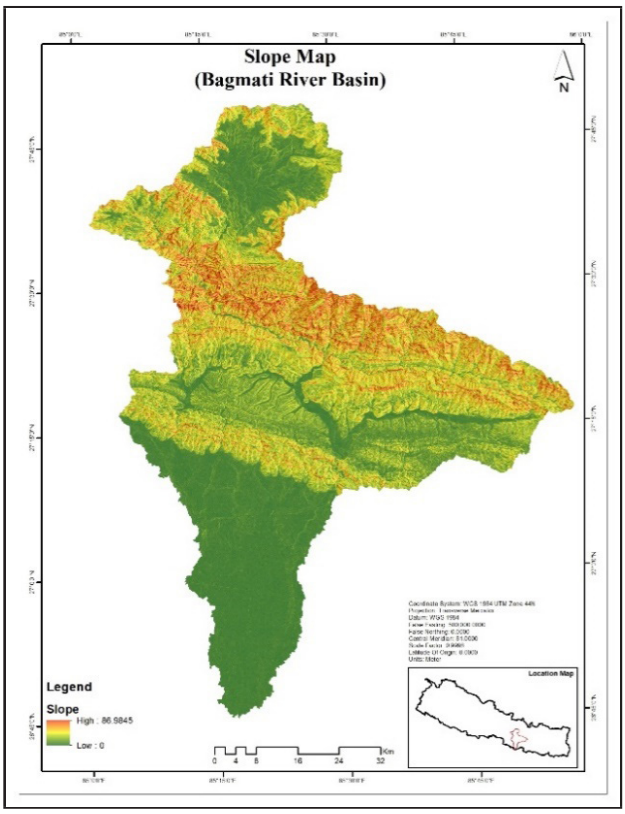

Figure 4. Slope map

2.4.3 Soil: Types of soil of the basin plays an important role for ground recharge and water holding capacity of the area as well. So, it is considered as the one of the important factors for ground water potential zonation (Kumar et al., 2016). There is major three types of soils in the study area namely Dystric Cambisols, Dystric Regosols and Eutric Fluvisols. Maximum portion of the area i.e 79% contains the cambisols , 7% by Regosols and rest 14% by Fluvisols soil type (Figure 5). Among them Cambisols are formed in materials with a medium to fine texture that come from a variety of rocks, primarily in alluvial, colluvial, and aeolian deposits and have medium capacity to recharge the ground water. Whereas Regoslos are weakly developed soils classified as Leptosols (very shallow soils), Arenosols (sandy soils), or Fluvisols are not included in the Regosols (in recent alluvial deposits) and have low infiltration and recharge capacity for ground water. On all continents and in all climate zones, fluvisols are found on alluvial plains, river fans, valleys, and tidal marshes. Periodic flooding is rather typical under natural conditions. The stratification of the soils is seen in the soils and very good recharge and infiltration capacity. Detail soil classification map is shown in Figure 6.

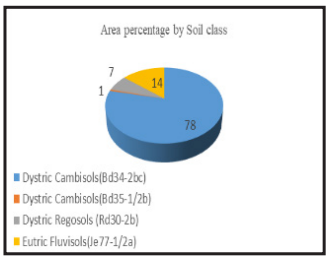

Figure 5 Soil Classification area

2.4.4 Geology: Lithology or say geology influence ground water potential significantly (Melese et al., 2021). The geology of the study area is made up of Mesozoic and Paleozoic intrusive and metamorphic rocks Neogene sedimentary rocks, undivided Paleozoic rocks, Quaternary sediments and undivided Precambrian rocks. Among these Quaternary sediments and Mesozoic and Paleozoic intrusive rocks mostly favours the infiltration and ground water recharge. Ranking of each geology class is presented in Table 5 and geological map of study area is shown in Figure 7.

2.4.5 Rainfall: Rainfall is a crucial factor in determining the potential of groundwater and the main hydrological sources of groundwater storage (Arulbalaji et al., 2019). Rainfall is maximum across the central part of the study area and decreases towards the north and south region as shown in Figure 8. Ranking of the rainfall class was directly proportional to the amount of rainfall as shown in Table 5.

2.4.6 Land use Land cover (LULC): Land use land cover plays an important role in recharge, occurrence and availability of groundwater (Selvam et. al., 2015). Land use land cover data used in this study was well prepared by ICIMOD using remote sensing techniques into eleven classes namely, waterbody, glacier, snow, forest, riverbed, built-up area, cropland, bare soil, bare rock, grassland and other wooden land. Ranking for each class is as per the Table 5 and land use land cover map is shown in Figure 9.

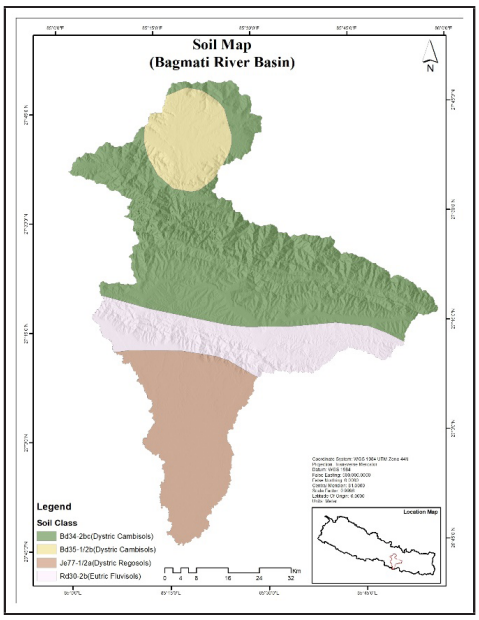

Figure 6. Soil map

2.4.7 Lineage density: Lineament is a linear geographical feature that represents underlying lithology in a landscape and is defined as the total length of the lineament per area of consideration and created using the hill shades of the study area at various angle of azimuth and altitudes. As lineament density is directly proportional to the ground recharge zone directly as with more lineament, more fracture will be in the area for water infiltration and mobility.

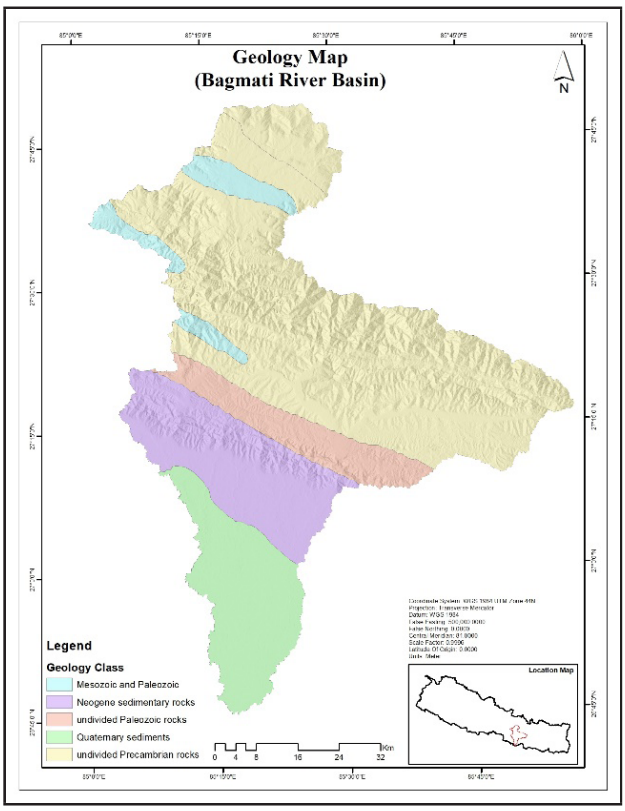

Figure 7. Geology map

2.5 Analytical Hierarchical Processing (AHP)

One of the best approaches to make the complex decision-making problems is Analytical Hierarchical Process (AHP) based multi-criteria decision analysis (MCDA) making. AHP is the widely accepted model used to define the weight of each criterion associated in the MCDA. (Saaty, 1980) defined AHP is a structured method for analysing and solving complex decision problems by decomposition, comparative judgments and synthesis of priorities. A problem's fundamental components are

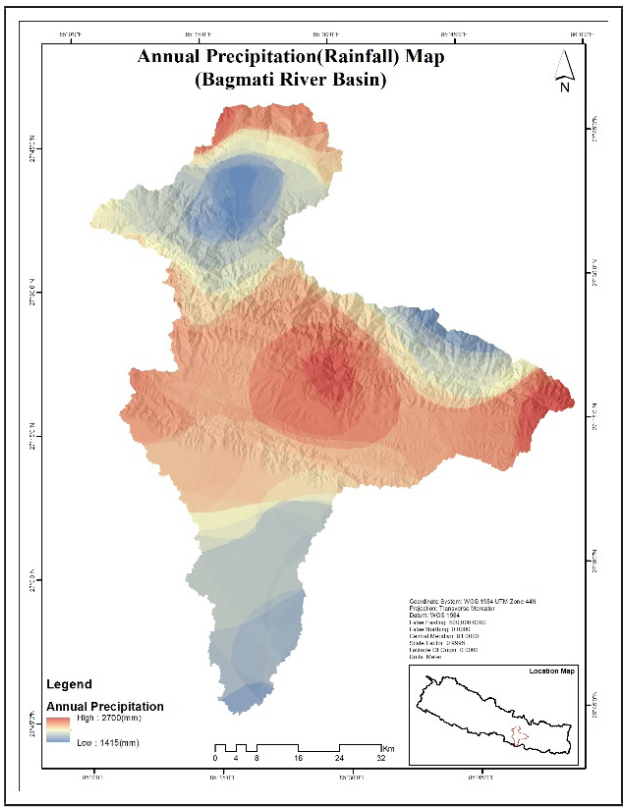

Figure 8. Annual precipitation (Rainfall) map

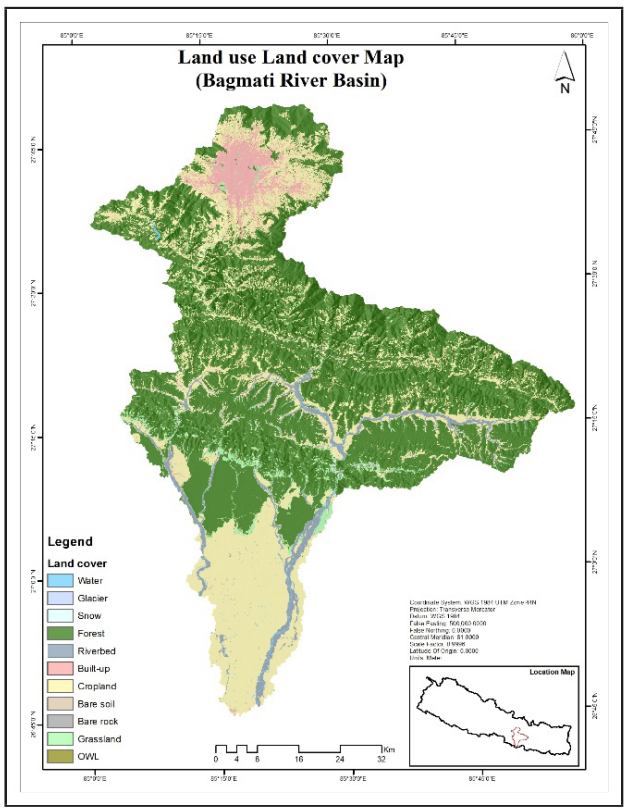

Figure 9. Land use land cover map

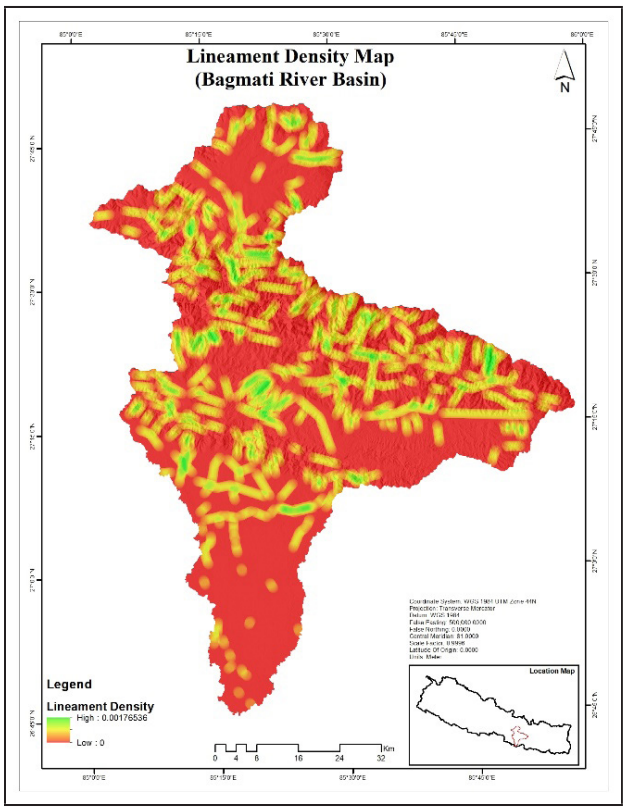

captured through its deconstruction, and a hierarchical structure is created by arranging the goal, objectives, attributes, and possibilities. By comparing two components at once, the pairwise comparison lowers the conceptual complexity of the issue. A comparison matrix is created to evaluate the relative relevance of each level's components in relation to those in the nearby high-level hierarchy, and expressed as

$$A = \begin{bmatrix} 1 & a_{12} & a_{13} & \cdots & a_{1n} \\ a_{21} & 1 & a_{23} & \cdots & a_{2n} \\ a_{31} & a_{32} & \cdots & \cdots & \cdots \\ \vdots & \vdots & \vdots & \vdots & \vdots \\ a_{n1} & a_{n2} & \cdots & \cdots & 1 \end{bmatrix}$$

, i

$$\text{where } a_{ij} = \frac{weight\ for\ attribute\ i}{weight\ for\ attribute\ j}$$

By normalizing the eigenvector of the pairwise comparison matrix that corresponds to the highest eigenvalue, the relative importance of each element is calculated. Based on the expert's opinion and review of pertinent literatures (Machiwal et al., 2011; Rahmati et al., 2015; Maheswaran et al., 2016; Arulbalaji et al.,2019; Ajay Kumar et al., 2022), influence level of each parameter for ground water potentiality was recognized and comparative weights for each factor was assigned. The AHP approach can be used to arrange both quantitative (objective) and qualitative (subjective) information concerning decision-making analysis. Each criterion was assigned a rank from 1 to 9 based on their relative importance as per Table 5 and pairwise comparison was matrix was prepared as shown in Table 3. While preparing pairwise comparison matrix, degree of preferences of one factor over another is analysed and ranked as per the Table 2 by the subject experts. Total of five expert's response was collected and averaged with one factor as per the literature as well (Machiwal et al., 2011; Rahmati et al., 2015; Maheswaran et al., 2016; Arulbalaji et al., 2019; Ajay Kumar et al., 2022).

The final weight of each prospect was calculated then by determining the principal Eigenvalue of the generated pairwise comparison matrix. The reliability of the weight assignment process was monitored by calculating the Consistency Index (CI) and Consistency Ratio (CR) values. One of the strengths of the AHP method is that it allows for inconsistent relationships while providing a CR as an indicator of the degree of consistency or inconsistency (Chen et al., 2010).

Table 2. Description of scales for pair comparison with AHP (source: Saaty 1990)

Scales	Degree of Preferences	Descriptions
1	Equally important	The contribution of the two factors is equally important.
3	Slightly important	Experiences and judgment slightly tend to a certain factor
5	Quite important	Experiences and judgment strongly tend to a certain factor.
7	Extremely important	Experiences and judgment extremely strongly tend to a certain factor
9	Absolutely important	There is sufficient evidence for absolutely tending to a certain factor
2,4,6,8	Intermediate values	There is sufficient evidence for absolutely tending to a certain factor

Table 3. Pairwise comparison matrix of seven parameters

Parameters	Geology	Soil	Slope	Rainfall	Lineage Density	LULC	Drainage Density	Geometric Mean	λ
Geology	1.00	1.13	1.20	1.58	1.58	1.88	2.40	0.20	7
Soil	0.88	1.00	1.06	1.39	1.39	1.66	2.12	0.18	7
Slope	0.83	0.94	1.00	1.32	1.32	1.56	2.00	0.17	7
Rainfall	0.63	0.72	0.76	1.00	1.00	1.19	1.52	0.13	7
Lineage Density	0.63	0.72	0.76	1.00	1.00	1.19	1.52	0.13	7
LULC	0.53	0.60	0.64	0.84	0.84	1.00	1.28	0.11	7
Drainage Density	0.42	0.47	0.50	0.66	0.66	0.78	1.00	0.08	7

(Saaty, 1990) recommended that, assigned weights are consistent only when the consistency ratio remains within 10% otherwise needs to be reconsidered to eliminate the irregularity. To calculate the Consistency Ratio, first Principal Eigen value (λ_{max}) is calculated as;

$$\lambda max = \frac{49}{7} = 7$$

Then, Consistency Index (CI) is calculated as.

$$CI = (\lambda \max - n)/(n - 1)$$

Where λ_{max} = 7 is the principal Eigen value and n = 7 is the number of factors used in the analysis.

Therefore,

$$CI = \frac{7-7}{7-1} = 0$$

Now, Consistency ration (CR) is calculated as the ratio of Consistency Index (CI) and Random Consistency Index (RCI) obtained from Saaty's standard for 7th order of matrix (Table 5).

$$CR = \frac{CI}{RCI} = \frac{0}{1.32} = 0$$

According to (Saaty, 1990), CR of 0.10 or less is sufficient to continue the analysis. If the consistency value is larger than 0.10, the judgment needs to be reviewed to identify the underlying causes of the inconsistency and make the necessary corrections. CR of 0 indicates there is the perfect level of consistency in the pair-wise comparison matrix.

2.6 Ground Water Potential Zoning (GWPZ)

The groundwater recharge potential map was generated by considering the comparative importance of various thematic layers and their corresponding classes. GWPZ, a dimensionless quantitative approach was adopted to delineate groundwater potential zone.

$$GWPZ = \sum(r_{ij} * w_i)$$

Where, (w_i) is the weight for each parameter layer and (r_{ij}) is the rank for each layer classes. The result of the Ground Water Potential Zoning using MCDA using AHP is shown in Figure 12 and 13 and discussed in following section.

Table 5. Weighted parameters and ranked class parameters

Wt.	Parameter	Class	Rank
18	*Soil*	Bd35-1/2b(Dystric Cambisols)	7
		Bd34-2bc (Chromic Cambisols)	4
		Rd30-2b (Dystric Regosols)	2
		Je77-1/2a (Eutric Fluvisols)	9
13	*Lineament Density*	(0 - 0.1523)m per sq. m	1
		(0.1524 - 0.4223)m per sq. m	2
		(0.4224 - 0.6785)m per sq. m	3
		(0.6786 - 0.9623)m per sq. m	4
		(0.9624 - 1.7654)m per sq. m	5
20	*Geology*	Mesozoic and Paleozoic intrusive	8
		Neogene sedimentary rocks	3
		Paleozoic rocks	7
		Quaternary sediments	9
		Precambrian rocks	6
11	*Land use land cover*	Waterbody	9
		Snow	7
		Forest	8
		Riverbed	7
		Built-up area	3
		Cropland	6
		Bare soil	4
		Bare rock	2
		Grassland	3
		Other wooded land	4
17	*Slope*	0 - 10	8
		11-25	6
		26-40	4
		41-55	3
		56-90	2
13	*Rain Fall*	(1,415 - 1,717) mm	3
		(1,718 - 1,919) mm	4
		(1,920 - 2,115) mm	6
		(2,116 - 2,282) mm	8
		(2,283 - 2,700) mm	9
8	*Drainage Density*	(59.3874 - 91.1996)m per sq. m	8
		(91.1997 - 109.2996)m per sq. m	6
		(109.2997 - 127.3996)m per sq. m	4
		(127.3997 - 149.3391)m per sq. m	3
		(149.3392 - 199.2513)m per sq. m	2

3. RESULTS AND DISCUSSION

The result of the Ground Water Potential Zoning (GWPZ) of Bagmati River Basin (BRB) with Multi Criteria Decision Analysis (MCDA) using Analytical Hierarchical Process (AHP) and Geographic Information System (GIS) is shown in Figure 12 and 13. The resulted map is zoned into five categories of ground water potential namely, very low,

low, moderate, high, and very high. From the map, most of the central region and the upper region of the study area is in the moderate zone, mountainous region of the central and lower region are categorized as the low ground water potential zone, and some patches in Siwalik regions have very low ground water potential. Valley and Lower plane land of the study area in the southern part and northern part of the study area are zoned in high and very high category.

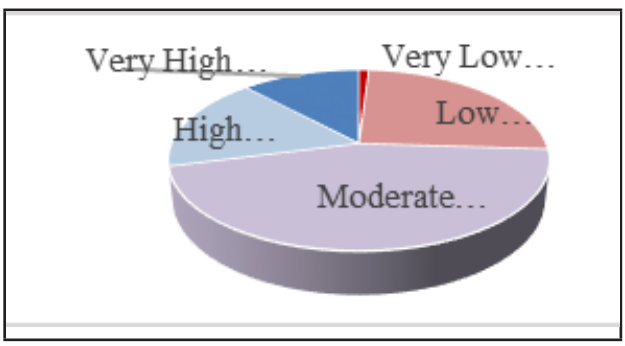

Figure 11. Aerial distribution of ground water potential zones of Bagmati river basin

As per figure 11, less than the half of the study area (45 %) is zoned in the moderate zone for ground water potential, 25 % and 1 % of the study area is in low and very low ground water potential zone respectively. Whereas 17 % of the study area shows the high potential of ground water potential and 12 % of the basin possess very high potential for ground water resource. From figure 13, it is seen that settlements are in the area with higher potential of ground water. Kathmandu Valley which comprises the valley of Kathmandu, Bhaktapur and Lalitpur districts has high potential of ground water. More than 50 % of people of Kathmandu valley uses groundwater frequently through sallow wells (USAID, 2021). Similarly, in the central region of Sindhuli district where there is the high potential of ground water, we can see the dense settlements. Moreover, in the low land area, there is very high dense settlements and has very high potential of ground water.

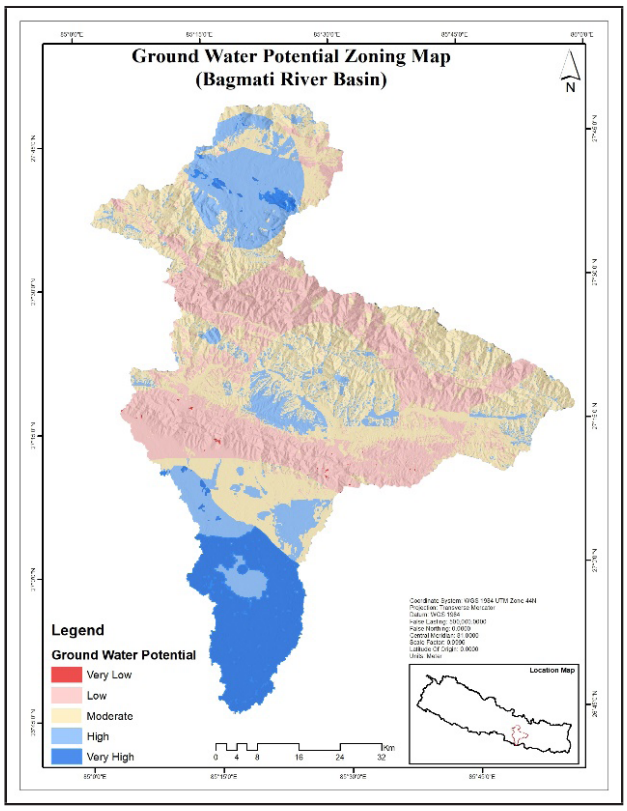

Figure 12. GWPZ and Administrative units and settlements in BRB

3.1 Cross-validation

The ground water potential zone map is further cross verified using the secondary data sources and comparing the result with the other research outputs. As water flows from aquifers into surface water bodies at seeps or springs, or infiltrates from rivers or lakes into aquifers, there is the strong relationship and dependency between the ground water level and waterbodies in the surface. Hence, the GWPZ map overlaid with the still water bodies such as lakes, ponds, reservoirs etc.... of the study area (Figure 14).

Almost 72 % of the waterbodies lie within the very high zone, approximately 20 % of the waterbodies lie on the high zone, 6% of it lie in the Moderate zone and the rest 2% of the water bodies lie in the low and very low zone of the ground water potential zone (Figure 15).

In figure 16, the relationship between the elevation and distance from river is shown with the ground water level,

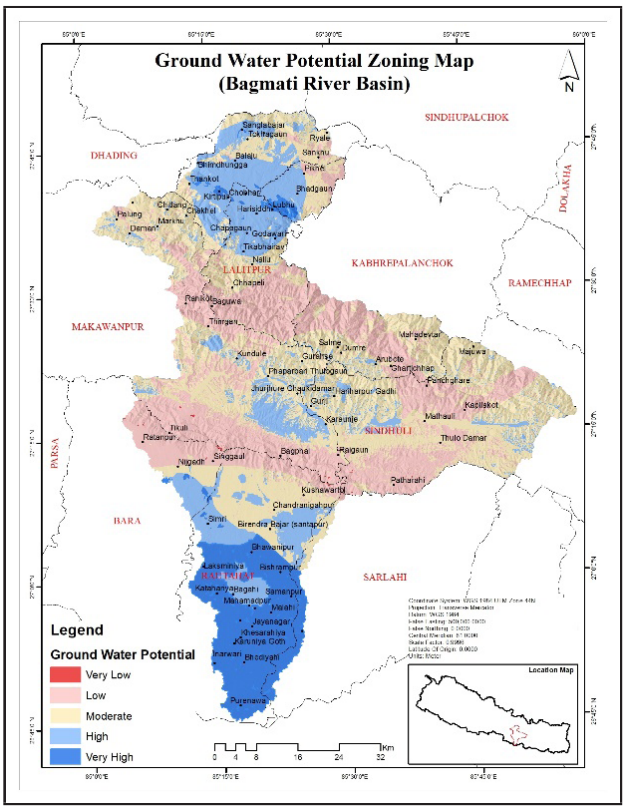

Figure 13. Ground water potential zoned map of Bagmati river basin

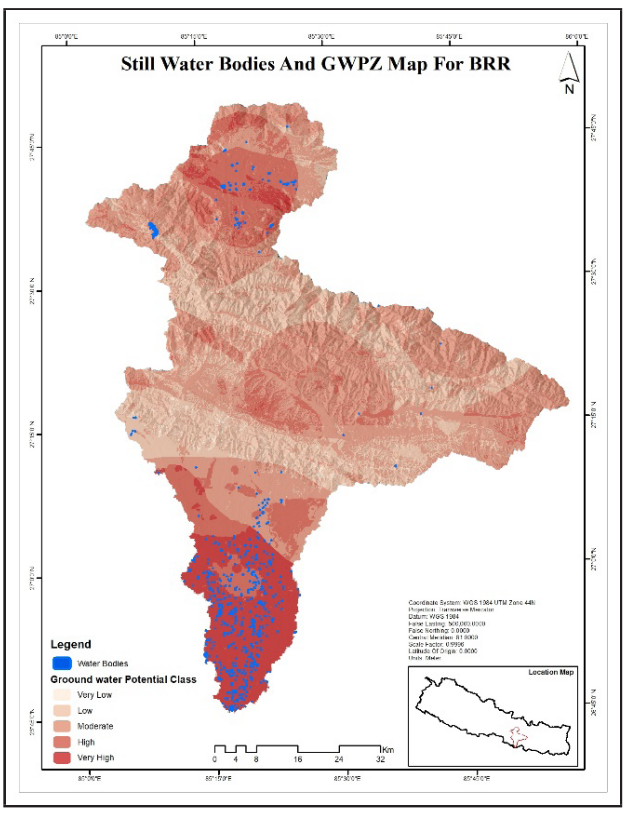

Figure 14. Still water bodies overlaid with GWPZ map

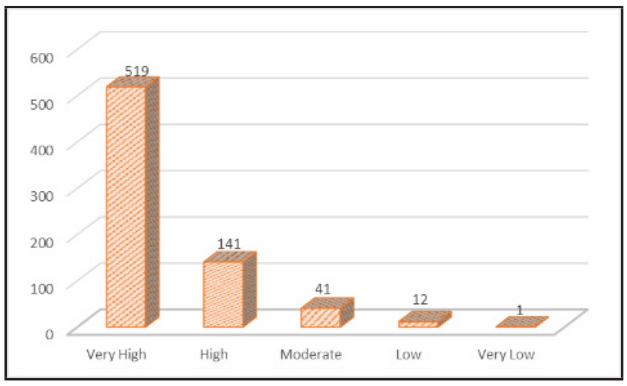

Figure 15. Number of Still water bodies in each zone of GWPZ map

and signifies that, near the distance from the river, near the ground water table from the surface i.e. more ground water potential (Akiyama et al.,2012). When overlaying the river area over the GWPZ map, figure 17 was obtained. In figure 17, most of the areas near the river possess higher potential of ground water and accumulation or amount of water in the river tends to increase the potential of ground water as well.

(Thakur et al., 2016) calculated the Water Poverty Index (WPI) for the upper basin region of Bagmati river basin. WPI explains about the poverty of water based on resource, access, capacity, use, and environment (Thakur et al., 2016). As per the figure 18(b), eastern part, Lubhu has the higher WPI index, inferring the proper accessibility of water resources. This could be due to the abundant availability of ground water resources in the area, which is also supported by the GWPZ map of the area. But in the northern part of the Kathmandu valley, Sundarijal also has a higher WPI but does not fall in the high or very high GWPZ, this is because Sundarijal is the gateway of the Melamchi River drinking water project and has lots of infrastructure for water access. Whereas the red circle in figure 18(b) suggests the area with low WPI and the area with low GWPZ. So, the comparative analysis of WPI for upper Bagmati river basin also supports the obtained result of GWPZ map.

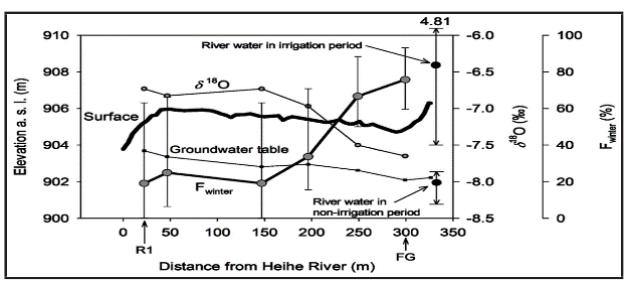

Figure 16. Relation between the distance from river and

ground water level (Akiyama et al., 2012)

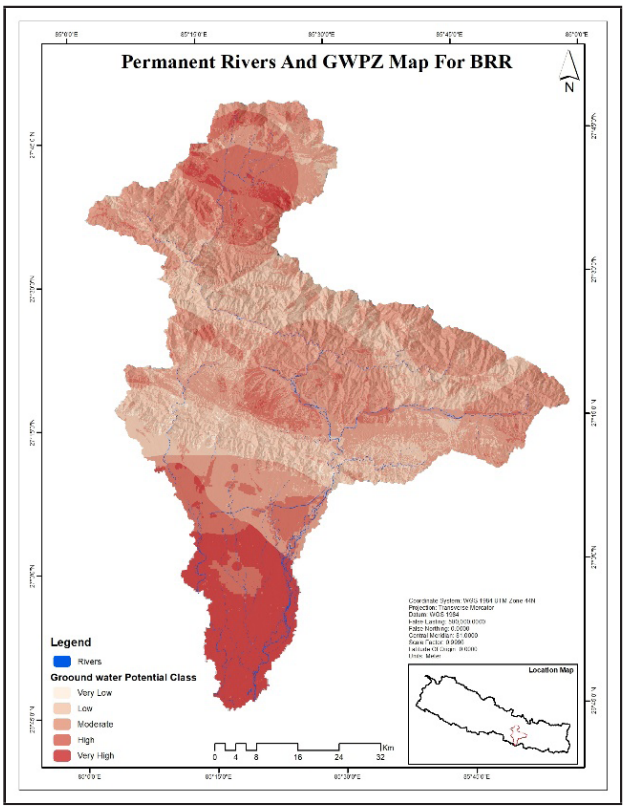

Figure 17. Rivers overlaid with GWPZ map of BRB

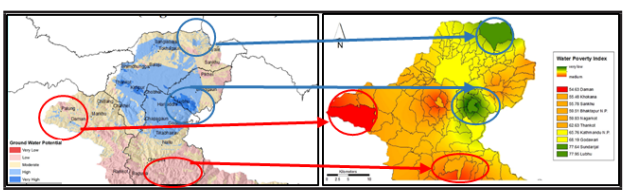

Figure 18. (a) GWPZ map of Upper BRB	Figure 18. (b) WPI map of Upper BRB (Thakur et al., 2016)

4. CONCLUSION

Ground water, yet being the important source of renewable water resource, has not been used and managed to fulfill the need of the drinking and sanitation need of the people. Identification and assessment of groundwater potential zone is the preliminary and vital step towards the use and management of ground water. MCDA techniques with the help of AHP in GIS platform has been proved to be the efficient way of modeling the ground water potential zones based on the various geomorphological, physiographical, lithological and climatic factors namely, Slope, Drainage density, Lineage density, Geology, Soil, Land use Land cover and Rainfall. Weight for each parameter was determined using the AHP process.

Weighted overlay of those seven variables was used to divide the study area into five zones namely, very low, low, moderate, high and very high zone for ground water potential, depending upon the value of each pixel. Plain lands and valley of the study area consist of high and very high potential zone for ground water and covers 17 % and 12% respectively of the Bagmati river basin. Siwalik region and higher mountainous regions tend to have very low and low potential for ground water with 25% and 1% of the study area. The rest of the region falls within the moderate zone for ground water potential. The map of ground water potential was cross verified using the still water bodies and past research in the similar study area and supports the obtained result.

So, Multi-criteria Decision Analysis (MCDA) using weighted overlay of various prospects of ground water using Analytical Hierarchical Process (AHP) in Geographic Information System (GIS) can be very useful for government bodies, policy makers, urban planners, infrastructure developers, environmentalist and any other enthusiasts about the ground water to get the basic insights regarding the ground water availability of the region and to develop the sustainable irrigation, drinking water and sanitation management system(model) by the optimum use of the renewable ground water.

REFERENCES

1. Ajay Kumar, V., Mondal, N. C., & Ahmed, S. (2020). Identification of groundwater potential zones using Rs, GIS and AHP Techniques: A case study in a part of Deccan Volcanic Province (DVP), Maharashtra, India. Journal of the Indian Society of Remote Sensing, 48(3), 497–511. https://doi.org/10.1007/s12524-019-01086-3

2. Akiyama, Tomohiro & Sakai, Akiko & Yamazaki, Yusuke & Fujita, Koji & Nakawo, Masayoshi & Kubota, Jumpei & Konagaya, Yuki. (2007). Surfacewater-groundwater interaction in the Heihe River basin, Northwestern China. Bulletin of Glaciological Research. 24. 87-94.

3. Arnous, M.O., 2016. Groundwater potentiality mapping of hard-rock terrain in arid regions using geospatial modelling: example from WadiFeiran basin, South Sinai, Egypt. Hydrogeol J, 24, 1375-1392.https://doi.org/10.1007/s10040-016-1417-8.

4. Arulbalaji, P., Padmalal, D., & Sreelash, K. (2019). GIS and AHP techniques based delineation of

groundwater potential zones: A case study from southern Western Ghats, India. Scientific Reports, 9(1). https://doi.org/10.1038/s41598-019-38567-x

5. Chen Y, Khan S, Paydar Z (2010) To retire or expand? A fuzzy GISbased spatial multi-criteria evaluation framework for irrigated agriculture. Irrig Drain 59(2):174–188. https://doi.org/10.1002/i

6. Choudhari K., Panigrahi B., Paul J. C. (2014). Morphometric analysis of Kharlikani watershed in Odisha, India using spatial information technology. International Journal of Geomatics and Geosciences 2014 Vol.4 No.4 pp.661-671 ref.17

7. Dadgar, M.A., Zeaieanfirouzabadi, P., Dashti, M. and Porhemmat, R., 2017. Extracting of prospective groundwater potential zones using remote sensing data, GIS, and a probabilistic approach in Bojnourd basin, NE of Iran. Arab J. Geosci. 10,114. https://doi.org/10.1007/s12517-017-2910-7.

8. Israil, M., Al-Hadithi, M. & Singhal, D. C. (2006) Application of a resistivity survey and geographical information system (GIS) analysis for hydrogeological zoning of a piedmont area, Himalayan foothill region, India. Hydrogeol. J. 14, 753–759.

9. Jaafarzadeh, M. S., Tahmasebipour, N., Haghizadeh, A., Pourghasemi, H. R., & Rouhani, H. (2021). Groundwater recharge potential zonation using an ensemble of Machine Learning and bivariate statistical models. Scientific Reports, 11(1). https://doi.org/10.1038/s41598-021-85205-6

10. Jha, M. K., Chowdary, V. M., & Chowdhury, A. (2010). Groundwater assessment in Salboni Block, West Bengal (India) using remote sensing, geographical information system and multi-criteria decision analysis techniques. Hydrogeology Journal, 18(7), 1713–1728. https://doi.org/10.1007/s10040-010-0631-z

11. Karki, S., Acharya, S., & Gautam, A. (2021). Evaluation of the vertical accuracy of open access digital elevation models across different physiographic regions and river basins of Nepal. https://doi.org/10.1002/essoar.10507129.1

12. Kumar, P., Herath, S., Avtar, R., & Takeuchi, K. (2016). Mapping of groundwater potential zones in Killinochi area, Sri Lanka, using GIS and remote sensing techniques. Sustainable Water Resources Management, 2(4), 419–430. https://doi.org/10.1007/s40899-016-0072-5

13. Kumar, R., Dwivedi, S. B., & Gaur, S. (2021). A comparative study of machine learning and Fuzzy-AHP technique to groundwater potential mapping in the data-scarce region. Computers & Geosciences, 155, 104855. https://doi.org/10.1016/j.cageo.2021.104855

14. Machiwal, D., Jha, M.K. and Mal, B.C., 2011. Assessment of groundwater potential in a semi-arid region of India using remote sensing, GIS and MCDM techniques. Water Resour Manage, 25(5), 1359-1386. https://doi.org/10.1007/s11269-010-9749-y

15. Maheswaran, G., Selvarani, A.G. and Elangovan, K., 2016. Groundwater resource exploration in Salem district, Tamil Nadu using GIS and remote sensing. J. Earth Syst. Sci. 125(2), .311-328. https://doi.org/10.1007/s12040-016-0659-0

16. Melese, Tadele & Belay, Tatek. (2021). Groundwater Potential Zone Mapping Using Analytical Hierarchy Process and GIS in Muga Watershed, Abay Basin, Ethiopia. Global Challenges. 6. 10.1002/gch2.202100068.

17. Mohammed, O. A., & Sayl, K. N. (2021). A GIS-based multicriteria decision for groundwater potential zone in the West Desert of Iraq. IOP Conference Series: Earth and Environmental Science, 856(1), 012049. https://doi.org/10.1088/1755-1315/856/1/012049

18. Pourghasemi, H. R., Sadhasivam, N., Yousefi, S., Tavangar, S., Ghaffari Nazarlou, H., & Santosh, M. (2020). Using machine learning algorithms to map the groundwater recharge potential zones. Journal of Environmental Management, 265, 110525. https://doi.org/10.1016/j.jenvman.2020.110525

19. Rahmati, O., Samani, A.N., Mahdavi, M., Pourghasemi, H.R. and Zeinivand, H., 2015. Groundwater potential mapping at Kurdistan region of Iran using analytic hierarchy process and GIS. Arab. J. Geosci, 8(9), 7059-7071.https://doi.org/10.1007/s12517-014-1668-4

20. Saaty, T. L. (1980). Analytic hierarchy process. Planning, priority setting, resource allocation.

21. Saranya, T., & Saravanan, S. (2020). Groundwater potential zone mapping using analytical hierarchy

process (AHP) and GIS for Kancheepuram District, Tamilnadu, India. *Modeling Earth Systems and Environment, 6*, 1105-1122.

22. Singh, L., & Katpatal, Y. (2018). Wetland Change Analysis and their impact on dense vegetation by spatial approach. Journal of Urban and Environmental Engineering, 12(1), 70–76. https://doi.org/10.4090/juee.2018.v12n1.070076

23. Selvam, S., Dar, F. A., Magesh, N. S., Singaraja, C., Venkatramanan, S., & Chung, S. Y. (2015). Application of remote sensing and GIS for delineating groundwater recharge potential zones of Kovilpatti Municipality, Tamil Nadu using if technique. Earth Science Informatics, 9(2), 137–150. https://doi.org/10.1007/s12145-015-0242-2

24. Sun, X., Zhou, Y., Yuan, L., Li, X., Shao, H., & Lu, X. (2021). Integrated decision-making model for groundwater potential evaluation in mining areas using the cusp catastrophe model and principal component analysis. Journal of Hydrology: Regional Studies, 37, 100891. https://doi.org/10.1016/j.ejrh.2021.100891

25. Thakur, J. K., Neupane, M., & Mohanan, A. A. (2017). Water poverty in Upper Bagmati River basin in Nepal. Water Science, 31(1), 93–108. https://doi.org/10.1016/j.wsj.2016.12.001

26. Water and sanitation (WASH). UNICEF Nepal. (n.d.). Retrieved November 01, 2022, from https://www.unicef.org/nepal/water-and-sanitation-wash

27. Winrock International, USAID Nepal (n.d.). Retrieved November 01, 2022, from https://winrock.org/wp-content/uploads/2021/08/Nepal_Country_Profile_Final.pdf

AUTHOR INFORMATION

Name	: Er. **Kamal Shahi**
Academic Qualification	: M.Sc. in Geospatial Technologies
Organization	: Land Management Training Center
Current Designation	: Instructor
Work Experience	: 10 years
Published Article	: 2

FLOOD RISK ASSESSMENT IN NARAINAPUR RURAL MUNICIPALITY USING ANALYTICAL HIERARCHY PROCESS

Rubi chaulagain[1], Rekha Paudel[1], Bijaya Adhikari[2]

[1]Paschimanchal Campus

pas077bge034@wrc.edu.np, pas077bge034@wrc.edu.np

[3]Department Of Water Resources And Irrigation - *bjayadk012@gmail.com*

ABSTRACT

Natural disasters are catastrophic events resulting from natural phenomena that cause significant damage to the environment, property, and human life.Narainapur Rural Municipality, located in Banke District of Lumbini Province, Nepal, is situated at approximately 27.4° N latitude and 81.6° E longitude. This municipality is char- acterized by its flat terrain and proximity to the Rapti River, which significantly influences its hydrology and flood dynamics. For the flood risk assessment using the Analytic Hierarchy Process (AHP), nine key factors were selected: curvature, soil type, distance to road, distance to stream, slope, rainfall, Topographic Wetness Index (TWI), Normalized Difference Vegetation Index (NDVI), and aspect. Each factor plays a significant role in flood susceptibility. AHP is a multi-criteria decision-making approach. The AHP is a decision support tool. It is used to solve complex decision problems, uses a multi-level hierarchical structure of objectives, criteria, sub-criteria and alternatives. Hence, the Consistency Index (CI) for all parameters combined was found to be 0.063, indicating an acceptable level of consistency in the pairwise comparisons. The individual CI values for each parameter were as follows: slope (0.054), NDVI (0.038), soil type (0.070), distance to stream (0.030), rainfall (0.014), TWI (0.022), distance to road (0.015), aspect (0.029), and curvature (0.026). The approach proved effective in identifying areas vulnerable to flooding, providing valuable insights for targeted disaster preparedness and management efforts.

KEYWORDS: Catastrophic, Multi-criteria analysis, Normalized Difference Vegetation Index, Standardization, Infiltration

1. INTRODUCTION

Natural disasters are catastrophic events resulting from natural phenomena that cause significant damage to the environment, property, and human life. The frequency and severity of natural disaster events and their associated social and economic impacts have been increasing (Djalante, 2018). Floods are considered as one of the most dangerous natural disasters spreading worldwide. A flood is a natural phenomenon that results in the short-term submergence of land areas due to extreme rainfall events within a short period of time. A flood occurs when there is partial or complete inundation of normally dry areas due to the rapid accumulation of runoff (Khanday et al., 2022). Climate change may increase the frequency, magnitude, and seasonality of floods, which means that concurrent flood hazards important for flood risk management may occur more frequently in the future (Danumah et al., 2016). The occurrence of floods is a complex phenomenon that has long attracted researchers worldwide to better understand and explore mechanisms for better management and prevention. It is estimated that approximately 1.5 billion people have been affected by floods over the past decades in the 21st century (Khanday et al., 2022). Several factors on which the occurrence of floods depends include land use, geology, slope, rainfall, elevation, and more (Stefanidis & Stathis, 2013; Gacu et al., 2022). Flood hazard evaluation is the basis of flood risk assessment, which has significant implications for the natural environment, human life, and the social economy (Liu et al., 2016). Various methods have been used to evaluate flood-prone areas, including multi-criteria decision analysis (MCDA) methods like Analytical Hierarchy Process (AHP), which rely on expert judgment but may involve uncertainty, and statistical techniques like frequency ratio (FR) and logistic regression, which depend on dataset size and explanatory variables. Physically based models like HEC-RAS and MIKE11 require extensive data and processing power. Newer machine learning methods, such as random forest (RF), artificial neural networks (ANN), and support vector machines (SVM), efficiently identify flood-prone areas and produce susceptibility maps (Choubin et al., 2019). Le Cozannet et al. (2013) assessed the applicability and usefulness of a multi-criteria decision mapping method AHP to map

physical coastal vulnerability to erosion and flooding in a structured way. One of the advantages of the AHP method is its extensibility and robustness. If the decision-maker wishes, they can modify the value of a criterion or add or eliminate criteria they deem relevant. The method allows them to readjust the evaluation previously carried out without repeating the entire hierarchy already established. GIS-based flood risk mapping integrated with multi-criteria analysis (MCA), particularly using the AHP, is an efficient, flexible, and low-cost approach for identifying flood prone areas by prioritizing criteria such as slope, distance to streams, soil type, and curve number. Studies have highlighted its adaptability in customizing risk maps based on social or economic vulnerabilities. Additionally, it has demonstrated that including effective precipitation improves accuracy, and its applicability is especially valuable in data-scarce regions, with potential for future enhancements, such as fuzzy logic integration (Rincón et al., 2018). In Nepal, floods frequently occur across various regions, causing significant impacts on lives and livelihoods. To better understand flood scenarios in Nepal, we conducted a thorough review of numerous research papers and studies highlighting the causes, impacts, and management strategies associated with flooding. Floods are among the most frequent natural disasters worldwide, causing substantial economic and social consequences, particularly in resource-constrained countries with limited disaster preparedness and response capacity. In Nepal, unique geographical and climatic conditions heighten vulnerability to multiple hazards such as floods, landslides, and earthquakes, with studies revealing that over 80% of the population is exposed to these risks. Historical events emphasize the severe impacts of multi-hazard scenarios, and the AHP serves as a crucial tool for multi-criteria decision-making in hazard assessments by systematically evaluating factors influencing vulnerability (Khatakho et al., 2021). Flood hazards in Nepal highlight the country's vulnerability due to a combination of geographical, climatic, and socio-economic factors. Nepal's steep mountain topography, high relief, and concentrated monsoon precipitation create an environment prone to severe flooding, leading to significant loss of life and property annually. These factors, along with communities' limited capacity to cope with disasters, contribute to the high vulnerability to floods (Khanal et al., 2007). Nepal faces a persistent struggle with flooding, intensified by its geological features, steep topography, and heavy monsoon rainfall. Floods have historically caused significant loss of life and property, with approximately 7,599 fatalities and economic losses of around 10.6 billion USD recorded between 1954 and 2018. Improper land use, unplanned settlements, and deforestation have further heightened community vulnerability, making effective flood control and prevention measures essential. Flood vulnerability assessments support early warning systems and emergency responses (Malla & Ohgushi, 2024). Similarly, flood assessment and vulnerability analysis highlight the increasing frequency and severity of disasters, emphasizing their profound impact on human lives and assets, particularly in vulnerable communities. The Sendai Framework for Disaster Risk Reduction emphasizes the importance of understanding vulnerability as the capacity of individuals or communities to cope with hazards for effective risk mitigation (Guragain & Doneys, 2022). Additionally, a community based flood damage assessment approach for the lower West Rapti River basin in Nepal, considering the impact of climate change, investigates the effects of climate change on flooding in the West Rapti River (WRR) basin, a vital agricultural region. Using community-based surveys and hydrological modeling, it estimates current and future flood damages, particularly referencing the significant 2007 flood event (Perera et al., 2015). The primary objective of this study is to develop a comprehensive flood risk assessment using the AHP. The secondary objectives include generating detailed thematic maps from high-resolution satellite imagery and Digital Elevation Models (DEMs), obtaining satellite imagery data for accurate ground truth collection, and evaluating the relationship between proximity to streams and slope gradients on flood susceptibility. Furthermore, the study seeks to analyze and classify the study area into high, medium, and low flood risk zones, and to assess the effectiveness of the AHP method in accurately identifying areas vulnerable to flooding.

2. MATERIALS AND METHODS

2.1 Study Area

Narainapur Rural Municipality, located in Banke District of Lumbini Province, Nepal, is situated at approximately 27.4° N latitude and 81.6° E longitude. This municipality is char- acterized by its flat terrain and proximity to the Rapti River, which significantly influences its hydrology and flood dynamics. The area experiences a subtropical monsoon climate, with the majority of its annual rainfall occurring from June to September, leading to substantial flood risks during the monsoon season. BIPAD (Building Information Platform Against Disaster) portal shows the average annual rainfall in Narainapur is around 1,500 mm, which is sufficient to trigger flooding, particularly in low-lying areas adjacent to the river. The demographic profile

of Narainapur includes a predominantly agricultural community, with rice, wheat, and sugarcane as the primary crops. The population is dispersed across several settlements, with many households located near the riverbanks, making them particularly susceptible to flood impacts. Historical flood events have caused significant damage to infrastructure, agricultural lands, and housing, displacing any residents and disrupting livelihoods.

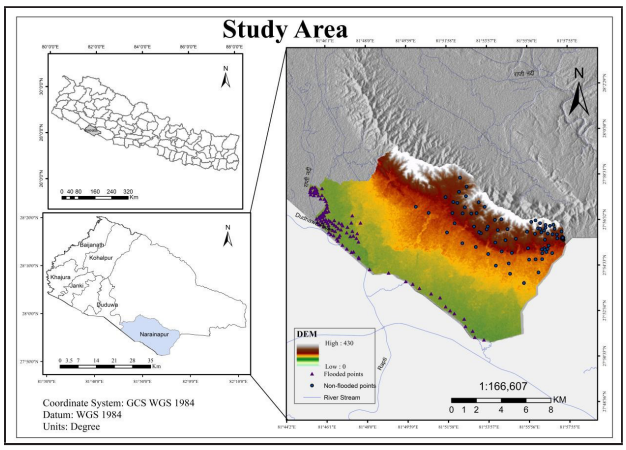

Figure 1. Study Area

2.2 Data Source

A high-resolution Landsat-08 satellite image acquired from March 2023 to October 2023, with a 30-meter spatial resolution, was utilized to generate a land use/ cover map of the study area. Additionally, a 30-meter Digital Elevation Model (DEM) was incorporated. This comprehensive geospatial dataset facilitated the production of detailed thematic maps, including slope, elevation, drainage density, distance to streams and aspect. These parameters are recognized as crucial factors in the generation of flood hazard maps.

Table 1. Data Source

Category	Type	Source	Resolution/ Scale
DEM	Raster	United States Survey(USGS)	30m
Landsat Images	Raster	United States Survey(USGS)	30m
Administrative boundary	Vector	National Geoportal	1 : 1000000
Rainfall	Raster	CHIRPS	5500m
Soil	Vector	National Soil Science Research Center NARC	1:10000

2.3 Flood Conditioning Factor

Slope

In the hydrological study, slope plays a vital role to regulate the flow of surface water, and slit is one of the most important topographic factors for such studies. Land surface slope is one of the effective factors in floods lower the slope higher is the intensity of flood and the higher the slope lower is the intensity of flood occurrence. The slope of a channel in a region is having a direct relationship with the flow velocity When the river slope increases then the flow velocity in the river also will increase. The slope has a direct relation to infiltration. An increase of the surface slope reduces the infiltration process but increases the surface runoff; as a result, in the regions having a lower surface slope, an enormous volume of water becomes stagnant and causes a flood situation. The slope map has been created from the Nasa Copernicus Digital elevation model (DEM) 30 m.

Normalized Difference vegetation index (NDVI)

The NDVI is another factor that is a valuable index in assessing vegetation coverage and its outcome on flooding in a study area. Normally NDVI value ranges from -1 to +1. NDVI map was prepared from satellite image of LANDSAT 8 OLI the NDVI values are calculated from below equation:

$$NDVI = (NIR - RED) / (NIR + RED) \quad \text{.....1}$$

The NDVI values ranged from -0.24 to 0.68 in the study area. Stated that the negative values show water and the positive values show vegetation. So, NDVI has negative relationship with flooding: higher NDVI values indicate lower probability of flood and lower NDVI values indicates higher flood probability.

Soil

The water holding capacity and surface infiltration characteristics of an area are determined by two main factors, such as soil type and texture . In this study, the study area was divided into 3 soil classes : Fluvial Non-Calcareous, Fluvial Calcareous and Sandstone/ Greywacke/Arkose . The soil type map was obtained from the NARC. The produced map was classified on the bases of the infiltration capacity; the weightage has been assigned to each soil type. Then after normalizing the values of soil types and making their pairwise comparsion, we get value 0.07 which is less than 0.1.

Distance from Stream

Distance from the river is one of the most important factors in flood hazard mapping. As the distance increases, the elevation and slope becomes higher. Also, Stream is generally the lowest point of that particular region. As a result of this, areas far from the river are having lower

vulnerability of flood occurrence. During floods, river banks get overflowed and submerge the dry land nearby the river. In this study we have classified distance from river in to five classes from very high (0 - 882 m), high (882 – 1,764 m), moderate (1,764 – 2647 m), low (2647 – 3529 m), and very low (3529 – 4,412). Lesser the distance from the river more is the flood vulnerability occurrence and more is the distance from the river lesser is the vulnerability.

Rainfall

It forms the most striking factor since the coastal area districts receive enough rainfall from both northeast and southwest monsoon, but northeast monsoon season (October to December is considered more rainy season than southwest monsoon. For the precipitation of the rainfall distribution map, the rainfall data of all the rain gauge stations have been calculated through the Inverse Distance Weighted (IDW) interpolation tool in ArcGIS 10.8.1 from Climate Hazards Group InfraRed Precipitation with Station data (CHIRPS).

Topographic Wetness Index (TWI) Topographic Wetness Index (TWI) indicates the effect of Topography on Runoff Generation and the amount of flow accumulation. The formula for calculating the TWI can be expressed as below:

$$TWI = In\ (As/tan\ \beta) \quad \text{..... 2}$$

Where, As represents the area and $\boldsymbol{\beta}$ indicates the local slope gradient in degree. Higher TWI regions have a higher potential of Vulnerability to flooding. Inversely, the lower TWI regions have a lower potential for Vulnerability.

Distance from Road

Distance from the road is also an important factor in quantifying flood vulnerability. During floods when water flows over banks of rivers incites as well as low lying areas flood water enters the roads and streams and damages the public properties and also damages the roads and houses as well.

Aspect

Aspect, or the direction a slope faces, is another vital factor in flood risk assessment, as it affects sun exposure, vegetation cover, and runoff patterns. For example, slopes facing away from direct sunlight tend to retain more moisture, leading to increased flood risk during heavy rainfall.

Curvature

Curvature is an important topographical parameter in flood risk assessment, as it determines the concavity or convexity of the land surface, which directly influences water flow and accumulation. Concave areas tend to collect water, increasing flood vulnerability, while convex areas facilitate water runoff, reducing flood risk.

2.4 Analytic Hierarchy Process

AHP is a multi-criteria decision-making approach and was introduced by Satty. The AHP is a decision support tool. It is used to solve complex decision problems, uses a multi-level hierarchical structure of objectives, criteria, sub criteria and alternatives. It determines the weights and ranks of different parameters for the flood vulnerable zones (FVZ). For preparing the all-thematic layers, the AHP model has been Grouping the prepared thematic maps into five vulnerable categories, an AHP-based pair-wise comparison matrix of different variables described above is constructed. The model is applied to assign varied weights for comparing the ten individual factors, and according to their relative importance, these nine parameters are rated from 1 to 9 as shown in table 2 on an absolute number scale. Pair-wise comparison scale weights on the bases of AHP scale. The selected factors considered for the analysis are as follows: Slope, Curvature, Distance to Stream, NDVI, Soil, Road, Aspect, Rainfall, and TWI. These factors were carefully chosen based on their significance and relevance to the study. The corresponding rating values assigned to each factor, which reflect their relative importance and contribution to the analysis, are presented below.

Table 2. Pair-wise comparison scale weights on the bases of AHP scale

Scale	Judgment of preference	Description
1	Equally Important	Two factors contribute equally to the objective
3	Moderate Important	Experience and judgment slightly favour one over the other
5	Important	Experience and judgment strongly important favour one over the other
7	Very strongly Important	Experience and judgment strongly important favour one over the other
9	Extremely Important	The evidence favoring one over the other is of the highest possible validity
2,4,6,8	Intermediate preference between adjacent scales	When compromised is needed

Consistency ratio

To rectify the constructed pair- wise matrix and its given weightage method is done by the following equation: evaluation through the consistency ratio (CR) was formulated where the acceptable CR must be blow 0.1. In the present study, the consistency of the derived Eigen vector- matrix following the index below found is 0.063 concludes that the set of decision considered is acceptable.

CR = CI/ RI 3

CI = $\lambda max - n / n - 1$ 4

Where CR represents the consistency ratio, CI stands for the consistency index, RI indicates the random index., λ max represents the principle Eigen value of the comparison matrix, and n is the number of components or factors in matrix. RI refers to the consistency of the randomly evolved pair-wise matrix depicted in normalized values. The values provided in the table 3 are subjected to various parameters involved in AHP.

Table 3. Random Index (RI) Value

Number of criteria	2	3	4	5	6	7	8	9	10	11
RI	0	0.58	0.9	1.12	1.24	1.32	1.41	1.45	1.49	1.51

FVI = ∑ Wi∗Ri $n\ i$=1where WI is the individual weights for individual flood conditioning of each parameter, and RI is the rating class.

The normalized values and the corresponding weight values in the standardized pair-wise comparison matrix are important for ensuring consistency in the Analytical Hierarchy Process (AHP).It ensures that the sum of the values in each column equals one, allowing for the determination of the priority vector or weightage for each criterion. The weightage derived from the normalized pair-wise comparison matrix, calculated based on table-4, is presented below in table-5 which represent the relative importance of each criterion and serve as the foundation for further analysis.

3. RESULT AND ANALYSIS

3.1 Flood Conditioning Factor Map

To ensure consistency and comparability in flood risk assessment, all factor maps were first normalized. This standardization process allows for a uniform scale of analysis, enhancing the accuracy of spatial interpretations. The factor maps were then processed and presented in raster format using a stretched scale to effectively capture variations across the study area. Each factor plays a significant role in flood susceptibility. Curvature influences water flow accumulation by defining terrain shape, while soil type affects infiltration capacity and surface runoff behavior. Distance to roads impacts drainage patterns, and distance to streams determines proximity to potential flood sources. Slope governs water velocity and runoff distribution, whereas rainfall is a direct contributor to flood potential. Topographic Wetness Index (TWI) helps identify moisture retention zones, and Normalized Difference Vegetation Index (NDVI) provides insights into vegetation cover, which influences soil permeability and runoff regulation. The spatial distribution of these factors is essential for understanding flood prone areas and their contributing elements.

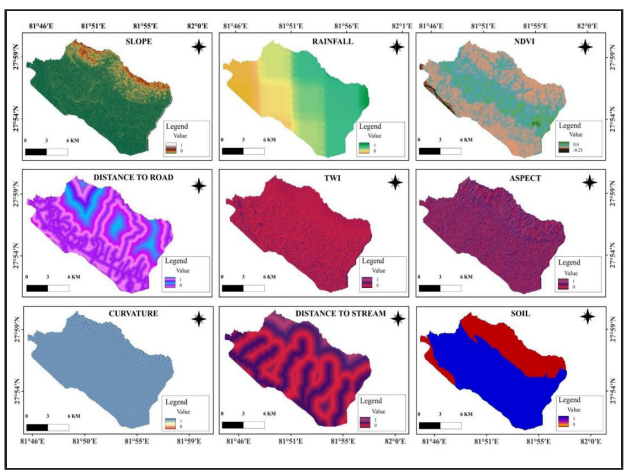

Figure 2. Parameters Map

3.2 Flood Susceptibility Map

The Analytic Hierarchy Process (AHP)

The Analytic Hierarchy Process (AHP) was utilized to assess the significance of various flood conditioning factors. Firstly, the Consistency Ratio (CR) for all factors was calculated to ensure the reliability of the pairwise comparisons, as presented in the table 5. A CR value of less than 0.1 indicates acceptable consistency in the judgments. After verifying consistency, the Pairwise Comparison Matrix was constructed to evaluate the relative importance of each factor in the study area. Based on this matrix, weightages for each factor were determined, which are displayed in the corresponding table 6. Once the weightages were finalized, they were applied to the factor maps to generate a comprehensive flood susceptibility map. The final maps were then classified into five distinct flood risk categories: Very Low, Low, Moderate, High, and Very High as shown in figure 3, ensuring a clear representation of flood-prone areas for effective risk assessment and management.

Table 4. Parameters Criteria

Criteria	Class	Weightage	Remark	C.R
Slope	0.00 -0.05	0.5	Very High	0.054
	0.05 -0.12	0.26	High	
	0.12 -0.22	0.13	Moderate	
	0.22 -0.54	0.07	Low	
	0.54 -1.00	0.03	Very Low	
NDVI	0.00 -0.05	0.52	Very High	0.038
	0.05 -0.16	0.25	High	
	0.16 -0.27	0.13	Moderate	
	0.27 -0.36	0.06	Low	
	0.36 -0.66	0.03	Very Low	
Soil Type	Fluvial Non-Calcareous	0.63	High	0.07
	Fluvial Calcareous	0.26	Moderate	
	Sandstone/Greywacke/Arkose	0.11	Low	
Distance to Stream	0.00 -0.12	0.51	Very Low	0.03
	0.12 -0.25	0.25	Low	
	0.25 -0.41	0.12	Moderate	
	0.41 -0.62	0.07	High	
	0.62-1.00	0.05	Very High	
Rainfall	0.00 -0.17	0.05	Very Low	0.014
	0.17 -0.36	0.08	Low	
	0.36 -0.53	0.13	Moderate	
	0.53 -0.71	0.21	High	
	0.71-1.00	0.53	Very High	
TWI	0.00 -0.24	0.06	Very Low	0.022
	0.24 -0.33	0.09	Low	
	0.33 -0.44	0.14	Moderate	
	0.44 -0.60	0.23	High	
	0.60-1.02	0.48	Very High	
Distance to Road	0.00-0.10	0.43	Very High	0.015
	0.10-0.25	0.26	High	
	0.25-0.43	0.16	Moderate	
	0.43 -0.66	0.09	Low	
	0.66-1	0.06	Very Low	
Aspect	0.00 -0.23	0.53	Very High	0.029
	0.23 -0.41	0.23	High	
	0.41 -0.57	0.12	Moderate	
	0.57 -0.74	0.07	Low	
	0.74 -1.00	0.04	Very Low	
Curvature	0.00 -0.25	0.42	Very High	0.026
	0.25 -0.41	0.26	High	
	0.41 -0.54	0.17	Moderate	
	0.54 -0.68	0.09	Low	
	0.68-1.00	0.06	Very Low	

Table 5.Pair-wise comparison of 9*9 decision matrix

Factors	Slope	Curvature	Distance Stream	NDVI	Soil	Road	Aspect	Rainfall	TWI
Slope	1.00	7.00	3.00	4.00	5.00	9.00	8.00	2.00	6.00
Curvature	0.14	1.00	0.20	0.25	0.33	3.00	2.00	0.17	0.50
Distance to Stream	0.33	5.00	1.00	2.00	3.00	7.00	6.00	0.50	4.00
NDVI	0.25	4.00	0.50	1.00	2.00	6.00	5.00	0.33	3.00
Soil	0.20	3.00	0.33	0.50	1.00	5.00	4.00	0.25	2.00
Road	0.11	0.33	0.14	0.17	0.20	1.00	0.33	0.13	0.25
Aspect	0.13	0.50	0.17	0.20	0.25	3.00	1.00	0.14	0.33
Rainfall	0.50	6.00	2.00	3.00	4.00	8.00	7.00	1.00	5.00
TWI	0.17	2.00	0.25	0.33	0.50	4.00	3.00	0.20	1.00
Total	2.83	28.83	7.59	11.45	16.28	46.00	36.33	4.72	22.08

Table 6. Normalized and the weight values in the standardized pair-wise comparison matrix

Factors	Slope	Curvature	Distance to Stream	Rainfall	Soil	Road	Aspect	NDVI	TWI
Slope	0.35	0.24	0.4	0.35	0.31	0.2	0.22	0.42	0.27
Curvature	0.05	0.03	0.03	0.02	0.02	0.07	0.06	0.04	0.02
Distance to Stream	0.12	0.17	0.13	0.17	0.18	0.15	0.17	0.11	0.18
Rainfall	0.09	0.14	0.07	0.09	0.12	0.13	0.14	0.07	0.14
Soil	0.07	0.1	0.04	0.04	0.06	0.11	0.11	0.05	0.09
Road	0.04	0.01	0.02	0.01	0.01	0.02	0.01	0.03	0.01
Aspect	0.04	0.02	0.02	0.02	0.02	0.07	0.03	0.03	0.02
NDVI	0.18	0.21	0.26	0.26	0.25	0.17	0.19	0.21	0.23
TWI	0.06	0.07	0.03	0.03	0.03	0.09	0.08	0.04	0.05

Therefore, based on the nine variables, the derived RI obtained in the study is 1.49 and the obtained CR is 0.063

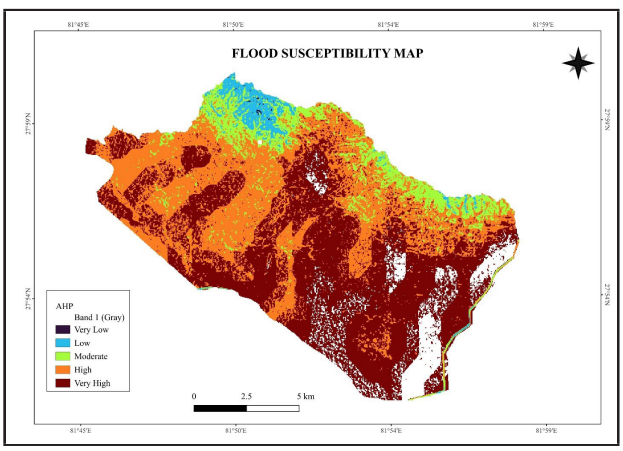

Figure 3. Flood Susceptibility Map

4.CONCLUSION

The flood risk assessment using the Analytic Hierarchy Process (AHP) was successfully conducted by integrating nine causative factors: curvature, soil, distance to road, distance to stream, slope, rainfall, Topographic Wetness Index (TWI), Normalized Difference Vegetation Index (NDVI), and aspect. By assigning appropriate weights through AHP based on the relative importance of each parameter, the study systematically classified the area into different flood risk zones. The approach proved effective in identifying areas vulnerable to flooding, providing valuable insights for targeted disaster preparedness and management efforts.

REFERENCES

1) Choubin, B., Moradi, E., Golshan, M., Adamowski, J., Sajedi-Hosseini, F., & Mosavi, A. (2019). An ensemble prediction of flood susceptibility using multivariate discriminant analysis, classification and regression trees, and support vector machines. *Science of The Total Environment*, *651*,2087–2096.

2) Danumah, J. H., Odai, S. N., Saley, B. M., Szarzynski, J., Thiel, M., Kwaku, A., Kouame, F. K., & Akpa, L. Y. (2016). Flood risk assessment and mapping in Abidjan district using multi-criteria analysis (AHP) model and geoinformation techniques, (cote d'ivoire). *Geoenvironmental Disasters*, *3*(1),

3) Djalante, R. (2018). Review article: A systematic literature review of research trends and authorships on natural hazards, disasters, risk reduction and climate change in Indonesia. *Natural Hazards and Earth System Sciences*, *18*(6), 1785–1810.

4) Efraimidou, E., & Spiliotis, M. (2024). A GIS-Based Flood Risk Assessment Using the Decision-Making Trial and Evaluation Laboratory Approach at a Regional Scale. *Environmental Processes*, *11*(1), 9.

5) Gayen, S., Villalta, I. V., & Haque, S. M. (2022). Flood Risk Assessment and Its Mapping in Purba Medinipur District, West Bengal, India. *Water*, *14*(7), Article 7.

6) Guragain, U. P., & Doneys, P. (2022). Social, Economic, Environmental, and Physical Vulnerability Assessment: An Index-Based Gender Analysis of Flood Prone Areas of Koshi River Basin in Nepal. *Sustainability*, *14*(16), Article 16.

7) Khatakho, R., Gautam, D., Aryal, K. R., Pandey, V. P., Rupakhety, R., Lamichhane, S., Liu, Y.-C., Abdouli, K., Talchabhadel, R., Thapa, B. R., & Adhikari, R. (2021). MultiHazard Risk Assessment of Kathmandu Valley, Nepal. *Sustainability*, *13*(10), Article 10.

8) Le Cozannet, G., Garcin, M., Bulteau, T., Mirgon, C., Yates, M. L., Méndez, M., Baills, A., Idier, D., & Oliveros, C. (2013). An AHP-derived method for mapping the physical vulnerability of coastal areas at regional scales. *Natural Hazards and Earth System Sciences*, *13*(5), 1209–1227.

9) Liu, R., Chen, Y., Wu, J., Gao, L., Barrett, D., Xu, T., Li, L., Huang, C., & Yu, J. (2016). Assessing spatial likelihood of flooding hazard using naïve Bayes and GIS: A case study in Bowen Basin, Australia. *Stochastic Environmental Research and Risk Assessment*, *30*(6), 1575–1590.

10) Malla, S., & Ohgushi, K. (2024). Flood vulnerability map of the Bagmati River basin, Nepal: A comparative approach of the analytical hierarchy process and frequency ratio model. *Smart Construction and Sustainable Cities*, *2*(1), 16.

11) Ologunorisa, T. E., & Abawua, M. J. (n.d.). Flood Risk Assessment: A Review. *Journal of Applied Sciences and Environmental Management*, *9*(1), 57–63.

12) Perera, E. D. P., Hiroe, A., Shrestha, D., Fukami, K., Basnyat, D. B., Gautam, S., Hasegawa, A., Uenoyama, T., & Tanaka, S. (2015). Community-based flood damage assessment approach for lower West Rapti River basin in Nepal under the impact of climate change. *Natural Hazards*, *75*(1), 669–699. https://doi.org/10.1007/s11069-014-1339-5

13) Rincón, D., Khan, U. T., & Armenakis, C. (2018). Flood Risk Mapping Using GIS and Multi-Criteria Analysis: A Greater Toronto Area Case Study. *Geosciences*, *8*(8),

14) Gacu, J. G., Monjardin, C. E. F., Senoro, D. B., & Tan, F. J. (2022). Flood risk assessment using GIS-based analytical hierarchy process in the municipality of Odiongan, Romblon, Philippines. *Applied Sciences, 12*(19), 9456

15) Cai, S., Fan, J., & Yang, W. (2021). Flooding risk assessment and analysis based on GIS and the TFN-AHP method: A case study of Chongqing, China. *Atmosphere, 12*(5), 623.

16) Khanal, N., Shrestha, M., & Chimire, M. (2007). Flood hazard, risk, and vulnerability in Nepal: The physical and socioeconomic environment.

17) Kumar, N., & Jha, R. (2023). GIS-based flood risk mapping: The case study of Kosi River Basin, Bihar, India. *Engineering, Technology & Applied Science Research, 13*(1), 9830–9836. https://www.etasr.com

18) Stefanidis, S., & Stathis, D. (2013). Assessment of flood hazard based on natural and anthropogenic factors using analytic hierarchy process (AHP). *Natural Hazards*, *68*(2), 569–585. https://doi.org/10.1007/s11069-013-0639-5

AUTHOR INFORMATION

Name	: Rubi Chaulagain
Academic Qualification	: BE in Geomatics Engineering
Organization	: Western Regional Campus
Current Designation	: Geomatics Engineer
Work Experience	: 3 months
Published Article	: 1

COMPARITIVE ANALYSIS BETWEEN AHP & FUZZY AHP: A CASE STUDY ON FLOOD SUSCEPTIBILITY OF KOSHI RIVER BASIN

Aashish Kumar Karki[1], Bipul Chaudhary[1], Dikshya Khadka[1], Pratiksha Dahal[1], Rupa Bajgain[1] , Dr. Reshma Shrestha[1], Er. Ajay Kumar Thapa [2]

[1]Department of Geomatics Engineering, Kathmandu University, Dhulikhel, Nepal

karkiaashish899@gmail.com, bipulchaudhary2000@gmail.com, dikshyakhadka524@gmail.com, dahalpratiksha409@gmail.com, rupabajgain33@gmail.com, reshma@ku.edu.np

[2]Florida Atlantic University–*ajaythapa0061@gmail.com*

ABSTRACT

The report compares the Analytic Hierarchy Process (AHP) and Fuzzy Analytic Hierarchy Process (FAHP) for flood susceptibility assessment in the Koshi Basin area. Both models are used in multi-criteria decision-making, but their effectiveness in handling complex environmental conditions varies. The study evaluates and compares the performance of these models in predicting flood-prone areas using the Area Under the Curve (AUC) of the Receiver Operating Characteristic (ROC) as a performance metric. The results show that the majority of the region falls under moderate flood risk, with low-risk zones accounting for 35.04% and 31.41%, and high-risk areas covering 12.67% and 13.33%. The topographical wetness index was the most weighted criteria in both models, while aspect was the least affecting criteria. The AHP model showed good predictive capability with an AUC of 0.758, while the FAHP model demonstrated superior performance with an AUC of 0.802, attributed to its incorporation of fuzzy logic..

KEYWORDS: Multi Criteria Decision Making/Analysis, AHP, FAHP, GIS, Flood, ROC & AUC Curve.

1. INTRODUCTION

1.1 Background

Flood is graded as one of the most calamitous disasters affecting 170 million people around the globe and is also accountable for more than 60 percent of deaths related to natural calamities (Bouamrane et al., 2022). The positive and negative effects of the catastrophe appear widely imbalanced as the negative effects weighs in more since the calamity is limited not only to affecting human and livestock's lives but also economy, food security, social insecurity etc. The impacts of flood are difficult to inspect on a larger area since it is highly influenced by various socioeconomic and demographic factors (Atiye Cikmaz et al., 2022). Due to the severity of the calamity, it is profoundly important to identify the areas under the flood risks and design various mitigation measures to address the catastrophe during its occurrence. With the advancement in the GIS and RS techniques and also with the development of statistical models such as AHP, we can precisely inspect the flood susceptible areas and in turn apply the various mitigation plans to minimize the effect of the catastrophe as much as possible (Atiye Cikmaz et al., 2022).

In the context of above topic, GIS can be defined as a decision support system involving the integration of spatially referenced data in a problem-solving environment (Sivakumar et al., 2003). With the help of varieties of tools in the working environment of GIS and RS, various qualitative and quantitative analysis can be created, understood, visualized and a meaningful result can be produced accordingly. The intent of dealing with a complex multi-dimensional dynamic issue such as flood is easily assisted by GIS along with the integration of some other disciplines as well.

Flood risk mapping is often a challenging task to provide a comprehensive risk assessment by covering social, economic, and geophysical processes as a whole (Noor et al., 2017). Conventionally, flood hazard assessment is conducted via hydrological and hydraulic modelling by estimating the flooding depth and extent for various return-periods but the application of these modelling

techniques requires a range of observed data that

are not always available (Sivakumar et al., 2003). When the focus primarily shifted to developing feasible models which would help better understand the various criterion of different phenomenon and the relationship between such criterion, the concept of various MCDA/MCDM models such as Frequency Ratio, AHP, Logistic Regression etc. came into existence (Bouamrane et al., 2022).

AHP is one of such MCDA models commonly used. In the AHP, the decision-making process of complex problems is conducted by dividing the problem into issues, which may be divided further to form a simple and comprehensible hierarchical structure (Bouamrane et al., 2022). Developed by Saaty in 1980, it is considered a mathematical approach to MCDM (Hammami et al., 2019). This technique evaluates the importance of factors, according to weight values from human judgement and preferences.

Another method in MCDA is the Fuzzy AHP method. The fuzzy set theory is used to address the ambiguity and uncertainty issue occurring in AHP and incorporate human judgement and preference with least amount of error. The weights in AHP are either in Crisp Scale or in Linguistic Terms. Fuzzy AHP assigns a membership function (one that defines the relationship between an independent variable and a dependent variable, degree of membership) to each linguistic terms rather than assigning a single value.

2. MATERIALS AND METHODS

2.1 Study Area

The study area covers the Koshi River within Nepal, where it flows through the eastern region and accounts for 45% of the total 87,311 km² transboundary basin.

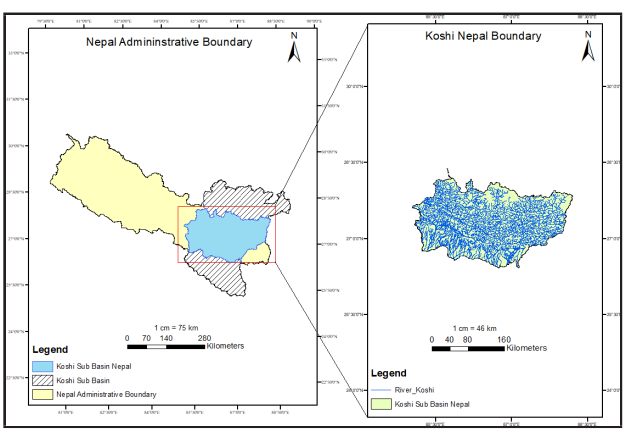

Figure 1: Koshi River Basin

2.2 Methodology

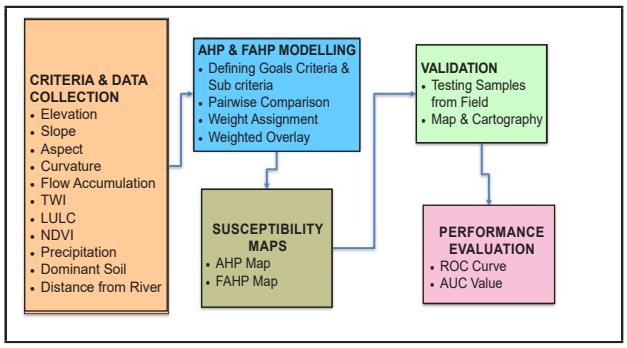

Figure 2. Methodological Workflow.

2.2.1 Data Collection

Various spatial and environmental datasets were collected from **Secondary Sources**, including Digital Elevation Model (DEM), land use/land cover (LULC), Normalized Difference Vegetation Index (NDVI), rainfall data, dominant soil type, and river shapefiles relevant to the study area.

2.2.2 Data Preprocessing and Analysis

i. DEM Processing: Mosaic, Extract by Mask, Slope/ Aspect/Curvature.

ii. Hydrological Analysis: Fill, Flow Direction, Flow Accumulation, TWI.

iii. Thematic Layers: Rainfall Interpolation, NDVI (GEE), Soil, LULC, River Distance.

iv. Standardization: Clip, Project Raster, Resample, Reclassify.

v. Overlay & Analysis: Weighted Overlay, Susceptibility Mapping, Validation.

2.2.3 Data Re-Classification

Determining how different thematic layers, such as elevation, slope, land cover, and proximity to rivers, naturally affect flooding is the first stage in flood susceptibility mapping. The subsequent reclassification of these layers into standardized classes and their normalization for comparative analysis in a multi-criteria evaluation are informed by this crucial understanding, which is derived from established hydrological principles, expert knowledge, and frequently preliminary spatial analysis.

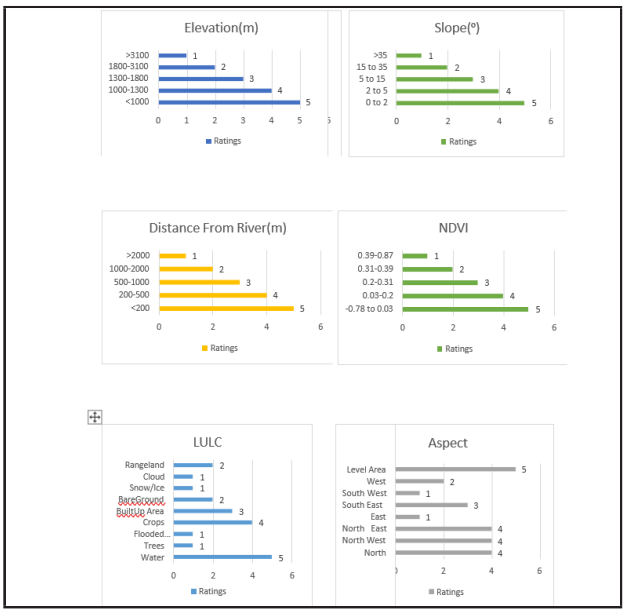

Figure 3. Criteria Reclassification (1)

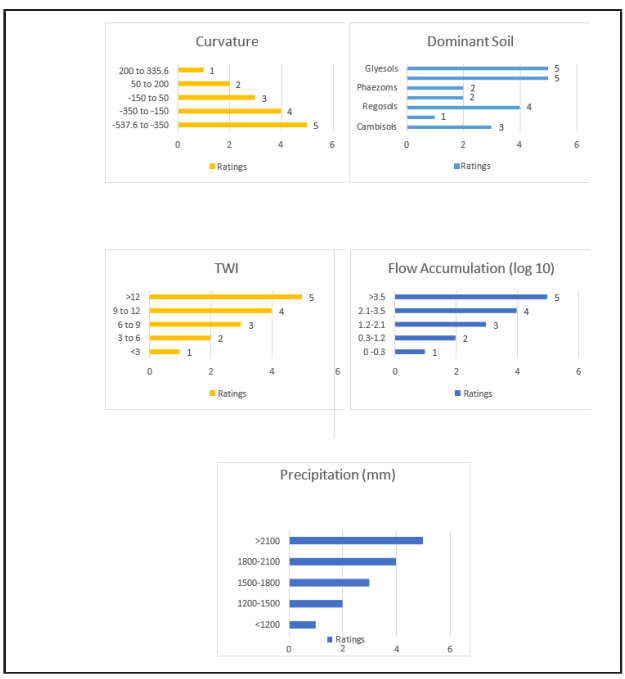

Figure 4. Criteria Reclassification (2)

Table 1. Criteria Rating Description

S.N.	Effect	Criteria Ratings
1	Very Low	1
2	Low	2
3	Moderate	3
4	High	4
5	Very High	5

The provided figures consist of horizontal bar charts representing the rating scales assigned to various criteria used in flood susceptibility mapping. These ratings reflect how different ranges or categories within each factor contribute to flood risk, typically for use in AHP or FAHP-based MCDA models. For instance, lower elevations and gentler slopes are given higher ratings due to their greater tendency to accumulate water, increasing flood susceptibility. Proximity to rivers (e.g., within 0–200 meters) is also rated higher, as areas closer to water bodies are more prone to flooding. Vegetation cover, measured by NDVI, and land use types (e.g., built-up or rangeland) are considered for their ability to absorb or repel water. Aspect (slope orientation) is rated based on its influence on microclimate and runoff patterns. Other critical terrain attributes like curvature (shape of the land), TWI (Topographic Wetness Index), and flow accumulation highlight the landscape's capacity to store or direct water, with higher values indicating greater risk. Soil types, such as Gleyerats or Regosols, are evaluated for permeability and retention capacity, while higher precipitation levels are also assigned higher flood susceptibility ratings. These charts collectively support a structured and evidence-based approach to quantifying flood risks spatially.

2.2.4 AHP/FAHP Methodology

AHP and FAHP methods were used to assign weights to flood susceptibility factors. Expert judgment was collected to build pairwise comparison matrices, and consistency was checked. FAHP incorporated fuzzy logic to handle uncertainty in data and expert opinions, allowing for more flexible decision-making.

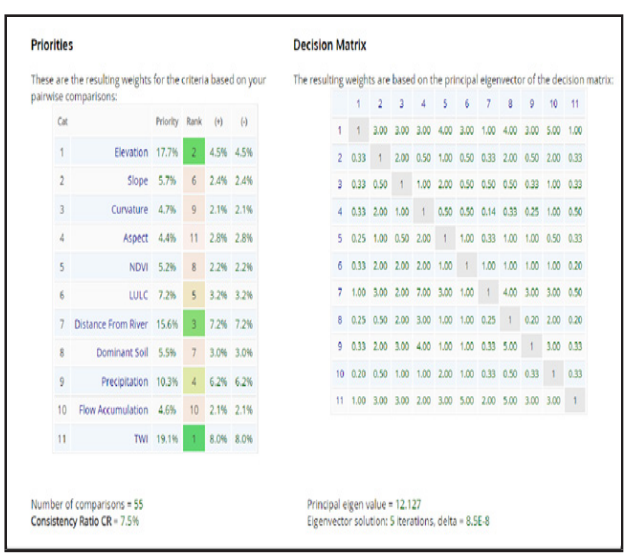

Figure 5. Criteria Weights in AHP

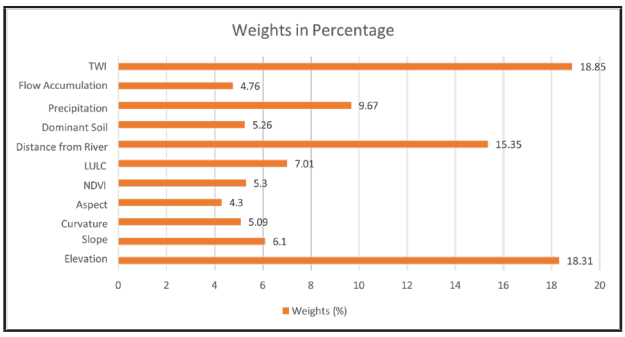

Figure 6. Criteria Weights in FAHP

2.2.5 Flood Susceptibility Mapping and Model Validation

The weighted criteria were used to generate a flood susceptibility map, classifying areas by risk. Model accuracy was validated with ROC curves, and adjustments were made to improve reliability.

3. RESULTS AND DISCUSSION

3.1 AHP and FAHP Results

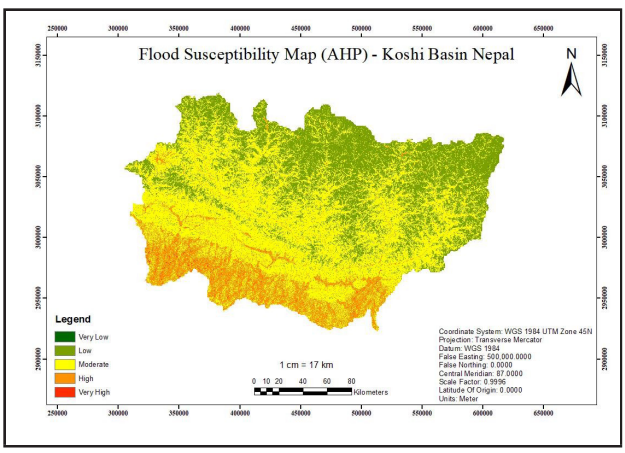

Figure 7. AHP Based Flood Susceptible Map

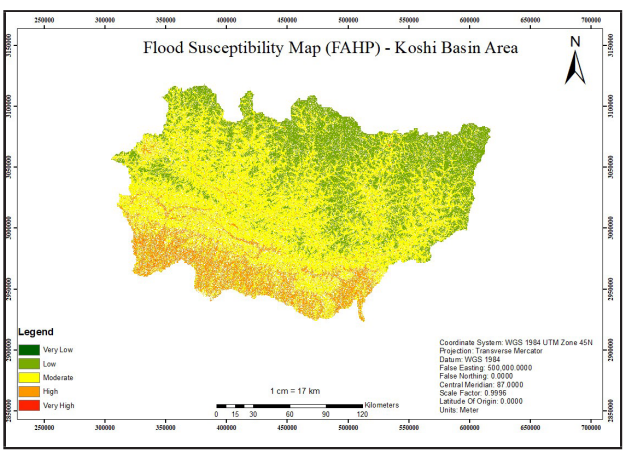

Figure 8. FAHP Based Flood Susceptible Map

ROC VALUE OF THE AUC CURVE FOR BOTH MODELS

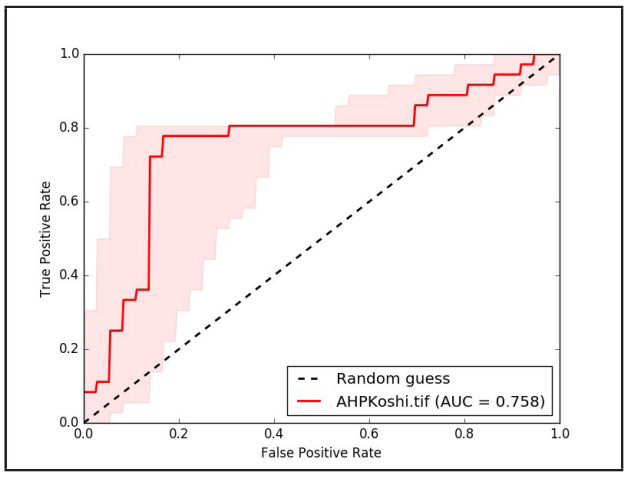

Figure 9. AHP Validation Curve

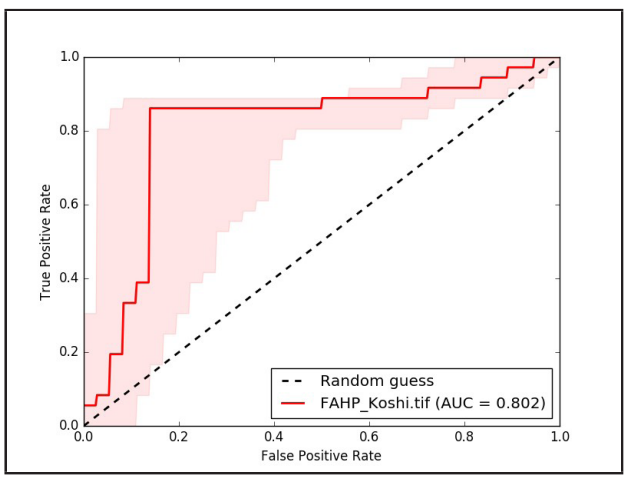

Figure 10. FAHP Validation Curve

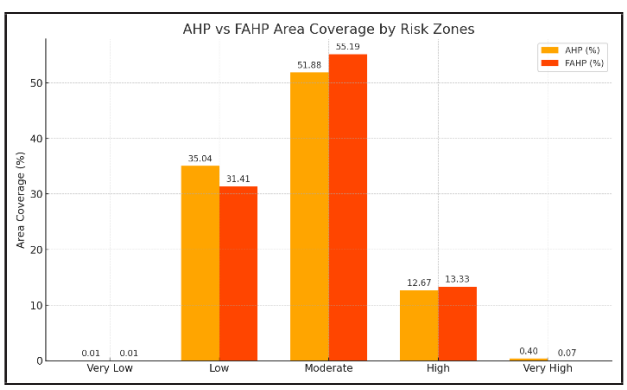

Figure 11. Area Coverage in the Models

In **Figure 7** and **8**, the AUC Value of the FAHP model is 0.802 while that of the AHP model is 0.758. An AUC of 0.758 indicates that the AHP model has good predictive performance for flood susceptibility. This means the model is able to correctly distinguish between flood-prone and non-flood-prone areas 75.8% of the time.

Similarly, an AUC of 0.802 indicates that the FAHP model has better predictive performance compared to the AHP model. This model correctly distinguishes between flood-prone and non-flood-prone areas 80.2% of the time. The predictive performance of these models is assessed using the Receiver Operating Characteristic (ROC) curve, which illustrates the trade-off between the true positive rate (sensitivity) and false positive rate (1 – specificity) at various threshold settings. The Area Under the Curve (AUC) provides a single quantitative measure of model accuracy. An AUC value of 0.5 corresponds to random guessing, indicating the model has no discriminatory power. Values closer to 1 signify better performance, meaning the model reliably differentiates between flooded and non-flooded areas. Thus, the higher the AUC, the more effective the model is at correctly predicting flood susceptibility beyond chance.

4. CONCLUSION

Our study compared the Analytic Hierarchy Process (AHP) and the Fuzzy Analytic Hierarchy Process (FAHP) to assess flood vulnerability in the Koshi Basin region with additional information about susceptible areas, highly affecting criteria etc. The flood susceptibility analysis of the Koshi Basin Area, using the Analytical Hierarchy Process (AHP) and the Fuzzy Analytical Hierarchy Process (FAHP), reveals that the majority of the region falls under moderate flood risk, covering 51.88% and 55.19% of the area respectively. Low-risk zones account for 35.04% (AHP) and 31.41% (FAHP), while high-risk areas cover 12.67% (AHP) and 13.33% (FAHP). Very low and very high-risk zones are minimal in both models. These findings highlight the necessity for targeted flood management in moderate and high-risk areas and the importance of multiple analytical approaches for effective flood prevention and resilience planning in the Koshi Basin. Topographical Wetness Index was the criteria with most weights in both the models, about nineteen percent. Aspect was the least affecting criteria with about only four percent weightage.

The AUC of the ROC was used to evaluate the performance of each model, resulting in an AUC of 0.758 for AHP and 0.802 for FAHP. The findings suggest that even though both models show strong predictive abilities, the FAHP model performs better than the AHP model. The FAHP model's AUC of 0.802 suggests a higher level of accuracy and dependability in forecasting flood-prone areas in comparison to the AHP model's AUC of 0.758. Bouamrane et al. conducted similar comparative assessment as "A comparison of the analytical hierarchy process and the fuzzy logic approach for flood susceptibility mapping in a semi-arid ungauged basin (Biskra basin: Algeria)" with similar conclusions as well. This enhancement is credited to the FAHP model's integration of fuzzy logic, enabling more effective management of uncertainty and imprecision in the input data and criteria weights. The superior capability of the FAHP model to capture the complex and uncertain flood susceptibility factors in the Koshi Basin area is emphasized by its enhanced performance. This enhances the FAHP model as a stronger tool for evaluating flood risk, offering important information for efficient flood control and reduction tactics.

REFERENCES

Atiye Cikmaz, B., Yildirim, E., & Demir, I. (2022). Flood Susceptibility Mapping using Fuzzy Analytical Hierarchy Process for Cedar Rapids, Iowa.

Bouamrane, A., Derdous, O., Dahri, N., Tachi, S. E., Boutebba, K., & Bouziane, M. T. (2022). A comparison of the analytical hierarchy process and the fuzzy logic approach for flood susceptibility mapping in a semi-arid ungauged basin (Biskra basin: Algeria). International Journal of River Basin Management,20(2),203213. https://doi.org/10.1080/15715124.2020.1830786

Chen, Y., Zhang, X., Yang, K., Zeng, S., & Hong, A. (2023). Modeling rules of regional flash flood susceptibility prediction using different machine learning models. Frontiers in Earth Science, 11. https://doi.org/10.3389/feart.2023.1117004

Hammami, S., Zouhri, L., Souissi, D., Souei, A., Zghibi, A., Marzougui, A., & Dlala, M. (2019). Application of the GIS based multi-criteria decision analysis and analytical hierarchy process (AHP) in the flood susceptibility mapping (Tunisia). In Arabian Journal of Geosciences (Vol. 12, Issue 21). Springer Verlag. https://doi.org/10.1007/s12517-019-4754-9

Helmy, S. E., Eladl, G. H., & Eisa, M. (2021). FUZZY ANALYTICAL HIERARCHY PROCESS (FAHP) USING GEOMETRIC MEAN METHOD TO SELECT BEST PROCESSING FRAMEWORK ADEQUATE TO BIG DATA. Journal of Theoretical and Applied Information Technology, 15(1). www.jatit.org

Kafle, M. R., & Shakya, N. M. (2018). Multi-Criteria Decision Making Approach for Flood Risk and Sediment Management in Koshi Alluvial Fan, Nepal. Journal of Water Resource and Protection, 10(06), 596–619. https://doi.org/10.4236/jwarp.2018.106034

Khosravi, K., Shahabi, H., Pham, B. T., Adamowski, J., Shirzadi, A., Pradhan, B., Dou, J., Ly, H. B., Gróf, G., Ho, H. L., Hong, H., Chapi, K., & Prakash, I. (2019). A comparative assessment of flood susceptibility modeling using Multi-Criteria Decision-Making Analysis and Machine Learning Methods. Journal of Hydrology,573,311–323. https://doi.org/10.1016/j.jhydrol.2019.03.073

Kwong, C. K., & Bai, H. (2002). A fuzzy AHP approach to the determination of importance weights of customer requirements in quality function deployment. Journal of Intelligent Manufacturing, 13(5), 367–377. https://doi.org/10.1023/A:1019984626631

Malczewski, J., & Rinner, C. (2015). Introduction to GIS-MCDA. In Advances in Geographic Information Science (Issue 9783540747567, pp. 23–54). Springer Heidelberg.

https://doi.org/10.1007/978-3-540-74757-4_2

Noor, A. Z. M., Fauadi, M. H. F. M., Jafar, F. A., Nordin, M. H., Yahaya, S. H., Ramlan, S., Shri, M. A., & Aziz, A. (2017). FUZZY ANALYTIC HIERARCHY PROCESS (FAHP) INTEGRATION FOR DECISION MAKING PURPOSES: A REVIEW.

Saaty, T. L., & Vargas, L. G. (2013). Decision Making with the Analytic Network Process (Vol. 195). Springer US.

https://doi.org/10.1007/978-1-4614-7279-7

Sivakumar, M. V. K., Roy, P. S., Harmsen, K., & Saha, S. K. (2003). Satellite Remote Sensing and GIS Applications in Agricultural Meteorology World Meteorological Organization (WMO) India Meteorological

Department (IMD) Centre for Space Science and Technology Education in Asia and the Pacific (CSSTEAP) Indian Institute of Remote Sensing (IIRS) National Remote Sensing Agency (NRSA) and Space Application Centre (SAC).

http://www.bishensinghbooks.com

Stofkova, J., Krejnus, M., Stofkova, K. R., Malega, P., & Binasova, V. (2022). Use of the Analytic Hierarchy Process and Selected Methods in the Managerial Decision-Making Process in the Context of Sustainable Development. Sustainability (Switzerland),14(18). https://doi.org/10.3390/su141811546

Vinogradova-Zinkevič, I., Podvezko, V., & Zavadskas, E. K. (2021). Comparative assessment of the stability of AHP and FAHP methods. Symmetry, 13(3).

https://doi.org/10.3390/sym13030479

AUTHOR INFORMATION

Name	:	**Dikshya Khadka**
Academic Qualification	:	BE in Geomatics Engineering
Organization	:	Kathmandu University
Current Designation	:	Student
Published Article	:	1

TRANSFORMING SURVEY OFFICES: TECHNOLOGY, MANAGEMENT AND COORDINATION

Ram Kumar Sapkota
Land Management Training Center - *ramksap1@gmail.com*

ABSTRACT

This article tries to explore practical and innovative ideas to enhance service delivery, transparency, and efficiency in Survey Offices through low-cost, technology-driven, and coordination-based initiatives. It outlines how simple interventions in office management, good governance, record preservation, and the use of information technology- when integrated with proper collaboration and coordination can transform survey offices of the country. Without considering major legal or structural changes, the article emphasizes creativity, leadership, and the tactical use of existing resources to improve public satisfaction, streamline workflows, and promote good governance in Survey Offices. Through the suggested measures, Survey Offices can enhance public trust, accelerate service delivery, reduce procedural delays, and contribute to more accountable and citizen-focused cadastral services.

KEYWORDS: Transformation, Good Governance, Record Management, Innovation, Low-cost Reform, NeLIS

1. BACKGROUND

The Survey office is a government institution under Survey Department, Ministry of Land Management, Cooperatives and Poverty Alleviation that provides services in sensitive areas of cadastre and supports parcel-based land administration of the country. Currently, such services are being provided through 135 survey offices across the country. In line with the concept of a Parcel-Based Land Administration System, the issuance of the Land Survey Act , 2019 led to the systematic preparation of cadastral maps and associated records through Survey Goshwaras. Later, updates to these maps were handled by the maintenance branch, which evolved through the survey branch into the current structure of survey offices. The core responsibilities of survey offices include preserving, storing, and updating cadastral maps, and associated registers. After the dissolution of the Survey Goshwaras in 2065 BS, in addition to updates of maps and records, resurveying is also being carried out by survey offices assigned by Survey Department. Essentially, survey offices handle tasks such as parcel subdivision, consolidation, field book and parcel register extraction, field demarcation, tile checks, and technical support for cadastral issues. Depending on available resources, they also carry out resurveying in allocated areas, preparing cadastral maps and field books, registering land, issuing land ownership certificates, preparing land registration records, and hand over to relevant land revenue offices. To make services timely, simple, efficient, transparent, and technology-friendly, many innovative and reformative actions can be implemented in survey offices. Some offices have already initiated such practices, while others are progressing. This article is prepared to help all survey offices introduce timely improvements and move forward innovatively based on practical experience, best practices, and study.

2. INTRODUCTION

This article presents possibilities for innovation in service delivery, operational tasks, office management, record preservation and utilization, and optimal use of available information technology within survey offices. While major reforms like infrastructure development and preparation of high-accuracy cadastral data require significant investment (high-cost demand), some innovations can be implemented at minimal cost (low-cost, no-cost, or low-hanging fruit). This article does not delve into major legal, policy, structural, or technical overhauls, but rather discusses how innovation can be achieved through creativity, modern work approaches, optimal use of existing IT, positive thinking, collective motivation, effective leadership, and high employee morale. It outlines five areas for innovation: office management, good governance, record management, technology utilization, and coordination.

3. AREAS OF INNOVATION

3.1 Office Management

3.1.1 Courteous Entry Message: Displaying welcoming messages such as "Welcome" or "Namaste" at the entrance of any public service office in local language and context can foster a positive impression among service recipients. Such messages can be attractively written or displayed on monitors/boards at the entrance of survey offices.

3.1.2 Cleanliness and Beautification: To improve the working environment and public perception, office premises and service rooms should be clean, peaceful, and aesthetically pleasing. Adequate parking should be arranged, and suitable flowers and decorative plants should be planted. Cleanliness should be maintained regularly in toilets, offices, passages, and waiting areas. Weekly group clean-up activities involving all staff foster a sense of ownership and send a message against littering. Waste should be sorted (biodegradable and non-biodegradable) and disposed accordingly. Educational and motivational displays related to surveying history, unit conversions, important reminders for buyers/sellers, and quotes from experts can also be showcased.

3.1.3 Waiting Area for Clients: A proper waiting area should be set up to avoid long lines and protect clients from weather while waiting. TV or display boards can provide entertainment and information, including awareness videos about services such as Merokitta system, buyer responsibilities, and available services. Free Wi-Fi and drinking water should be available. Charging stations can be arranged in coordination with service providers like Nepal Telecom.

3.1.4 Staff Responsibility Board with Photos: To avoid confusion about service desk and officials, a display board with photos and responsibilities of staff, categorized by area (municipality/ward), should be placed aside of the entrance or visible area. Additional service flow charts and required documents for each service should also be displayed clearly.

3.1.5 Clear Division of Work: Each employee must have a clearly defined role and responsibilities documented in writing. Technical employee (Assistant Surveyor, Surveyor, Survey Officer, Chief Survey Officer) should be assigned service areas (VDCs/municipalities or wards) and allocate responsibility. In survey offices where Nepal Land Information System (NeLIS) has implemented, responsibilities should be assigned as per the provision on that system.

3.1.6 Uniformity in Service Desks: All service desks should follow a consistent layout with similar furniture and furnishing. Desks must be able to hold maps and documents, and dual monitor systems should be used so both staff and clients can view the same screen. Counters should restrict unauthorized access to official documents.

3.1.7 Regular Monthly Meetings: At least one staff meeting per month should be held to discuss performance, challenges, solutions, directives, and good practices in the office. This fosters collective ownership and improves office operations.

3.1.8 Capacity Development Training: Staff should be provided opportunity to participate in relevant training, workshops, and orientation programs. In-house peer learning and group discussions should be encouraged. Training on GIS, remote sensing, GNSS, LiDAR, satellite imagery, UAVs, and topics like office management, professional ethics, and stress management can enhance performance and motivation.

3.1.9 Employee Recognition: Implementing a system of rewards and penalties can discourage poor performance and promote excellence. Monthly and yearly best employee awards can motivate staff and enhance the office's image.

3.1.10 Recreational Activities: Organizing recreational programs like picnics or exposure visits time to time promotes team bonding, creativity, and employee morale.

3.1.11 Auction of Unusable Items: Old, damaged, and irreparable items should be auctioned off as per regulations to avoid clutter and improve aesthetics and space management.

3.2 Good Governance

3.2.1 E-Attendance System: To enforce discipline and punctuality among staff, an electronic attendance system (E-attendance) can be introduced. This would require mandatory clock-in and clock-out at designated times, encouraging a culture of arriving and leaving on time. It also provides an objective basis for evaluating staff performance for rewards or disciplinary action. Coordination with the Department of Information Technology may be required for technical and logistics support

3.2.2 Operation of Customer Care Desk: Besides registration and inquiry desks, a Customer care desk can be established to assist clients, especially those who are illiterate. Assistance may be about writing applications, providing stamps and photocopies, preparing and verifying files, confirming required documents, and guiding clients to the appropriate service desks. This reduces reliance on third parties or middlemen.

3.2.3 One-Door Service System: Implementing a one-door system streamlines service delivery. Instead of sending clients to multiple rooms, one designated desk handles the entire process. After submitting necessary documents, a designated office clerk handles all processing, calling the client only if additional verification is needed. For example, map printing services could be fully completed from the room where the token was issued.

3.2.4 Public Display of Service Status: In NeLIS-based offices, digital systems track applications. By displaying real-time updates (e.g., which phase does the document is in; registered, processing, under review, or completed) on monitors, clients can track progress. This boosts transparency and reliability. A Service Tracking System can also be developed for online status checks.

3.2.5 Special Service Desk: For senior citizens, pregnant women, and people with disabilities, a special service desk can be set up in a convenient location. Dedicated staff can assist these clients with applications, document preparation, and services eliminating the need to visit various service units. Accessible ramps must also be mounted.

3.2.6 Daily Service Display: Daily data on services delivered such as parcel subdivisions, map prints, and revenue collected can be displayed for general public using a digital board. This enhances accountability and transparency.

3.2.7 Daily Work Log: Each staff member should maintain a logbook of tasks performed daily. The log should include receipt and completion times for any application or files. This supports performance analysis and discourages delays.

3.2.8 Delineation Service Management: Delineation services, especially in urban offices, are in high demand and typically scheduled between Kartik and Jestha. To avoid delays and dissatisfaction of the clients, appointment dates should be given on the day of request, and inform client for making arrangement of the local representatives to be present at the time of delineation. An application system including the information and documents regarding request dates, responsible staff, field reports, and status updates should be developed.

3.2.9 Information and Grievance Officers: Survey offices must assign Information Officers to ensure transparency and communication. Similarly, Grievance Officers must handle client complaints regarding services or staff conduct. Their contact details and photos should be prominently displayed.

3.2.10 Regular Monitoring: Chief of Survey offices should regularly monitor operations via CCTV and also by the application installed in mobile systems. Regular visits to each section of the office and weekly field visits to the areas where surveying/surveying is being conducted by the chief improve accountability of all the staffs and allow prompt issue resolution.

3.2.11 Client Feedback Form: Client feedback mechanisms are vital for improving service quality. Feedback forms or booklets with questionnaires can be provided, along with QR codes for digital submission. This helps to assess satisfaction and identify areas for improvement.

3.3 Record Management

3.3.1 Organized Storage of Maps, Field Books, and Plot registers: Modern plan chests with lockable chambers for storing cadastral maps can be brought in use. Special care should be taken to protect field books from sunlight, moisture, and insects. Only retrieve original cadastral maps with proper logs authorized by the office chief. Plot registers and Fieldbooks should be digitized/scanned and systematically organized

3.3.2 Digitization of Incomplete Maps: All remaining maps, including those from resurvey or file maps, should be digitized. Images of field books and plot registers should be linked in the reference system for faster retrieval. Coordination can be made with the Survey Department to integrate those data into the NeLIS system.

3.3.3 Digital Archiving System: All incoming and outgoing correspondence should be scanned and stored digitally on secure servers or desktops with regular backups. A document management system can be developed for easy retrieval based on date, subject, or sender/recipient.

3.3.4 Map Preservation: Old and fragile original maps can be preserved using transparent plastic folders with

reinforced backing and sealed edges. In NeLIS-enabled offices, even trace maps can be preserved similarly as they do not need to be retrieved frequently.

3.3.5 Binding of Kittakat Traces: All kittakat trace prepared during parcel subdivision process should be systematically binded in volumes of about 100, with dates clearly labeled. Until enough are collected for binding, they can be stored in loose files.

3.3.6 Integrated Record of Public Land: Based on field books and plot registers, a detailed record of government/ public land including location, map sheet number, parcel number, and area should be prepared. Satellite overlays can help as a reference to identify parcel boundaries and verify historical data.

3.4 Use of Information Technology

3.4.1 Digital Citizen Charter: A digital Citizen Charter outlining services, required documents, processing time, fees, responsible officers, and grievance handling officer contacts can be displayed. Charters cab be made multilingual and may include jingles or videos. QR codes can be arranged to provide full information of the services.

3.4.2 Use of Dual Monitors: Dual monitors at service desks can be installed so that service seekers can observe maps and data from the monitor facing towards them. This helps clients to have an idea of the location, orientation and shape of their parcels which enhances transparency.

3.4.3 Token System: A queue management system can be implemented to manage crowds for services like map printing. Clients collect tokens and are called to counters in order, reducing wait times and confusion.

3.4.4 CCTV Monitoring: CCTV in key areas like entrance, service desks, records rooms, waiting areas can be installed to enhance transparency and deter misconduct. Office head can monitor footage on-site or remotely via internet/mobile.

3.4.5 Internal Communication and Intercom: Intercom systems can be installed for internal communication, minimizing physical movement and preserving confidentiality. Staff may also use internal groups on messaging apps like WhatsApp or Viber.

3.4.6 Fingerprint Door Locks: Sensitive records like maps, field books, and plot registers can be safeguard from the unauthorize access using fingerprint locks on access doors. Access only to the responsible staff ensure document confidentiality and security.

3.5 Coordination

3.5.1 Coordination with Local Governments: Effective service delivery by survey offices requires close coordination with local governments and their representatives. Regular formal or informal meetings can foster cooperation. Key areas for coordination include: sharing information on required documents for land related services, public awareness on land transactions, online services, responsibilities of landowner during resurvey, role of ward representatives in field delineation, land use classification, and controlling encroachment on government and public land. Providing local governments with detailed cadastral maps including old VDC/municipality and map numbers enhances service facilitation for local government.

3.5.2 Coordination with Provincial Government: Provincial land ministries often support record management and infrastructure development through annual programs. Coordination with the related ministry can help in managing budget and program for strengthening survey offices and improving records management.

3.5.3 Coordination with Land Revenue Offices: Survey Offices and land revenue offices are closely linked for land related services. For example, deed for partial ownership transfer or parcel subdivision are prepared by the land revenue offices and parcel split based on that deed is being carried out by the survey offices. Coordination ensures accuracy, legal compliance, and smooth service delivery. Issues related to land transaction and land registration such as record amendment as per the evidence, registration of unregistered land, and update ownership record also require coordination.

3.5.4 Coordination with District Administration Offices: District administration offices oversee peace, security, and inter-agency coordination. For complex service delivery issues or coordination with other offices, the district administration's support is crucial. Best practices from survey offices can also be shared during regular district meetings to inspire replication by others.

3.5.5 Coordination with the Survey Department: In case of policy, legal, administrative, or technical challenges, direction from the parent agency, Survey Department is

vital. Offices must adhere to circulars and directives from the department and report innovative practices to the department so other offices can take-up ideas on good practices.

3.5.6 Coordination with Building Construction Division Offices: For physical infrastructure development or repair, technical assistance from the Urban Development and Building Construction Division is essential. Coordination with these offices may provide support and financial & technical assistance for general construction and renovation,

4. CONCLUSION

This article tries to present low-cost, coordination-based transformations that survey offices can adopt and implement using their resources or in collaboration with other institutions. While policy, structural, legal, and procedural reforms requiring departmental or ministerial involvement are beyond this article's scope, it emphasizes practical measures to improve service delivery, transparency, record management, and staff capacity. These ideas aim to enhance survey offices by modernizing record preservation, improving staff performance, and fostering good governance. By maximizing the use of available technologies, survey offices can ensure quality services, effective management, and accountability, ultimately contribute to improve land administration and cadastral services of the country.

(*The views expressed in this article are based solely on the personal experience and insight of the author*)

AUTHOR INFORMATION

Name	:	Ram Kumar Sapkota
Academic Qualification	:	M.Sc. in Geodesy and Geoinformation
Organization	:	Land Management Training Center
Current Designation	:	Director
Work Experience	:	17 Years
Published Article	:	7

LEVERAGING UAV TECHNOLOGY IN LOCAL GEOID MODELING

Er. Sushmita Timilsina[1], Er. Bhagirath Bhatt[2]

[1]Survey Department, Geodetic Survey Division - *qust04sharma@gmail.com*

[2]Land Management Training Center - *bhagirath.bhatt@nepal.gov.np*

ABSTRACT

TLeveraging UAV (Unmanned Aerial Vehicle) technology in local geoid modeling is a promising approach, particularly in areas with challenging terrain and sparse GNSS, leveling and gravity infrastructure. In this study, UAV was utilized to capture high-resolution images of the area surrounding the Land Management Training Center (LMTC) from an altitude of about 120 meters. These aerial images were carefully georeferenced using a coordinate set of ellipsoidal height (h) and orthometric height (H). A sufficient number of points were then generated from these images, which included both ellipsoidal and orthometric height data. The next step involved calculating the geoid height (N). This calculation provided the point-specific geoid heights, which were then used to construct a comprehensive geoid model for the region. The evaluation of this geoid model was done by comparing it with the recent global gravity model. This assessment demonstrated that UAV technology can be useful for local geoid modeling, offering accurate and reliable data for understanding geoid variations on a local scale.

KEYWORDS: UAV, GGM, Geoid, DEM, Orthometric height

1. INTRODUCTION

Geoid is a complex surface yet the most relevant physical figure of the Earth. The significance of geoid modeling is well comprehended from former times. However, it is not an easy task to determine an accurate geoid model, it involves complex methods that are often time-consuming, costly and tedious (Timilsina. S., et al., 2021). In the field of geophysics and geodesy, the geoid is a vital reference surface that represents the shape of the Earth under the influence of gravity and rotation, which serves as the basis for measuring elevations and is essential for various applications, such as mapping, navigation, and environmental monitoring. To construct accurate geoid models, precise measurements of the Earth's surface, gravity, and topography are necessary. For this, satellite measurements, terrestrial surveys, and gravimetric data have been relied upon to gather such information. The advancement of GGMs, particularly with the help of satellite missions, has significantly enhanced our understanding of the Earth's gravitational field and determination of geoid (Barthelmes. F, 2014). In geoid modeling, GGMs are essential because they provide high-resolution gravity data that allow for accurate determination of the geoid.

The advent of unmanned aerial vehicles (UAVs) has brought a significant breakthrough in 3D modeling, which has also aided in geoid modeling. Geoid modeling has gotten simpler with the advancement of technologies like UAV and LIDAR. This involves the acquisition of a rich amount of accurate data in a very short time and processing them automatically to compute continuous models of the earth such as DEM and geoid (Raufu. (I.O., et al., 2023).

The UAV is a powered aerial vehicle that does not require a human pilot. This technology's ease of use, portability, and fascinating hardware, as well as its capacity to support a broad range of applications including military, agricultural, search and rescue, surveying, and mapping, have been contributing to its increasing popularity. For mapping local regions that are comparatively smaller in area, UAV technology can provide a cost-effective solution.

The major good aspect of using this technology is that it is a close-range sensing technology providing a platform for different sensors (visible, infrared, LiDAR) with high data acquisition speed and automation of data processing, providing accurate geoinformation. When coupled with surveyed ground control points (GCPs), UAV technology

can capture spatial data with a richness of detail that can meet high accuracy standards.

2. OBJECTIVE OF THE STUDY

The objective of this study was to assess the applicability of UAV technology in local geoid modeling.

3. STUDY AREA

The study area for this study was Bhakhundol -4 of Dhulikhel municipality in Nepal. The total area of the project covers around half a square kilometer (0.552 sq.km). The flight for UAV was taken from the roof of the administration building of the Land Management Training Center (LMTC). The UAV used for the data acquisition was DJI Mavic 2 Interprise quadcopter. The Ground Control points were established using GNSS instruments for registration of aerial images.

4. METHODOLOGY

4.1 GNSS Observation

GNSS observations were done at five points. These points were used as ground control points for UAV image acquisition, processing and georeferencing. These points were accurately determined and processed using precise ephemeris and differential observation. The three-dimensional coordinates with ellipsoid height were computed for each point.

4.2 Precise Levelling

Precise leveling was conducted in order to obtain the orthometric height on the above-mentioned five ground control points. Each set of ground control points contained latitude, longitude, ellipsoid height and orthometric height.

4.3 UAV operations

4.3.1 Mission Planning

Effective mission planning is crucial to ensure the safe and efficient success of any UAV operation. After selection of the appropriate UAV, a single grid flight plan considering environmental factors was designed and pre-flight checks were performed. Five Ground Control Points (GCP) were established in the Area of Interest (AOI). The large forward overlap of 80% and cross/side overlap of 60% was planned to be used in order to compensate for aircraft instability and subsequent generation of the dense point cloud.

4.3.2 Image Acquisition

The presence of GNSS/INS onboard is usually exploited to guide the image acquisition. During flight, the platform is normally observed with a control station which shows real-time flight data such as position, speed, attitude and distances, GNSS observations, battery or fuel status, rotor speed, etc. GNSS coordinates and elevations were recorded for each image with the roll, pitch, and heading of the platform.

4.4 Processing and Output Generation

Image processing of UAV was done using Pix4D (photogrammetric software package) for initial data processing, point cloud densification and 3D model generation. The initial processing was done for 840 images of AOI and five ground control points to obtain an average Ground Sampling Distance of 3.02 cm. Point cloud (each point has an associated elevation) was generated from UAV images containing elevation data. High-density point clouds were automatically generated through image matching. Large overlaps and high visuals content led to better results, generating around 66 million 3D points with an average density of 152.72 m^3.

The Digital Surface Model (DSM) was obtained using the inverse distance weighting method and Orthomosaic of resolution 3.02cm was generated in GeoTIFF format.

5. RESULTS AND DISCUSSION

Two digital elevation models were generated using two set of GCPs. At first the generation of DSM using point cloud and 3D Ground control points with ellipsoid height was done. A DEM (DEM_ell) was then generated then by removing non ground points from the model and is shown in figure 1. For this, WGS-84 was chosen as the vertical and horizontal reference datum.

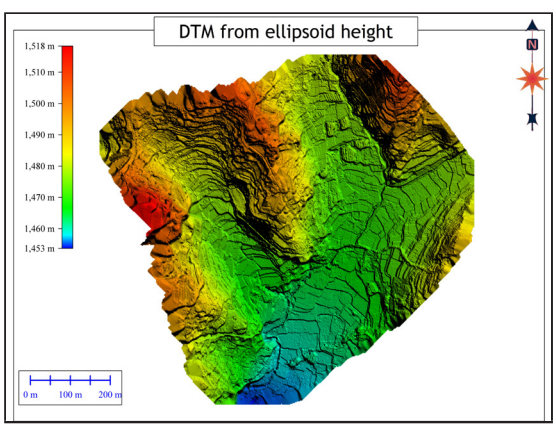

Figure 1. DEM from ellipsoid height

On the other hand, another DSM was generated by using point cloud and 3D ground control point with orthometric height (the orthometric height was computed by using differential leveling). The DEM (DEM_orth) was then generated by removing ground control points from the derived model and is shown in figure 2.

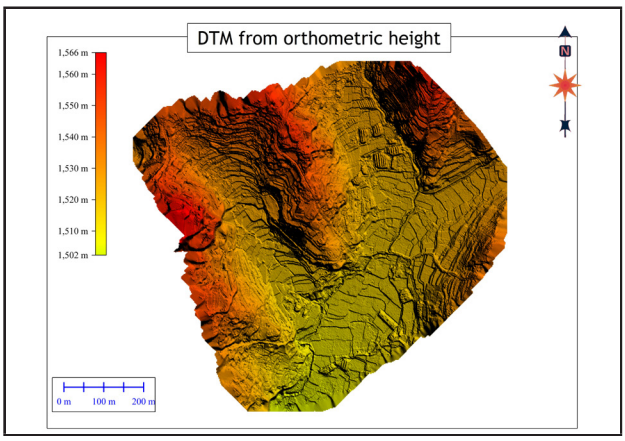

Figure 2. DEM from orthometric height

EGM_2008 was chosen as the vertical reference date. The DEM_ell contains each point/cell with ellipsoid height (h) and the DEM_orth contains each point/cell with orthometric height (H). The corresponding difference between these two points or models is h-H, which is the difference between ellipsoid height and orthometric height, commonly known as geoid height (N). The difference between these two models principally generates a geometric geoid model.

6. ACCURACY ASSESSMENT

The accuracy assessment of the obtained geoid model was done by comparing it with geoid height from the latest global gravity model XGM2019e. XGM2019e is a combined global gravity field model represented through spheroidal harmonics up to d/o 5399, corresponding to a spatial resolution of 2' (~4 km). As data sources, it includes the satellite model GOCO06s in the longer wavelength area combined with terrestrial measurements for the shorter wavelengths (Zingerle, P. et al., 2019).

Thirty geoid height points were taken as test points from a geoid model derived from UAV and their corresponding geoid height points were computed from XGM2019e using MATLAB (Bucha B. et al., 2014). They were then compared to assess the reliability of the geoid model. The comparison result showed the overall variation of 27 cm with minimum of 5mm and maximum 89 cm as shown in figure 3.

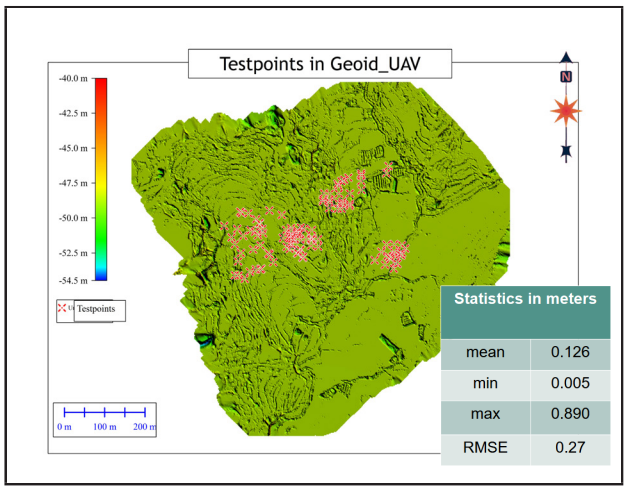

Figure 3. Geoid model from UAV with test points (pink)

7. CONCLUSION

The advancement of UAV technology in 3D modeling has shown a promising future in modeling of continuous surfaces such as geoid. The differences between UAV-derived ellipsoid height and UAV-derived orthometric height can be used to determine the geometric geoid at the local level. The UAV-derived geoid model, while compared with the global model, showed a good result. Geoid can be determined in a short time, less and less tedious, using UAV technology.

The number of ground control points for this study was very limited. A larger number of control points can be used for more accurate results. Further, the establishment of reliable GNSS-Levelling points for proper validation of the geoid model can assess its reliability even more accurately. For larger areas, LIDAR sensor data can be used in developing similar geoid models.

Although this method is not the most accurate method to compute a geometric geoid model, the results have shown that UAV technology can be a cost-effective solution for modeling of local geoid as it reduces time, cost and effort.

8. WAY FORWARD

Nepal is a mountainous country where large portions contain hills and mountains, creating smaller than obvious variations in gravity. Surface gravity observations to quantify these variations in all places might not be practical. In order to take this mass and density variation into account and comprehend the terrain effect, deploying UAV technology can be a way forward in local modeling of geoid.

REFERENCES

B. Bucha, J. J. (2014). A MATLAB- based graphical user interface program for computing functionals of geopotential up to ultra-high degrees and orders: Efficient computation at irregular surfaces. *Computers and Geosciences, Volume 66*, 219-227.

Barthelmes, F. (2014). *Global Models.* Potsdam: German Research Centre of Geosciences.

I.O. Raufu., H. T. (2023). *Modelling local geoid undulation using unmaned aerial vehicles (UAVs): a case study of Federal University of Technology.* Akura, Nigeria: Federal University of Technology.

P. Zingerle, R. P. (2019). *The experimental gravity field model XGM2019e.* GFZ Data Services.

S. Timilsina, R. P. (2021). Regional geiod model for Nepal using Least Squares Collocation. *Terrestrial, Atmospheric and Oceanic Sciences (TAO), 32*, 847-856.

AUTHOR INFORMATION

Name	:	**Sushmita Timilsina**
Academic Qualification	:	M.Sc. in Geodesy and Geoinformation
Organization	:	Survey Department
Current Designation	:	Survey Officer
Work Experience	:	10 years
Published Article	:	7

URBAN HEAT ISLAND EFFECT ANALYSIS OF KATHMANDU METROPOLITAN CITY IN NEPAL

Sudipta Poudel[1], Ishwor Pd. Dhital[1]

[1]Department of Geomatics Engineering ,Kathmandu University

poudelsudipta4014@gmail.com, dhitali164@gmail.com

ABSTRACT

Rapid urbanization and anthropogenic activities have significantly altered the thermal environment of Kathmandu Metropolitan City, creating pronounced Urban Heat Island (UHI) effects that threaten urban livability and climate resilience. This study examines the spatial-temporal evolution of UHI patterns in Kathmandu over a decade (2015-2024) using multi-temporal satellite remote sensing data. The research integrates Normalized Difference Vegetation Index (NDVI), Normalized Difference Built-up Index (NDBI), and Land Surface Temperature (LST) derived from Landsat 8/9 thermal infrared bands and Sentinel-2 multispectral imagery to quantify land cover transformations and their relationship with urban thermal patterns. Results indicate drastic urban expansion accompanied by severe vegetation loss, leading to intensified heat island effects across rapidly developing areas. Maximum LST increased substantially from 26.28°C in 2015 to 35.85°C in 2023, representing a 9.57°C increase over eight years. The urban-rural temperature gradient intensified from 5.2°C to 8.7°C, while built-up areas expanded by 15.2% with dense vegetation declining by 8.7% of the total area. Strong correlations were observed between NDBI and LST (r = 0.78), NDVI and LST (r = -0.72), confirming the cooling effect of vegetation and heating effect of built surfaces. The eastern and northern sectors of the city experienced the most pronounced thermal intensification, with newly developed areas showing temperature increases of 7.1-8.2°C. Urban heat islands are increasingly problematic in an era of rapid urbanization and climate change.

KEYWORDS: Urban Heat Island, Normalized Diffference Vegetation Index(NDVI), Normalized Difference Built up Index(NDBI), Land Surface Temparature (LST)

1. INTRODUCTION

Urban Heat Island (UHI) is a situation where cities become much warmer than the areas around them, mainly because buildings, roads, and other artificial surfaces trap heat from the sun(Sarif, Rimal, and Stork 2020). This extra heat can make city life uncomfortable, increase energy use, worsen air pollution, and harm the local environment. According to United Nations Environmental Protection Agency (EPA), the annual mean air temperature of a city with 1 million people or more experience 1-3°C warmer temperature compared to its rural surroundings. Due to the excess heat, the quality of life in urban areas has been compromised.

The Urban Heat Island (UHI) effect arises from multiple interrelated factors. Predominantly, urban surfaces such as pavements, roads, and buildings possess higher thermal absorptivity compared to natural vegetated areas, resulting in increased solar radiation retention(Feng et al. 2019). The significant reduction in vegetation cover within urban environments diminishes evapotranspiration processes, thereby limiting the natural cooling effects typically provided by plant transpiration. Furthermore, anthropogenic heat emissions from transportation, industrial activities, and air conditioning systems contribute additional thermal energy to the urban atmosphere. The complex urban morphology, characterized by tall buildings and narrow street canyons, impedes airflow and traps heat, creating thermal accumulation. Lastly, the generally low albedo of urban materials leads to decreased reflectivity and enhanced absorption of solar radiation, collectively intensifying the temperature disparity between urban centers and their rural surroundings(City 2022).

Kathmandu, the capital city of Nepal, has experienced unprecedented urbanization in recent decades, transforming from a cultural hub into a sprawling metropolitan center(Chaudhary, Pradhan, and Naryan 2021). According to United Nations Department of

Economic and Social Affairs (UN DESA), Kathmandu has a growth rate of 3.94% and 29% of the country's total urban population. The land use of Kathmandu valley has changed significantly in the last four decades(Nations 2018). The city has expanded as much as 412%, with the majority of land converted from agricultural land to built-up areas, which has changed the valley's landscape considerably. The growth of built-up areas in the most urban settlements is haphazard and uncontrolled with a rapid decrease in agricultural land(Wu et al. 2019). Covering only one percent of the country's total area, Kathmandu valley accommodates 31% of the total urban population of the country. Central Bureau of Statistics (CBS) of Nepal has stated Kathmandu valley is characterized by sustained population growth in the urban core and rapid urban sprawl. With 51% growth from 2001 to 2011, the total population of Kathmandu valley is expected to reach almost 6 million by 2031. This unplanned urban development has contributed to dramatic changes in urban footprint of the valley. More people moving to cities creates two compounding effects: larger populations are exposed to the negative impacts of heat islands (increased energy consumption, compromised health, elevated air pollution), and as cities become larger and more densely populated, heat island intensity typically increases(Reality 2024).

This research aims to provide a comprehensive analysis of UHI patterns and their relationships with land cover changes over the past decade (2015-2024) by integrating multiple remote sensing indices (NDVI, NDBI, LST). Studying the UHI effect in Kathmandu from 2015 to 2024 will help us understand how much the city has warmed, what is causing it, and what can be done to make the city cooler and more comfortable.

2. MATERIALS AND METHODS

2.1 Study Area:

For Analyzing the UHI effect trend in Kathmandu Metropolitan city the study area, situated at approximately 1400 meters above sea level at Latitude Range: 27.67°N to 27.74°N and Longitude Range: 85°16'5" E to 85°22'32" E covering area about 50.67 sq. km, is delineated to include the metropolitan boundaries and adjacent rural surrounding.

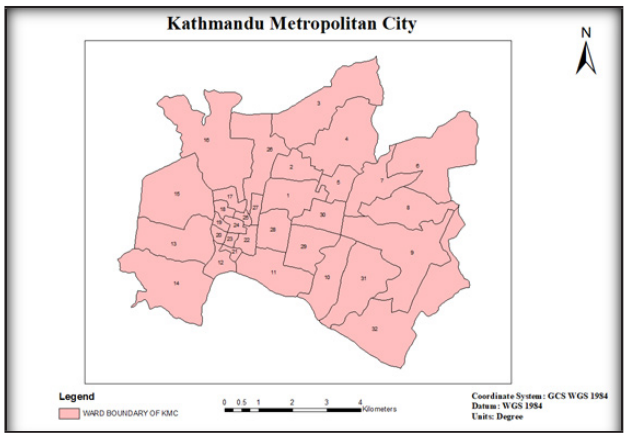

Figure 1. Study Area Map

2.2 Data acquisition

For data acquisition, multispectral Sentinel-2 imagery, cloud masked and processed, with 10 m spatial resolution is utilized to calculate the indices such as NDVI, using the red (Band 4, 665 nm) and near-infrared (Band 8, 842 nm) bands. NDVI serves as an indicator of vegetation density and health, which is critical in assessing urban cooling effects through evapotranspiration.Landsat 8/9 Operational Land Imager (OLI) and Thermal Infrared Sensor (TIRS) data provide thermal bands (Band 10 and Band 11) used to derive Land Surface Temperature (LST) and Normalized Difference Built-up Index (NDBI). NDBI, calculated from shortwave infrared (SWIR) and near-infrared bands, identifies built-up areas contributing to heat accumulation. LST is estimated using the mono-window algorithm, which incorporates atmospheric correction and emissivity adjustment to convert thermal band data into accurate surface temperature measurements. All satellite data processing, including image acquisition, pre-processing, and index calculations, is conducted on the Google Earth Engine (GEE) platform, enabling efficient handling of large temporal datasets from 2015 to 2024.

Table 1:Parameters of UHI Analysis

Index	Equation	References(s)
NDVI (Normalized Difference Vegetation Index	$NDVI=\frac{NIR-RED}{NIR+RED}$	(Ustuner et al. 2014)
NDBI (Normalized Difference Built-up Index)	$NDBI=\frac{SWIR-NIR}{SWIR+NIR}$	(Zha et al. 2003)
LST (Land Surface Temperature)	$LST = \frac{TB}{1 + (\lambda \sigma TB/(hc)) \ln \epsilon}$ with atmospheric correction and emissivity adjustment applied to thermal band data.	(Weng and Schubring, 2004)

The major parameters for UHI which are indices such as NDVI, NDBI, and LST are analyzed spatially and temporally to understand the relationship between land cover changes and surface temperature variations. NDVI highlights vegetated areas that mitigate heat, while NDBI maps urban expansion and impervious surfaces that exacerbate heat retention. LST quantifies the thermal intensity across the valley, allowing identification of urban heat hotspots and the extent of the UHI effect. This integrated methodology provides a comprehensive framework to assess how urbanization and land cover dynamics influence thermal patterns in Kathmandu, supporting urban planning and heat mitigation strategies.

Table 2. Parameters for Classification based on Normalized Difference Vegetation index

Land Cover Class	Range	Reference
Water	0 to 0.015	*Nepal Land Cover Monitoring System (FRTC, 2023)*
Built-up Area	0.015-0.14	*Idrees et al. ,2022*
Barren Land	0.14-0.18	*Idrees et al. ,2022*
Grassland	0.18-0.27	*Nepal Land Cover Monitoring System(FRCT,2023)*
Sparse Vegetation	0.27-0.36	*Bedunkevich,2025*
Dense Vegetation	0.36-0.63	*(USGS,2017)*

3. RESULTS AND ANALYSIS

Table 3. NDBI TREND ANALYSIS

Year	NDBI Maximum	NDBI Minimum	Mean NDBI
2015	0.274864	-0.717677	-0.221
2016	0.259421	-0.486409	-0.113
2017	0.312301	-0.420260	-0.054
2018	0.431514	-0.369096	0.031
2019	0.441835	-0.355450	0.043
2020	0.446978	-0.348627	0.049
2021	0.452155	-0.341803	0.055
2022	0.383615	-0.321303	0.067
2023	0.315075	-0.300803	0.079
2024	0.315075	-0.239641	0.091

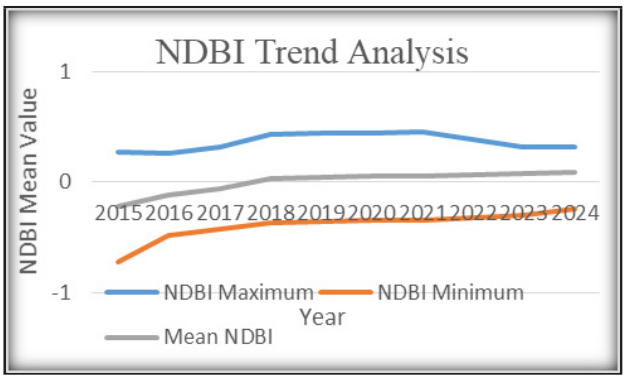

Figure 2. Line Char of NDBI Value per Time (2015-2024)

Over the timeline, the mean NDBI values steadily rose from -0.221 in 2015 to 0.091 in 2024, transitioning from negative to positive values, which indicates a significant expansion of built-up areas. The maximum NDBI values increased gradually, reaching a peak of 0.452 in 2021 before declining to 0.315 by 2023 and 2024. Meanwhile, the minimum NDBI values also rose from -0.718 in 2015 to -0.240 in 2024, reflecting a reduction in the extent of non-urban land cover. This overall positive trajectory in mean NDBI values, especially the rapid increase observed between 2017 and 2018, highlights accelerating urban growth. The slight decline in maximum values after 2021 suggests that core urban areas may be approaching saturation, while the increase in minimum values points to a decrease in undeveloped or vegetated land. Together, these trends indicate a marked transformation of the landscape towards more built-up environments over the analyzed period.

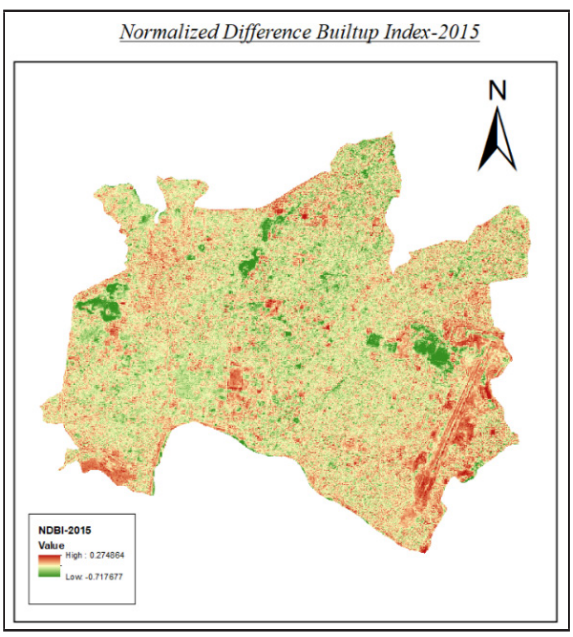

Figure 3. NDVI-2015 Map

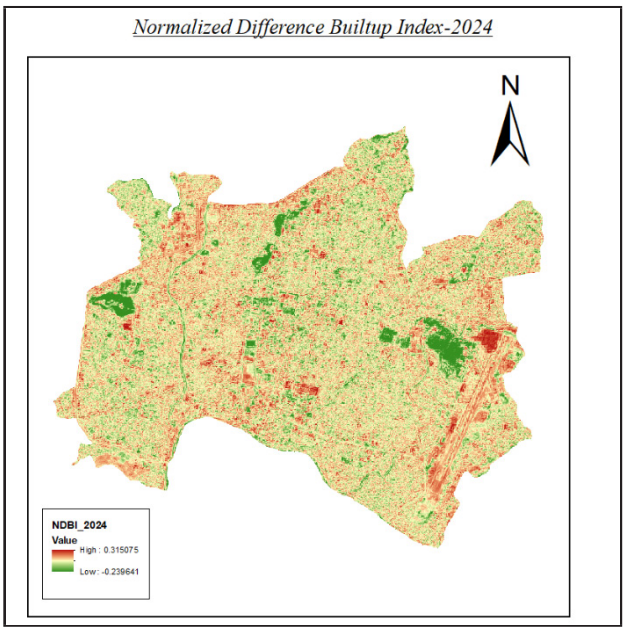

Figure 4. NDBI-2024 Map

Table 4. LST Trend Analysis

Year	LST Maximum (°C)	LST Minimum (°C)	LST Range (°C)
2015	26.2754	17.2979	8.98
2016	30.7906	19.2838	11.51
2017	32.8773	21.6029	11.27
2018	36.0611	23.5854	12.48
2019	27.5007	15.9581	11.54
2020	32.8226	19.2154	13.61
2021	28.2014	16.5118	11.69
2022	29.5857	18.6446	10.94
2023	35.8458	20.7108	15.14
2024	32.3806	17.7559	14.62

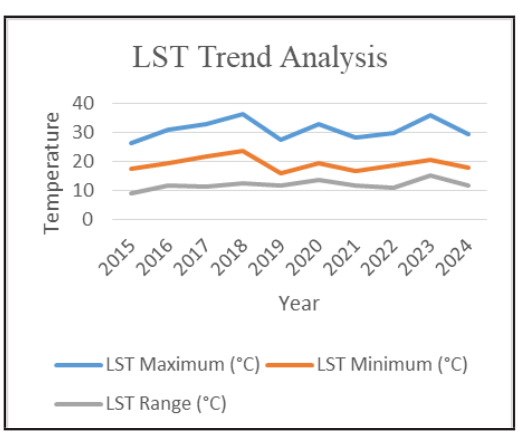

Figure 5. LIne Chart of LST per Year

The Land Surface Temperature (LST) data from 2015 to 2024 shows notable fluctuations in temperature extremes and variability over the years. The maximum LST values generally increased from 26.28°C in 2015 to a peak of 36.06°C in 2018, followed by some variation, with another high of 35.85°C recorded in 2023. Minimum LST values also rose from 17.30°C in 2015 to a maximum of 23.59°C in 2018, indicating a warming trend in both daytime and nighttime temperatures. The LST range, which represents the difference between maximum and minimum temperatures, varied between 8.98°C and 15.14°C, with the widest range occurring in 2023. These variations suggest increased temperature extremes and greater diurnal temperature variability in recent years, which could be linked to factors such as urban expansion, changes in land use, and climatic influences in the region.

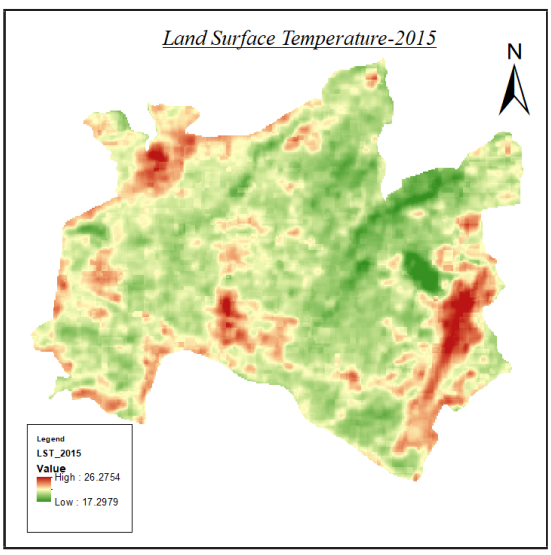

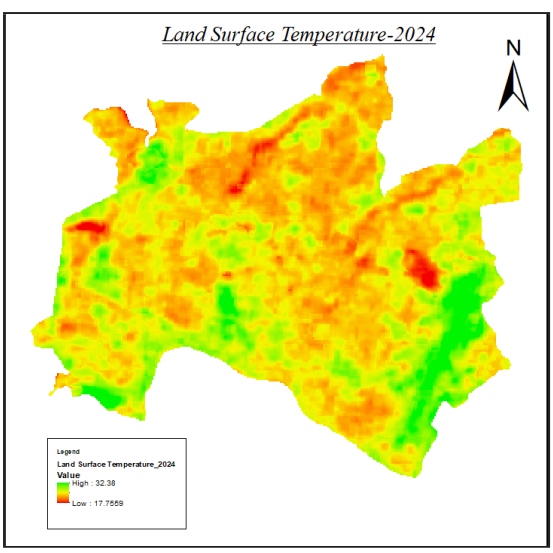

Table 5. NDVI Trend Analysis

Year	NDVI Maximum	NDVI Minimum	Mean NDVI
2015	0.724301	0.0103063	0.367
2016	0.689103	-0.0390573	0.325
2017	0.724808	0.0217074	0.373
2018	0.63254	-0.182822	0.225
2019	0.744496	-0.0251177	0.360
2020	0.767177	-0.0635003	0.352
2021	0.742636	-0.127451	0.308
2023	0.50842	-0.0299878	0.239
2024	0.315075	-0.239641	0.038

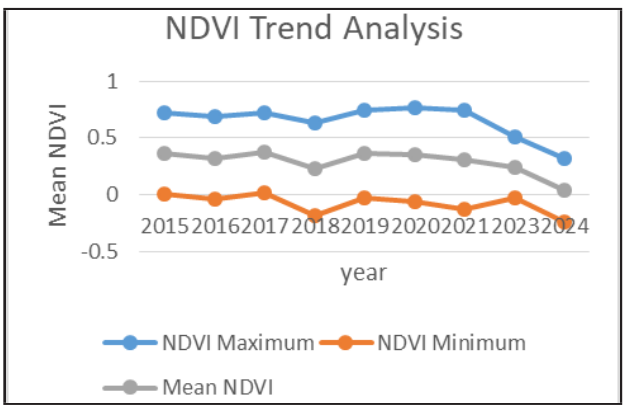

Figure 6. NDVI-Value per year

The NDVI analysis from 2015-2024 reveals a catastrophic vegetation decline in Kathmandu Metropolitan City, with mean NDVI plummeting from 0.367 in 2015 to a critically degraded 0.038 in 2024, representing an 89.7% loss of vegetation health and density. Maximum NDVI values decreased from 0.724-0.767 (indicating dense, healthy vegetation) to 0.315 by 2024, while minimum NDVI values dropped to -0.240, signifying extensive conversion of vegetated areas to barren or built surfaces. The most dramatic decline occurred between 2021 (mean NDVI 0.308) and 2024 (mean NDVI 0.038), indicating accelerated deforestation and land cover conversion during recent urbanization phases. This vegetation collapse directly correlates with urban heat island intensification, as the city lost its natural cooling capacity through evapotranspiration, with the 2024 NDVI values falling well below the 0.14 threshold that defines built-up areas, confirming that Kathmandu's landscape has fundamentally transformed from a vegetation-dominated to a critically vegetation-depleted urban environment requiring immediate large-scale reforestation and green infrastructure implementation.

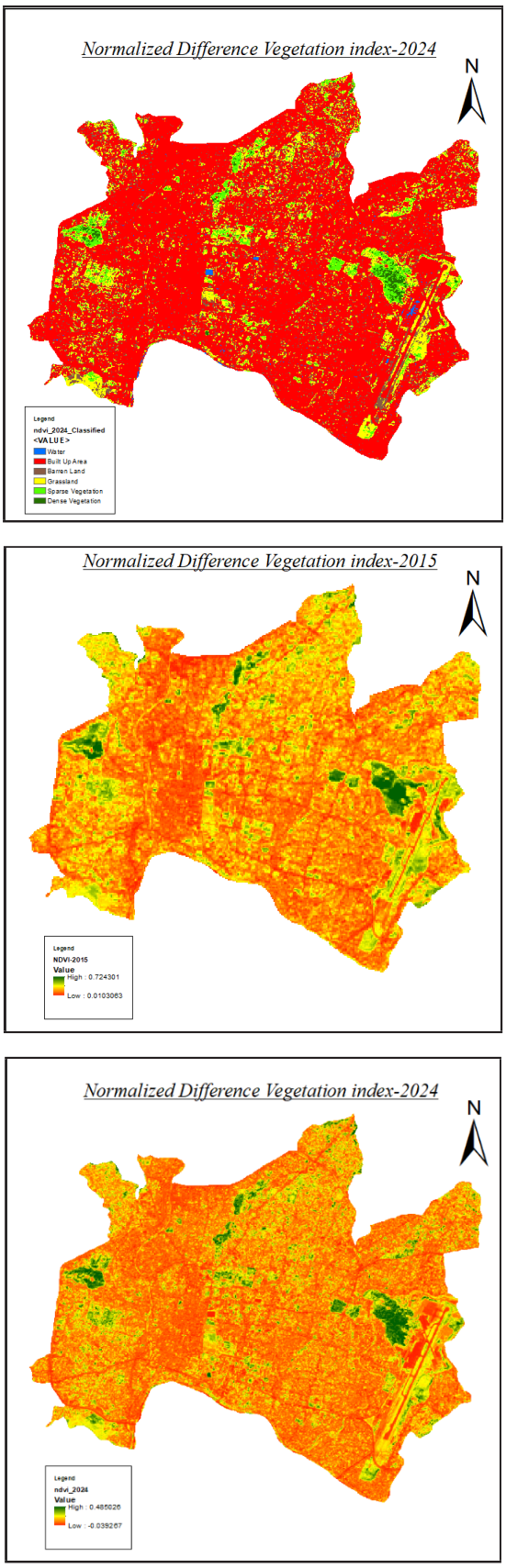

Figure 7. Classified NDVI Map

Table 3. Correlation Analysis

Correlation Pair	Correlation Coefficient (r)	Determination Coefficient (r^2)
NDBI vs. LST	0.78	0.61
NDVI vs. LST	-0.72	0.52
NDVI vs. NDBI	-0.81	0.66

Visual inspection of the spatial data reveals distinct and consistent patterns linking land surface temperature (LST), normalized difference built-up index (NDBI), and vegetation cover. Central urban areas consistently exhibit higher LST and NDBI values, indicating that densely built-up zones correspond with elevated surface temperatures. The eastern section of the city shows the most pronounced increase in built-up area, which aligns with observed urban expansion along major transportation corridors, especially in the eastern and northern sectors. Dense vegetation areas, identified as dark green zones, correspond with lower LST values, reflecting the cooling effect of vegetation. Conversely, built-up areas, marked red in NDVI classification, strongly correlate with hotspots in LST maps, demonstrating the urban heat island effect. These strong correlations confirm the cooling effect of vegetation (negative NDVI-LST correlation) and the heating effect of built-up surfaces (positive NDBI-LST correlation). The negative correlation between NDVI and NDBI (-0.81) reflects the land cover conversion process where vegetated areas are replaced by built structures

SUMMARY

The temporal analysis of the indices trends in the study has highlighted initial baseline period (2015-2017) has relatively stable thermal conditions with moderate urban development. Land surface temperatures ranged from 26.3°C to 32.9°C maximum, indicating natural thermal variation. The NDBI values remained low (mean -0.221 to -0.054), suggesting limited built-up areas, while vegetation indices maintained healthy levels above 0.32 mean NDVI. This period represents the pre-intensive urbanization baseline against which subsequent changes are measured. Period of 2018-2020 marks critical transformation with rapid urbanization. The year 2018 experienced the highest maximum LST of 36.1°C, coinciding with significant NDBI increases to positive values (0.031 mean). Built-up and fallow lands record high temperatures, whereas the vegetated areas and water bodies exhibit lower temperature. The LST range expanded to 13.61°C by 2020, indicating intensifying thermal heterogeneity across the urban landscape. Mean NDBI values consistently increased from negative to positive, reflecting substantial land cover conversion from natural to built surfaces. Finally, period of 2021-2024 marks as thermal intensification period that shows the establishment of severe urban heat island conditions. The year 2023 recorded the highest maximum LST of 35.8°C with the greatest temperature range of 15.14°C, indicating extreme thermal differentiation. NDBI values continued increasing to 0.091 mean by 2024, while NDVI values declined dramatically to 0.038 mean value. Maximum LST increased by 9.6°C from 2015 to 2023, representing a warming rate of 1.2°C per year during peak development phases. The temperature range expanded from 8.98°C to 15.14°C, indicating increasing spatial thermal heterogeneity within the metropolitan area. The transition from negative to positive mean NDBI values (from -0.221 to 0.091) represents a fundamental shift from vegetation-dominated to built-up dominated landscapes. This transformation correlates directly with vegetation loss, as evidenced by NDVI decline from 0.367 to 0.038 mean values. The data also confirms the urban rural temperature gradient intensified from 5.2°C in 2015 to 8.7°C in 2023, representing a 67% increase in thermal differentiation. Kathmandu metropolitan city needs to implement mandatory green building codes requiring 30% vegetation coverage for new developments, establish protected green corridors along major rivers, enforce reflective surface mandates for existing infrastructure, create strategic urban forest zones targeting the thermally vulnerable eastern sectors, implement strict development density controls in rapidly converting peripheral areas, and integrate climate-responsive zoning that prioritizes vegetation preservation.

REFERENCES

Bedunkevich, N. (2025, April 16). NDVI classification: Understanding vegetation health for better crop management.

Cropler Blog. Retrieved June 22, 2025, from https://www.cropler.io/blog-posts/ndvi-classification-understanding-vegetation-health

Chaudhary, Bishnu, Inu Pradhan, and Khem Naryan. 2021. "Urban Heat Island : A Case Study of Kathmandu Valley." 8914: 68–79.

City, Valley. 2022. "Assessing Surface Urban Heat Island Related to Land Use / Land Cover Composition and Pattern in the Temperate Mountain."

Feng, Yuning, Shihong Du, Soe W. Myint, and Mi Shu. 2019. "Do Urban Functional Zones Affect Land Surface Temperature Differently? A Case Study of Beijing, China." Remote Sensing 11(15).

Forest Research and Training Centre (FRTC). (2023). National land cover monitoring system of Nepal [PDF]. Government of Nepal. Retrieved June 22, 2025, from https://frtc.gov.np/noticefiles/GoN_National-land-cover-monitoring-system-for-Nepal-1718522489.pdf

Idrees, M. O., Omar, D. M., & Babalola, A. (2022). Urban land use land cover mapping in tropical savannah using Landsat-8 derived NDVI threshold. South African Journal of Geomatics, 11(1), 100–110. https://doi.org/10.4314/sajg.v11i1.8

Nations, United. 2018. 12 Demographic Research World Urbanization Prospects. https://population.un.org/wup/Publications/Files/WUP2018-Report.pdf.

Qin, Z., Karnieli, A., Berliner, P. (2001). A mono-window algorithm for retrieving land surface temperature from Landsat

TM data and its application to the Israel-Egypt border region. International Journal of Remote Sensing, 22(18), 3719-3746.

Reality, Virtual. 2024. "Er p a d e w 2024 e i v Re Eek r e a Is Orki s I." (May): 19–24.

Rouse, J.W., Haas, R.H., Schell, J.A., Deering, D.W. (1974). Monitoring vegetation systems in the Great Plains

with ERTS. Third Earth Resources Technology Satellite-1 Symposium.

Sarif, Md Omar, Bhagawat Rimal, and Nigel E. Stork. 2020. "Assessment of Changes in Land Use/Land Cover and Land Surface Temperatures and Their Impact on Surface Urban Heat Island Phenomena in the Kathmandu Valley (1988–2018)." ISPRS International Journal of Geo-Information 9(12).

Wu, Qiong et al. 2019. "Multi-Scale Relationship between Land Surface Temperature and Landscape Pattern Based on Wavelet Coherence: The Case of Metropolitan Beijing, China." Remote Sensing 11(24): 1–22.

Zha, Y., Gao, J., Ni, S. (2003). Use of normalized difference built-up index in automatically mapping urban areas from

TM imagery. International Journal of Remote Sensing, 24(3), 583-594.

United States Geological Survey (USGS). (2017, July 23). Landsat normalized difference vegetation index. USGS.gov. Retrieved June 22, 2025, from https://www.usgs.gov/landsat-missions/landsat-normalized-difference-vegetation-index

AUTHOR INFORMATION

Name	:	**Sudipta Poudel**
Academic Qualification	:	BE in Geomatics Engineering
Organization	:	Kathmandu Metropolitan City
Current Designation	:	Intern
Work Experience	:	3 months
Published Article	:	4

GUIDELINES FOR JOURNAL OF LAND MANAGEMENT AND GEOMATICS EDUCATION

Author Name[1], Author Name[2], Author Name[3]

[1]Author Affiliation and Email Address

[2]Author Affiliation and Email Address

[3]Author Affiliation and Email Address

ABSTRACT

These guidelines are provided for preparation of papers for publications in the journal going to be prepared by Land Management Training Centre. These guidelines are issued to ensure a uniform style throughout the journal. All papers that are accepted by the editorial board of this journal will be published provided they arrive by the due date and they correspond to these guidelines. Reproduction is made directly from author-prepared manuscripts, in electronic or hardcopy form, in A4 paper size 297 mm x 210 mm (11.69 x 8.27 inches). To assure timely and efficient production of the journal with a consistent and easy to read format, authors must submit their manuscripts in strict conformance with these guidelines. The editorial board may omit any paper that does not conform to the specified requirements.

KEYWORDS: Manuscripts, Journals, LMTC, Guidelines for Authors, StyleGuide

1. MANUSCRIPT

1.1 General Instructions

The maximum paper length is restricted to 8 pages. The paper should have the following structure:

1. Title of the paper
2. Authors and affiliation
3. Keywords (6-8 words)
4. Abstract (100 – 250 words)
5. Introduction
6. Main body
7. Conclusions
8. Acknowledgements (if applicable)
9. References
10. Appendix (if applicable)

1.2 Page Layout, Spacing and Margins

The paper must be compiled in one column for the Title and Abstract and in two columns for all subsequent text. All text should be single-spaced, unless otherwise stated. Left and right justified typing is preferred.

1.3 Length and Font

All manuscripts are limited to a size of no more than eight (8) single-spaced pages (A4 size), including abstracts, figures, tables and references. ISPRS Invited Papers are limited to 12 pages. The font type Times New Roman with a size of nine (9) points is to be used.

Table 1. Margin settings for A4 size paper

Setting	**A4 size paper**	
	mm	inches
Top	25	1.0
Bottom	25	1.0
Left	20	0.8
Right	20	0.8
Column Width	82	3.2
Column Spacing	6	0.25

2. TITLE AND ABSTRACT BLOCK

2.1 Title

The title should appear centered in bold capital letters, at the top of the first page of the paper with a size of twelve (12) points and single-spacing. After one blank line, type the author(s) name(s), affiliation and mailing address (including e-mail) in upper and lower case letters,

centred under the title. In the case of multi-authorship, group them by firm or organization as shown in the title of these Guidelines.

2.2 Key Words

Leave two lines blank, then type "**KEY WORDS:**" in bold capital letters, followed by 5-8 key words. Note that ISPRS does not provide a set list of key words any longer. Therefore, include those key words which you would use to find a paper with content you are preparing.

2.3 Abstract

Leave two blank lines under the key words. Type "**ABSTRACT:**" flush left in bold Capitals followed by one blank line. Start now with a concise Abstract (100 - 250 words) which presents briefly the content and very importantly, the news and results of the paper in words understandable also to non-specialists.

3. MAIN BODY OF TEXT

Type text single-spaced, **with** one blank line between paragraphs and following headings. Start paragraphs flush with left margin.

3.1 Headings

Major headings are to be centered, in bold capitals without underlining, after two blank lines and followed by a one blank line.

Type subheadings flush with the left margin in bold upper case and lowercase letters. Subheadings are on a separate line between two single blank lines.

Subsubheadings are to be typed in bold upper case and lower case letters after one blank line flush with the left margin of the page, with text following on the same line. Subsubheadings may be followed by a period or colon, they may also be the first word of the paragraph's sentence.

Use decimal numbering for headings and subheadings

3.2 Footnotes

Mark footnotes in the text with a number (1); use the same number for a second footnote of the paper and so on. Place footnotes at the bottom of the page, separated from the text above it by a horizontal line.

3.3 Illustrations and Tables

3.3.1 Placement: Figures must be placed in the appropriate location in the document, as close as practicable to the reference of the figure in the text. While figures and tables are usually aligned horizontally on the page, large figures and tables some-times need to be turned on their sides. If you must turn a figure or table sideways, please be sure that the top is always on the left-hand side of the page.

3.3.2 Captions: All captions should be typed in upper and lower case letters, centered directly beneath the illustration. Use single spacing if they use more than one line. All captions are to be numbered consecutively, e.g. Figure 1, Table 2, Figure 3.

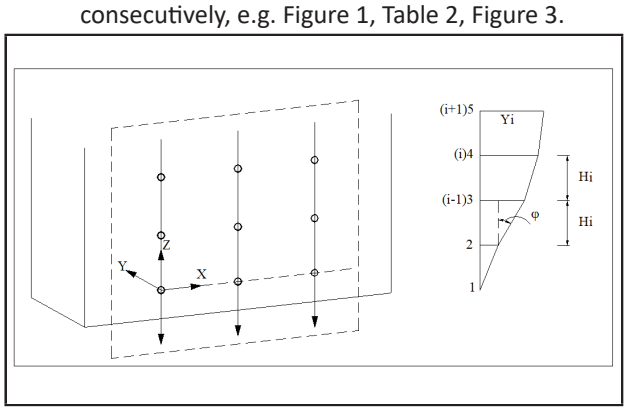

Figure 1. Figure placement and numbering

3.4 Equations, Symbols and Units

3.4.1 Equations: Equations should be numbered consecutively throughout the paper. The equation number is enclosed in parentheses and placed flush right. Leave one blank lines before and after equations:

$$x = x_0 - c\frac{X - X_0}{Z - Z_0} \; ; \; y = y_0 - c\frac{Y - Y_0}{Z - Z_0} \qquad (1)$$

where *c* = focal length

x, y = image coordinates

X_0, Y_0, Z_0 = coordinates of projection center

X, Y, Z = object coordinates

3.4.2 Symbols and Units: Use the SI (Système Internationale) Units and Symbols. Unusual characters or symbols should be explained in a list of nomenclature.

3.5 References

References should be cited in the text, thus (Smith, 1987a), and listed in alphabetical order in the reference section. The following arrangements should be used:

3.5.1 References from Journals: Journals should be cited like (Smith, 1987a). Names of journals can be abbreviated according to the "International List of Periodical Title Word Abbreviations". In case of doubt, write names in full.

3.5.2 References from Books: Books should be cited like (Smith, 1989).

3.5.3 References from Other Literature: Other literature should be cited like (Smith, 1987b) and (Smith, 2000).

3.5.4 References from websites: References from the internet should be cited like (Maas et al. 2017). Use of persistent identifiers such as the Digital Object Identifier or (DOI) rather than a URLs is strongly advised. In this case last date of visiting the web site can be omitted, as the identifier will not change.

3.5.5 References from Research Data: References from internet resources should be cited like (Dubaya et al., 2017).

3.5.6 References from Software Projects: References to a software project as a high level container including multiple versions of the software should be cited like (GRASS Development Team, 2017).

3.5.7 References from Software Versions: References to a specific software version should be cited like (GRASS Development Team, 2015).

3.5.8 References from Software Project Add-ons: References to a specific software add-on to a software project should be cited like (Lennert and GRASS Development Team, 2017).

3.5.9 References from Software Repository: References from internet resources should be cited like (Gago-Silva, 2016).

ACKNOWLEDGEMENTS (OPTIONAL)

Acknowledgements of support for the project/paper/author are welcome.

REFERENCES

Dubayah, R.O., Swatantran, A., Huang, W., Duncanson, L., Tang, H.,Johnson, K.,Dunne, J.O., and Hurtt, G.C., 2017. CMS: LiDAR-derived Biomass, Canopy Height and Cover, Sonoma County, California, 2013. ORNL DAAC, Oak Ridge, Tennessee, USA https://doi.org/10.3334/ORNLDAAC/1523.

Gago-Silva, A., 2016. GRASS GIS in Grid Environment. Figshare https://doi.org/10.6084/m9.figshare.3188950.

GRASS Development Team, 2017. Geographic Resources Analysis Support System (GRASS) Software, Open Source Geospatial Foundation http://grass.osgeo.org (20 September 2017).

GRASS Development Team, 2015. Geographic Resources Analysis Support System (GRASS) Software, Version 6.4. Open Source Geospatial Foundation http://grass.osgeo.org (1 June 2017).

Lennert, M. and GRASS Development Team, 2017. Addon i.segment.stats. Geographic Resources Analysis Support System (GRASS) Software, Version 7.2, Open Source Geospatial Foundation https://grass.osgeo.org/grass7/manuals/addons/i.segment.stats.html (1 June 2017).

Maas, A., Rottensteiner, F., Heipke, C., 2017. Classification under label noise using outdated maps. In: *ISPRS Annals of the Photogrammetry, Remote Sensing and Spatial Information Sciences*, Vol. IV-1/W1, pp. 215-222, doi.org/10.5194/isprs-annals-IV-1-W1-215-2017.

Smith, J., 1987a. Close range photogrammetry for analyzing distressed trees. *Photogrammetria*, 42(1), pp. 47-56.

Smith, J., 1987b. Economic printing of color orthophotos. Report KRL-01234, Kennedy Research Laboratories, Arlington, VA, USA.

Smith, J., 1989. *Space Data from Earth Sciences*. Elsevier, Amsterdam, pp. 321-332.

APPENDIX (OPTIONAL)

Any additional supporting data may be appended, provided the paper does not exceed the limits given above.

Note: The format for the journal is taken and modified from the format of ISPRS archives of the Photogrammetry, Remote Sensing and Spatial Information Sciences

Short-Term Trainings Conducted in Fiscal Year 2081-82

SN	Training Name	Place	Number of Trainees
1	Refreshment Training for High Level Officials Related to Land Management	LMTC	50
2	Training on Informal Land Tenure	LMTC	392
3	Training on Informal Land Tenure	Janakpur	36
4	Land Administration and Management Training (Officer Level)	Kathmandu	26
5	Land Administration and Management Training (Assistant Level)	LMTC	17
6	Training of Trainers (TOT)	LMTC	50
7	Digital Cadastral Survey and Office Management Training (In-service Training for Amin)	LMTC	20
8	Digital Cadastral Survey and Office Management Training (In-service Training for Surveyors)	LMTC	19
9	Orientation Training for Newly Appointed Survey Officers	LMTC	9
10	Orientation training for Honorable District Judges	LMTC	20
11	Training on Surveying, Mapping and Land Administration for the Employees Working in the Supreme Court, Subordinate Courts, the Office of the Attorney General, and its Subordinate Bodies	LMTC	19
12	Training on Operation of NeLIS	LMTC	32
13	GIS Training for Local Level	Kanchanpur	24
14	GIS Training for Local Level	Dailekh	22
15	GIS Training for Local Level	Dadeldhura	17
16	Instrument Handling Training for Local Level	LMTC	19
17	Basic GIS Training	LMTC	22
18	Basic Remote Sensing Training	LMTC	14
19	Advanced Remote Sensing Training	LMTC	21
20	GIS and Instrument Handling Training for Local Level	Dang	23
21	GIS and Instrument Handling Training for Local Level	Kanchanpur	47
22	GIS and Instrument Handling Training for Local Level	Kailali	21
23	Training on Cadastral Surveying and Land Registration for Technical Employees Working in Survey Offices	Banke	14
24	Training on Cadastral Surveying and Land Registration for Technical Employees Working in Survey Offices	Sunsari	15
25	Land Use/Land Management Training for Local Level	Dhankuta	23
26	Land Use/Land Management Training for Local Level	Palpa	26
27	Training on LiDAR Data Application and Processing	LMTC	17
28	UAV and GNSS Training	LMTC	22
29	Total Station Calibration Training	LMTC	21
30	Map Reading Training for Employees Working in Government Offices of Kavre District	LMTC	21
31	Map Reading Training for School Level	Schools	816
32	Land Literacy Training in Collaboration with Non-Governmental Organizations	LMTC	26
33	Surveying and Advanced Surveying Training for Students of Masters in Geoinformatics in Collaboration with Nepal Open University	LMTC	16

Key Programs Planned for Year 2082/83

SN	Program	Number of Trainings/ Programs	Venue
1.	Training of Trainers	3	LMTC Premises
2.	Annual Review and Planning Formulation Program	1	LMTC Premises
3.	Orientation Training for Newly Recruited Survey Officers	1	LMTC Premises
4.	Digital Cadastral Survey and Office Management Training (In-service Training for Amin)	1	LMTC Premises
5.	Digital Cadastral Survey and Office Management Training (In-service Training for Surveyors)	1	LMTC Premises
6.	Land Use/Land Management Training for Local Level	1	Local Level
7.	Basic Remote Sensing Training	1	LMTC Premises
8	Advanced Remote Sensing Training	1	LMTC Premises
9.	Basic GIS Training	1	LMTC Premises
10.	Advanced GIS Training	1	LMTC Premises
11.	GIS Training for Local Level	3	Local Level
12.	Orientation Training for District Judges	1	LMTC Premises
13.	Training on Informal Land Tenure for Officials of the Land Problem Settlement Commission	1	LMTC Premises
14.	Training on Cadastral Surveying and Land Registration for technical Staffs Involved in Informal Land Tenure Management	1	Local Level
15.	Training on Cadastral Mapping and Land Registration for Technical Staffs Working in Survey Offices	1	LMTC Premises
16.	Training on Surveying and Mapping/Land Administration for Officer Level Employees Working in Court	1	LMTC Premises
17.	Training on Surveying and Mapping/Land Administration for Assisstant Level Employees Working in Court	1	LMTC Premises
18.	Land Administration and Management Training for officer-level Employees Working in Land Revenue Offices	1	LMTC Premises
19.	Training on Cadastral Surveying and Mapping Using GNSS and UAV	2	LMTC Premises
20.	Land Administration and Management Training for Assistant-level employees Working in Land Revenue Offices	1	LMTC Premises
21.	Instrument Handling and Data Processing Training	2	LMTC Premises
22.	Land Literacy Program	2	LMTC Premises
23.	Training on the LiDAR Data Application and Processing	1	LMTC Premises
24.	NeLIS Training	1	LMTC Premises
25.	Training on Operation of LRIMS and PAM for Employees Working in Land Revenue Offices	1	LMTC Premises
26.	Study, Research and Survey on Issues Related to Land Management	2	
27.	Shadowing With Real Work	6	

Calendar of International Geoinformatics Events

1 **ISPRS ICWG III/II: 2025 Workshop and Tutorial in GeoAI Advancements and Applications**
Date: 14-15 Jul 2025
Website: https://rcaig.com/2025-workshop-and-tutorial-in-geoai-advancements-and-applications/
Place: Hong Kong, Hong Kong

2 **ISPRS ICWG IV/III/II: Academic Track of FOSS4G) Europe 2025**
Date: 14-20 Jul 2025
Website: https://2025.europe.foss4g.org/
Place: Mostar, Bosnia-Herzegovina

3 **ISPRS TC IV: 9th International Workshop on Dynamic and Multi-dimensional Geospatial Information Simulation**
Date: 22-24 Aug 2025
Website: https://dmgis2025.scievent.com/
Place: Beijing, China

4 **ISPRS ICWG V/IV: Unleashing the power of Geospatial and Frontier Technologies for a Sustainable Future**
Date: 01-03 Sep 2025
Website: http://giftssummit.com/
Place: Pune, Maharashtra State, India

5 **ISPRS WG IV/1: 3D GeoInfo & SDSC 2025**
Date: 02-05 Sep 2025
Website: https://www.csis.u-tokyo.ac.jp/3d_geoinfo_sdsc_2025/overview.html
Place::Tokyo, Japan

6 **ISPRS ICWG II/Ib: The 15th International Workshop on Structural Health Monitoring (IWSHM)**
Date: 09-11 Sep 2025
Website: https://iwshm2025.stanford.edu/
Place: Stanford, CA, USA

7 **ISPRS ICWG II/Ia: UAV-g Uncrewed Aerial Vehicles in Geomatics 2025**
Date: 10-12 Sep 2025
Website: https://uav-g2025.com/
Place: Finland,ON, Canada

8 **ISPRS WG V/6 Workshop: Applied Photogrammetry and Remote Sensing for Environmental and Industry**
Date: 23-25 Sep 2025
Website:https://www.phedcs.com/phedcs-2025-tashkent/
Place: Tashkent, Uzbekistan

9 **ISPRS WG III/3: The 9th Asia-Pacific Conference on SAR Technology and Applications for Sustainability**
Date: 05-09 Oct 2025
Website: http://apsar2025.ce.t.kyoto-u.ac.jp/
Place: Matsue, Shimane, Japan

10 **ISPRS WG IV/5: Symposium on Geospatial Technologies: Visions and Horizons 2025**
Date: 08-10 Oct 2025
Website: http://geovisions2025.org/
Place: Çanakkale, Turkey

11 **ISPRS WG IV/2: The 8th ISPRS Geospatial Conference 2025**
Date: 13-15 Oct 2025
Website: https://geospatialconf2025.ut.ac.ir/
Place: Tehran, Iran

12 **13th International FIG Workshop on the Land Administration Domain Model & 3D Land Administration**
Date: 03-05 Nov 2025
Website:https://gdmc.nl/3DCadastres/workshop2025
Place: Florianópolis, Santa Catarina, Brazil

13 **ISPRS ICWG V/IV: Navigating Excellence in Geospatial Technology for Smart Cities**
Date: 07-09 Nov 2025
Place: Jaipur, India

14 **ISPRS WG IV/6: 2nd International Workshop on Geo-spatial Computing for Understanding Human Behaviors**
Date: 15-16 Nov 2025
Website: https://geohb2025.tongji.edu.cn/
Place: Shanghai, China

15 **ISPRS TC I, WG I/6, WG I/7, ICWG I/IV: Workshop on Evaluation and Benchmark of Sensors and Systems in Photogrammetry and Remote Sensing**
Date: 20-21 Nov 2025
Website: https://geobench.fbk.eu/
Place: Wroclaw, Poland

16 **ISPRS ICWG III/IV: Conference on Geoinformation 2025**
Date: 24-28 Nov 2025
Website: https://www.selper.org.mx/conferencia-de-geoinformacion-2025/
Place:Yucatán,Mexic0

17 **INTERGEO 2025**
Date: 07-09 Oct 2025
Website: https://dvw.de/intergeo/en/welcome-to-intergeo/registration
Place: Frankfurt, Germany

18 **FOSS4G :NA 2025**
Date: 03-05 Nov 2025
Website: https://www.foss4gna.org/
Place: Reston, Virgina, USA

19 **FOSS 4G Auckland 2025**
Date: 17-23 Nov 2025
Website: https://2025.foss4g.org/
Place: Auckland, New Zealand

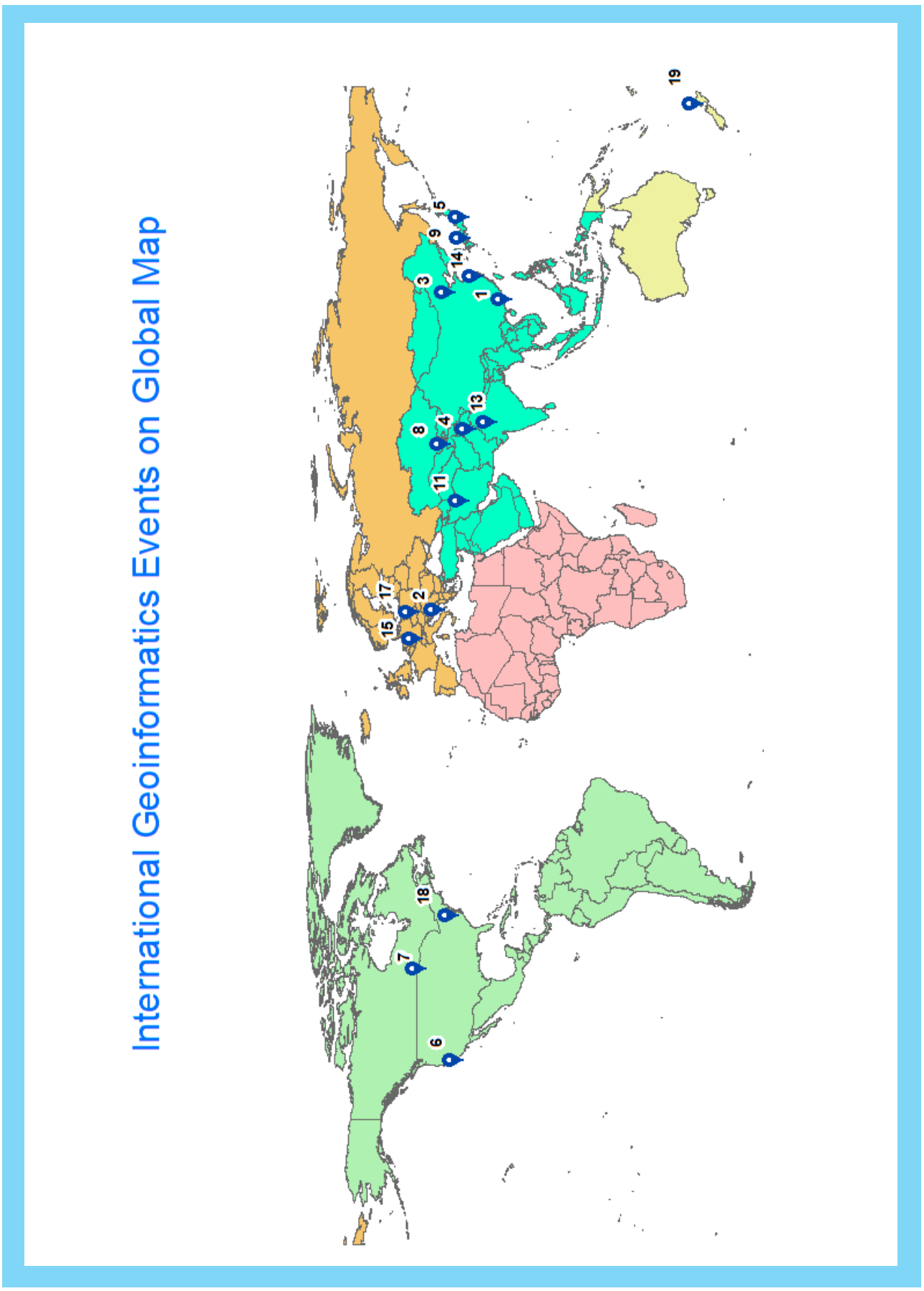
International Geoinformatics Events on Global Map
19
5
9
14
3
1
13
8
4
11
17
2
15
18
7
6

Articles Published in Previous Editions

Volume I (Published in 2076 B.S.)

1. **Comparison of Machine Learning and Classical Algorithms based on Supervised Classification for Forest Types Discrimination using Rapid Eye Imagery**
   Sanjeevan Shrestha, Stavros Sakellariou

2. **Effects of Service-Specific On-the-Job Training-A Case Study of the Digital Cadastre and Office Management Training Programme**
   Bhuwan Ranjit, Sudarshan Gautam

3. **Assessing the Overall Accuracy of UAV Photogrammetry: A Methodology for Different Combination of Imagery Parameters and Terrain Type**
   Basant Awasthi, Shashank Karki, Pratikshya Regmi, Deepak Singh Dhami, Shangharsha Thapa, Uma Shankar Panday

4. **Management of Public Land for Urban Open Space: In Case of Disaster Risk Reduction**
   Sanjaya Manandhar, Janak Raj Joshi

5. **Outburst Flood Hazard Assessment of Tsho-Rolpa Glacial Lake**
   Sanjeevan Shrestha, Karuna Shrestha, Yashoda Acharya

6. **Vulnerability Assessment of Indigenous Communities to Climate Change in Nepal**
   Pawan Thapa, Dr. Pradeep Sapkota Upadhyaya

Volume II (Published in 2077 B.S.)

1. **A Collaborative Model and "Knowledge Transfer Vehicle" For Capacity Development: Geo-Information and Land Administration Education at Kathmandu University Jointly with Land Management Training Center**
   Reshma Shrestha, Ganesh Prasad Bhatta

2. **Assessment of Pre-Processing Methods of Digital Elevation Models for Stream Delineation**
   Shangharsha Thapa, Lone Mokkenstorm, Julika Wolf, Birkan Çalışkan

3. **German School of Thoughts on Geography and Its Implication in Nepal**
   Sanjaya Manandhar

4. **Comparison of Early Season Characteristics of Nepalese Forest Fires Retrieved by MODIS and VIIRS**
   Him Lal Shrestha, Mahesh Poudel

5. **Impact of Labour Migration on Land Use Change: A Case of Nepal**
   Gobinda Ghimire

6. **Ultra-High Resolution UAV Images for Land Pooling**
   Aman Manandhar, Sagar Bayalkoti

7. **Identifying Suitable Resettlement Areas for Squatters Using Multi Criteria Evaluation**
   Atul Man Joshi, Bhuwan Ranjit

Volume III (Published in 2078 B.S.)

1. **Encroachment of Forest Cover in Chitwan and Parsha Districts of Nepal: A Spatiotemporal Quantification Over 25 Years**
   Pratikshya Regmi, Nimisha Wagle

2. **Assessing the Status of Land Tenure System of Nepal Using Swot Matrix Method**
   Sharad Chandra Mainali

3. **Route Planning Using Least Cost Path Analysis (A Case Study of Janakpur – Birgunj Section)**
   Sushmita Subedi, Bishal Kumar Jha, Shova Acharya, Nandeshwar Kushwaha

4. **Land Slide Susceptibility Mapping of Budhigandaki River Sub-Basin Using Analytic Heirarchy Process and Machine Learning Methods**
   Sudarshan Gautam, Binod Humagain, Sanjeevan Shrestha

5. **Landslides In Nepal: A Case Study of Postearthquake Landslides in Upper Bhotekoshi**
   Sharad Chandra Mainali, Sudarshan Gautam, Khem Raj Devkota

6. **Quantification of Surface Velocity and Ice Thickness of Glacier: A Case Study of G9 Glacier, Hidden Valley Nepal**
   Nabin Raj Bhatt, Sujan Sapkota, Dinesh Prasad Bhatt, Shangharsha Thapa, Dr. Rijan Bhakta Kayastha

7. **Comparative Analysis of Different Methods of Spatial Interpolation: Interpolating Annual Precipitation on The Koshi Basin**
   Sudarshan Gautam, Binod Humagain, Rebanta Aryal, Prakash Lakandri , Jagannath Aryal

Volume IV (Published in 2079 B.S)

1. **Comparison of Random Forest, Support Vector Machine and Artificial Neural Network Classifiers for Land Cover Classification Using Sentinel-2 Imagery**
   Bhagirath Bhatt, Suraj KC, Sanjeevan Shrestha
2. **Suitability Analysis to Identify the Suitable Dumping Site on Kanchacnpur Using MCDA (Multi Criteria Decision Analysis)**
   Binod Prasad Bhatta, Sudeep Kuikel, Reshma Shrestha
3. **Smoke Scene Detection from Satellite Imagery Using Deep Learning**
   R. Aryal, P. Thapa, M.Karki
4. **Landslide Susceptibility Mapping Along Pokhara-Beni Highway Using Frequency Ratio Techniques**
   Sagar Karki, Bishal Thapa, Rajan Kumar Adhikari, Shreeram Bhandari
5. **Gravimetry in Survey Department: A Brief History and Current Practices**
   Stallin Bhandari, Sandesh Upadhyaya, Shanker KC
6. **Using Geospatial Technologies for Disaster Management in Developing Countries**
   Pawan Thapa

Volume V (Published in 2080 B.S.)

1. **The Land-use Planning and its Economic Implication**
   Prof. Achyut Wagle
2. **Land Banking Initiative in Nepal for Sustainable Land Management: Unfinished Agenda of Decentralizing Land Use Planning and Land Reform**
   Bhupendra Jung Keshari Chand
3. **A Brief History of Advances in Geodesy with National Cases**
   Shanker K.C., Tri Dev Acharya
4. **Perceiving, Preserving and Promoting Indigenous Land Use Role Model with Drone Mapping in Nepal**
   Sunil Bogati
5. **Reutilization Of Abandoned and Fallow Agricultural Land in Nepal: Lensing Through the Vedic Wisdom Perspective**
   Basu Dev Kaphle
6. **Landcover Classification Using Decision Tree Algorithm**
   Dhruba Poudel, Sanjeev Kumar Raut
7. **Identification of Land Market Impact Factors in The Context of The Introduction of The Land Use Regulation in Nepal: Stakeholders' Perspective**
   Dr. Nab Raj Subedi, Professor Kevin McDougall, Dr Dev Raj Paudyal
8. **Summary Report on International Workshop on Land Use Planning and Land Administration: Integration and Decentralization**
   Ganesh Prasad Bhatta, Rheecha Sharma, Sharad Chandra Mainali

Volume VI (Published in 2081 B.S.)

1. **Mapping Burn Severity of Wildfire and its Analysis with Topographical Factors: A Case Study of Chitwan District**
   Aagya Dhungana, Anjali Singh, Anju Lage, Punam Koirala, Man Kumari Chaulagain, Sunil Thapa , Dr.Reshma Shrestha
2. **Spatio-Temporal Analysis of Air Pollutants Before, During and After Covid-19 Outbreak Over Kathmandu Valley**
   Binod Prasad Bhatta, Mamta Kadel, Gorakh Nath Pandey, Sadikshya Adhikari, Manoj Kumar Bhat
3. **Practical Learning about Time using Sundial at Land Management Training Center**
   Bhagirath Bhatt, Sushmita Timilsina, Shivaji K.C., Hareram Yadav
4. **Ecotourism and Ecovillage Mapping in Kavrepalanchowk District, Nepal**
   Prakash Ghimire, Rheecha Sharma
5. **Concepts and Principles for Identification of Logical Errors in Cadastral (Parcel) Database Developed by Digitization of Analogue Cadastral (Parcel) Maps**
   Er. Mahesh Thapa
6. **Modernizing Nepal's Height System: Leveraging GNSS and Gravity Observations for Global Compatibility**
   Sushmita Timilsina
7. **Dependency of Orientation of Image Capture on Vegetation Indices**
   Sanjeev Kumar Raut, Dhurba Poudel, Umang Raj Dotel, Shree Krishna Adhikari
8. **Land Management Training Center: The Center of Excellence in Land Management and Geomatics Education**
   Tina Baidar, Ram Kumar Sapkota
9. **Effective Land Administration in Nepal: Navigating Governance, Legal and financial Pathways within the Climate Change- Land Nexus: Summary Report**
   Umang Raj Dotel, Sushmita Timilsina
10. **Land Literacy Program: A Joint Effort of the Government and Non-Governmental Organizations Towards Land Issues Awareness on Communities**
    Dharma Raj Joshi

Lecture of the Month Series Organized at LMTC

S.N.	Episode	Date	Theme	Expert/ Speaker
1	Episode 1	2080/11/27	Professional ethics and integrity on civil service at work place	Mr.Gopinath Mainali, Former Secretary, Government of Nepal
2	Episode 2	2080/12/30	Geographical Names and Romainization system for Nepal.	Mr. Sureshman Shrestha, Former Deputy Director General, Survey Department
3	Episode 3	2081/01/28	Positivity for a Happy life	Mrs. Sumi Manav, Motivational Speaker/Social Worker
4	Episode 4	2081/02/25	Low cost GNNS and Application of RTK in mobile maps	Mr. Prashant Malla, Geospatial Expert/Application Developer
5	Episode 5	2081/03/26	Future human resources and future of human resources in Nepal	Mr.Madhusudan Adhikari, Former Secretary, Government of Nepal
6	Episode 6	2081/04/25	Harnessing Remote Sensing and Geo-information	Dr.Arun Kumar Pratihast, Researcher and senior data scientist Wageningen University
7	Episode 7	2081/05/31	Health Issues at Work Place	Dr.Rajendra Koju, Senior Cardiologist
8	Episode 8	2081/06/11	Professional Ethics and Integrity	Dr. Bhishma Kumar Bhusal, Joint Secretary, Government of Nepal
9	Episode 9	2081/08/23	Public service delivery and Good Governance	Dr. Rajan Khanal, Executive Director, Nepal Administrative Staff College
10	Episode 10	2081/08/27	Role of Young Surveyor's for Climate Resilient Lands	Mr. Buddhi Narayan Shrestha, Former Director General, Survey Department
11	Episode 11	2081/12/29	Empowering local governance through Geospatial Innovations	Mr. Ashok Kumar Byanju, Mayor, Dhulikhel Municipality
12	Episode 12	2082/01/30	Efforts initiated in resolving land issues in Nepal	Dr. Jagat Basnet, Expert Member, Land Issues Resolving Commission (LIRC)

GOVERNMENT OF NEPAL
MINISTRY OF LAND MANAGEMENT, COOPERATIVES AND POVERTY ALLEVIATION

LAND MANAGEMENT TRAINING CENTER

Dhulikhel, Kavrepalanchok

INTRODUCTION

Land Management Training Center (LMTC), under the Ministry of Land Management, Cooperatives and Poverty Alleviation, Government of Nepal was established in 1968. LMTC is the oldest and the only governmental institution continually and significantly producing human resources and enhancing the capacity of government personnel in the field of Surveying Mapping, and Land Management since its establishment. The center has already produced more than 10,000 land professionals at different levels through various types of training courses.

LMTC is certified with ISO 9001:2015 for Quality Management on 29 June 2022 A.D. The center has been conducting a wide range of long and short-term training incorporating state-of-the-art modern technologies. Along with this, LMTC has collaborated to run academic courses with Kathmandu University (KU). Additionally, the Center contributes to the capacity building of Provincial and Local Governments.

VISION

To be the Center of Excellence in Land Management and Geomatics Education.

MISSION

Building and Enhancing Individual and Institutional Capacity in Land Management and Geomatics Sector.

GOAL

To produce qualified and skilled human resources in the field of Land Management and Geomatics.

OBJECTIVES

- To conduct various professional courses.
- To carry out Pre-service and In-service Training, Refresher courses, and Orientation programs.
- To collaborate with national and international academia and professional organizations.
- To promote Research and Development
- To support provincial and local governments in developing qualified human resources.

OUR FACULTIES/TRAINERS

Our courses are delivered by passionate and dedicated faculties/trainers who possess wealth of national and international experiences, and high qualification obtained from renowned national and international universities.

ANNUAL PUBLICATION

JOURNAL OF LAND MANAGEMENT AND GEOMATICS EDUCATION

OFFICIAL WEBSITE

www.lmtc.gov.np

ACADEMIC COURSES (In Collaboration)

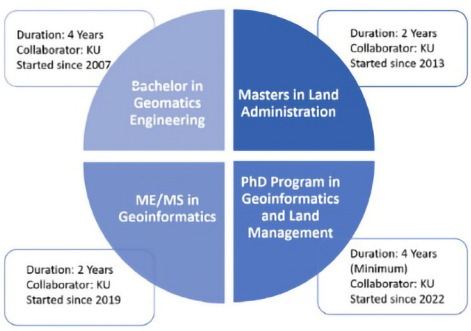

TRAINING COURSES

LONG TERM TRAININGS

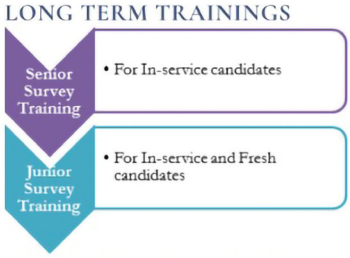

SHORT TERM TRAININGS

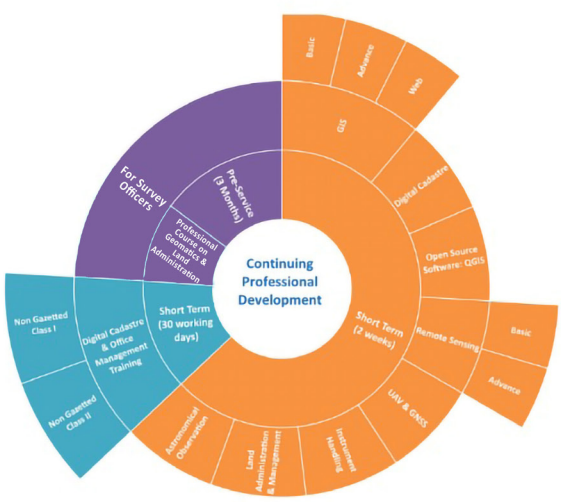

FUTURE PLANS

- To contribute in Policy Research in the sector of Geomatics and Land Management
- To contribute to capacity Building of Local Governments in the sector of Geomatics and Land Management
- To extend collaboration with academia and regional training institutions

Government of Nepal
Ministry of Land Management, Cooperatives and Poverty Alleviation

LAND MANAGEMENT TRAINING CENTER

ACHIEVEMENT OF FY 2081/82

NOVEL SUCCESSES

Achievements of 2081/82

- Recertification of ISO 9001:2015 Quality Standards
- Approval of ten years strategic plan (2022-2032)
- Publication of Land Literacy: Reference Book
- Successfully Conducted 8 episodes of Lecture of the Month Series
- Refresher Course for High Level Officials Working in the Field of Land Management

TRAININGS LAUNCHED THIS FISCAL YEAR

GIS Training for Local Level	63
Training for District Judges	20
Instrument Handling & Orientation	19
Land Use/Land Management	49
Informal Land Tenure Training	428
LiDAR Data Application and Processing Training	17

ADDITIONAL CAPACITY BUILDING SHORT TRAININGS

- NeLIS (32)
- Orientation Training for New Officers (9)
- UAV & GNSS (22)
- Remote Sensing (35)
- Land Administration & Management Gazetted Class III (26)
- Land Administration & Management Non-Gazetted (17)
- Total Station Calibration Training (21)
- Map Reading Training for School Level (816)
- Map Reading Training for Government Employees (21)
- Cadastral Surveying and Land Registration (29)

LONG TERM TRAININGS

- Senior Survey Training Inservice (16)
- Junior Survey Training Fresh (23)
- Junior Survey Training Inservice (24)

INSERVICE TRAINING GRANTING 2 POINTS

Digital Cadastre & Office Management Training (Non-Gazetted Class I)	17
Digital Cadastre & Office management Training (Non-Gazetted Class II)	20

The figures in the parenthesis are the numbers of trainees

Photo Gallery

56th Anniversary of Land Management Training Center

Inaguration of 5th FIG Young Surveyors Asia-Pacific Meeting by FIG President Dr. Diane Dumashie

Opening Ceremony of 5th FIG Young Surveyors Asia-Pacific Meeting

Participants of the 5th FIG Young Surveyors Asia-Pacific Meeting at LMTC for Social and Technical Tour

Participants of Meeting of High Level Officials Related to Land Management

Participants of 56th Anniversary of LMTC

Participants from World Bank, LMTC and Kathmandu University, on Interaction Program Focusing on Exploring Collaboration Opportunities to Improve the Drone Ecosystem in Nepal

Participants of Orientation Training for Survey Officers, SOSET-5

Graduation Ceremony of Senior Survey Training Batch 2080-81

Graduation Ceremony of Junior Survey Training (Inservice)-59th Batch

Graduation Ceremony of Junior Survey Training (Fresh), 58th Batch

Participants of Orientation Training on Land Administration for Honourable District Judges

Participants of Training on Land Related Frauds for Investigation Officers of CIB

Participants of GIS Training for Local Level at Kanchanpur

Participants of Basic Remote Sensing Training

Participants of Land Use-Land Management Training for Local Level at Palpa

Plantation Program at LMTC Premises on the Ocassion of World Environment Day 2025

Terrestrial LiDAR Survey During LiDAR Data Application and Processing Training at LMTC Premises

LiDAR Data Processing by Director Mr. Ram Kumar Sapkota on LiDAR Data Application and Processing Training

Trainees of Junior Survey Training (Inservice)-59th Batch Trainees at Tanahun Hydropower Limited During Educational Tour

Field Inspection By Executive Director Mr. Janak Raj Joshi

Trainees of Junior Survey Training (Inservice)-59th Batch Conducting UAV Survey During Field Camp

Students of Geomatics Engineering BE 8th Semester Performing Field Activities at LMTC Premises

LMTC Staff Team on Sports Week 2025